UNIVERSITÀ
DEGLI STUDI
FIRENZE

DOTTORATO DI RICERCA IN FISICA ED ASTRONOMIA

INDIRIZZO FISICA - XXXII CICLO

Settore disciplinare - FIS02

Wilson loops at weak and strong coupling in $\mathcal{N} = 4$ Super Yang-Mills with defects

Dottorando:
Sara Bonansea

Tutore:
Prof. Domenico Seminara

Coordinaotre:
Prof. Raffaello D'Alessandro

Anni 2016-2019

Contents

Introduction **i**

1 The ADS/CFT correspondence **1**

1.1 Supersymmetric gauge theories 1

1.1.1 Supersymmetry 3

1.1.2 Conformal symmetry 5

1.1.3 Representation of the conformal group 7

1.1.4 Correlation functions 9

1.1.5 Superconformal symmetry 10

1.1.6 Representation of the superconformal algebra 11

1.1.7 $\mathcal{N} = 4$ Super Yang-Mills Theory 12

1.2 'T Hooft expansion of gauge theories and string theory 18

1.3 The $AdS_5 \times S^5$ correspondence 21

1.3.1 AdS space 22

1.3.2 Type IIB supergravity 24

1.3.3 D-branes and open strings perspective 25

1.3.4 D3-branes and closed strings perspective 29

1.3.5 The Maldacena conjecture 30

1.3.6 Comparing the symmetries and correlation functions 32

2 Supersymmetric Wilson loop operators **35**

2.1 Wilson loops in non-abelian gauge theories 35

2.2 BPS Wilson loops in $\mathcal{N} = 4$ SYM theory 37

2.2.1 Supersymmetry variation of the Wilson loop . . . 39
2.2.2 Straight line . . . 40
2.2.3 The circular Wilson loop . . . 41
2.2.4 Zarembo construction . . . 42
2.2.5 DGRT construction . . . 43
2.3 The circular Wilson loop at weak coupling . . . 44
2.4 The holographic Wilson loop . . . 48
2.4.1 Minimal surface for the circular Wilson loop . . . 49
2.5 Operator product expansion expansion of the Wilson loop . . . 51

3 $\mathcal{N} = 4$ SYM theory with the insertion of a defect 55
3.1 $\mathcal{N} = 4$ dCFT: field theory construction . . . 55
3.1.1 Symmetries . . . 56
3.1.2 Correlation functions . . . 57
3.1.3 Vacuum expectation values . . . 58
3.2 D3-D5 brane system . . . 59
3.2.1 Brane construction and near horizon limit . . . 60
3.2.2 D5 probe brane . . . 63
3.3 Quantum check of AdS/CFT . . . 65
3.3.1 Tree level one-point functions . . . 65
3.3.2 Higgsing problem and one loop one-point functions . . . 66

4 Circular Wilson loop in defect $\mathcal{N} = 4$: strong coupling 69
4.1 Prelude . . . 70
4.1.1 Setting-up the geometric description . . . 70
4.2 General solution for the connected extremal surface . . . 73
4.2.1 Allowed regions for the parameters j, m and $\tilde{\sigma}$ . . . 77
4.3 The structure of the solutions . . . 81
4.3.1 The distance from the defect . . . 81
4.3.2 The Area . . . 86
4.3.3 Transition: connected solution vs dome . . . 90

5 Circular Wilson loop in defect $\mathcal{N} = 4$: weak coupling 95
5.1 Perturbation theory: the non-BPS case . . . 95
5.1.1 Comparing perturbative analysis with the strong coupling analysis . . . 98

5.1.2 Perturbation theory: the BPS case 100

6 Correlator of two circles in the defect case **105**
6.1 String solutions between two concentric circles without the defect . . 106
6.2 String solutions for two concentric circles with the defect 110

Conclusions and outlook **115**

Acknowledgments **119**

A Representation of $\mathfrak{su}(2)$ **121**

B Massive propagators **123**

C Expression for the distance from the defect **125**

D Expansion of n, $g(\tilde{\sigma})$ and $\frac{\partial \eta}{\partial m}$ around the boundary $j^2 = -1/m^2$. **127**

E The Expansion of the area and comparison with the perturbative results **129**

F Connected solution as correlator between two circle of different radii **133**

G Basis for chiral primary operators **135**

Bibliography **147**

Introduction

This thesis will be focused on some particular aspects of $\mathcal{N} = 4$ Super Yang-Mills theory (SYM) which is a non-abelian interacting theory with the maximal amount of supersymmetry in four dimensions. The theory content is given by a massless vector multiplet with one gauge boson of spin one, six real scalars and four Weyl spinors.

Supersymmetry (SUSY) provides a balance for the bosonic and fermionic degrees of freedom at every mass level of the spectrum and put a strong constraint on the structure of the theory. The power of supersymmetry leads to cancellations between divergent diagrams of the field theory due to the presence of fermionic and bosonic loops that appear with opposite sign. In the superspace formalism, this mechanism recasts into the so-called "non-renormalization theorem." Not only supersymmetry is fascinating by itself from a mathematical point of view, but it plays a pivotal role in the studies of quantum field theories (QFTs), and it has strongly influenced the experimental search in Particle Physics in the last decades. It can also be used to solve some important phenomenological problems as the hierarchy problem for the Higgs mass, and the lowest SUSY particle could provide a candidate for dark matter. In order to build a SUSY version of the Standard Model, one has to introduce a supersymmetric partner for each existing particle, but so far none of these new particles has been observed. Thus, if SUSY exists in Nature, it has clearly to be broken at very high energy scales. Even if we do not have an experimental proof for SUSY, studying supersymmetric models can be very useful because often they are easier to solve than non-supersymmetric ones due to the strong constraints coming from the higher degree of symmetry. Thus, they may serve as toy models where exact analytic results can be obtained thanks to the rich structure of the theory that dramatically simplifies the computations. Moreover, SUSY may serve as a qualitative guide to understand the behavior of more realistic theories as the strong coupling dynamics responsible for phenomena like quark confinement in the

quantum Chromo Dynamics (QCD). There are also non-perturbative techniques, as localization and integrability, that allow us to understand supersymmetric gauge theories deeply. In particular, localization is a mechanism through which the path integral can be reduced to an integration over a subspace of the configuration space.

Supersymmetry is also a crucial ingredient for string theory which is a promising candidate for a quantum version of gravity. When the standard quantum field theory techniques are applied to gravity, very concerning problems arise due to its renormalizability. Non-renormalizable theories are typically viewed as effective field theories, valid only up to some cut-off energy scale beyond which they are not trustable. This is because of the real ultraviolet degrees of freedom are missing. For instance, in QCD, there are quarks at high energies, and pions are the composite degrees of freedom at low energy where the quarks are strongly coupled. The pion Lagrangian is non-renormalizable since it breaks down around 1 GeV and the ultraviolet completion of the chiral model is QCD, which is an asymptotically free theory and thus UV-finite since it has a gaussian fixed point in the UV.
There are several all-orders arguments that string theory provides a theory that is finite in the UV. Its fundamental characteristic is that pointlike particles are replaced by extended objects, the elementary constituents of the theory, which propagating span the worldsheet, a two-dimensional surface. The very consistency of the theory demands the presence of gravity and the graviton appears as a vibrational mode of closed strings while gauge interactions are provided by the open string sector. In this way, General Relativity, Electromagnetism, and Yang-Mills gauge theories all appear in a surprising but also natural fashion. String theory introduces extra dimensions, but it can be defined in four dimensions using the Kaluza-Klein idea, namely considering the extra dimensions to be compact and small. Bosonic string theory is a non-realistic model since it contains only bosons and also tachyons, but is the easiest to study. It requires 26 dimensions in order not to break Lorentz invariance at the quantum level. Superstring theory, which is obtained introducing fermions both on the worldsheet and in space-time, lives in ten dimensions. In string theory, there are also non-perturbative extended objects which play a fundamental role: the Dp-branes that can be viewed as hypersurfaces extended in $p+1$ directions (p spatial + time) where open strings can end. They can be obtained by quantizing the open string with endpoints along these hyperplanes (Dirichlet boundary conditions).

Thus, SUSY is a very intriguing element since it plays a central role both in superstring theory and in QFT. While in closed string theory there is always a massless spin-2 particle that naturally describes gravity, usually in QFT gravity is not present. These two descriptions can be connected through the holographic principle [1, 2], which states that a theory that contains gravity, that could be string theory, in the bulk space, and a field theory without gravity living on the boundary of this space are equivalent. All of the information that is needed to specify a state of a theory of quantum gravity is encoded in the quantum state of a QFT living in a lower dimension. The holographic principle has added a new aspect to string theory: it is not only a fundamental microscopic theory of all particles and their interactions but can be viewed as a framework that allows a detailed and quantitative study of many physical systems thanks to its complementary to a QFT description. The first concrete argument in support of the existence of a relation between gauge and string theories was suggested initially by 't Hooft in [1] with a very general argument. He took into account a generic non-abelian gauge theory with gauge group $SU(N)$ in the limit in which the number of colors N is large. He showed that a gauge theory in the large N limit admits a topological graphs expansion in powers of $1/N$ that reminds a string theory loop expansion. This result suggests the existence of a dual string description for any gauge theory. A concrete realization of the holographic principle is the AdS/CFT correspondence [3–5]. It is founded on a map between ordinary QFTs with conformal invariance (CFT) without gravity, and higher-dimensional models of gravity and strings on anti-De Sitter background. If conformal invariance is added to a supersymmetric field theory, the resulting theory is superconformal. It becomes even more constrained, and the exact computation of physical observables is accessible. It seems that dualities are present also between non-supersymmetric theories, but are more difficult to realize than among rather supersymmetric ones. The AdS/CFT duality can be realized at various levels, and there are several examples. The first best established formulation of the correspondence, due to Maldacena, is the conjecture that there is a mapping between $\mathcal{N} = 4$ SYM theory in four dimensions with gauge group $SU(N)$ and type IIB superstring theory on the ten-dimensional background given by $AdS_5 \times S^5$. $\mathcal{N} = 4$ SYM has not only the maximal number of supercharges for a four-dimensional theory without gravity (namely sixteen Poincarè supercharges), but it is finite and exactly conformal invariant at the quantum level since the coupling constant g_{YM} does not run with the energy scale. Both perturbative arguments and general considerations sug-

gest that the β function of the theory is zero to all loop orders. The parameters of the theories are on the gauge side the coupling g_{YM} and the rank of the gauge group N, while on the other hand, we have the radius of the AdS_5 and the S_5 spaces, indicated with L, and the string coupling constant g_s. They are related through the 't Hooft coupling constant λ in the following way:

$$\lambda = g_{YM}^2 N = 4\pi g_s N \quad , \quad \sqrt{\lambda} = \frac{L^2}{\alpha'}$$

One of the crucial aspects of the Maldacena conjecture is that the correspondence is a weak-strong duality which relates the weak coupling regime of the gauge theory with the strongly coupled string theory and vice versa. Thus, the correspondence opens the possibility to investigate the strong coupling behavior of the gauge theory using a classical gravitational theory. This weak-strong duality has many advantages but, at the same time, it makes very hard to check the validity of the conjecture since there is no overlap between the regions of the validity of the two calculations with the standard tools. In the particular case of $\mathcal{N} = 4$ SYM, the plentiful symmetry structure sometimes allows to extract strong coupling results and provides non-trivial checks of the conjecture.

A simple but non-trivial set-up, where to test the duality on the field theory side, is to consider objects (called BPS) that are invariant under a certain fraction of supersymmetry. Respect to the non-BPS ones, it is more probable that they can be computed exactly, thus providing functions interpolating between weak and strong coupling regimes. Examples of this type of observables are supplied by the chiral primary operators (CPOs) or by the supersymmetric Wilson loop. The latter is a gauge-invariant non-local operator, whose importance in non-abelian gauge theories has been known for a long time. From a geometrical point of view, it is the trace of the holonomy of the gauge connection of the theory. On rectangular contour, it measures the potential of a pair of heavy quarks providing a tool to inspect the confinement of the theory. The Wilson loop operators have been generalized to $\mathcal{N} = 4$ theory by Maldacena in [6], and they are known as the Maldacena Wilson loops. They become locally supersymmetric and possess a string theory counterpart [6, 7]: at large N and strong coupling ($\lambda \to \infty$), they are described by a minimal surface that extends in the bulk of AdS and which is anchored to the contour of the

Wilson loop located at the holographic boundary. A notable example of operators for which a global fraction of the original supersymmetry can be preserved is the circular Wilson loop [8, 9]. Pestun has rigorously proved in [10] that its vacuum expectation value is fully captured by a hermitian matrix model with a gaussian potential. Thanks to the holographic interpretation of the operator, it is possible to calculate the expectation value of the circular Wilson loop also in the gravity side and compare it to the non-perturbative result: quite surprisingly the two computations match. Performing the expectation value of the circular Wilson loop on both sides of the correspondence has been one of the first successful tests of the duality.

This Ph.D. thesis is devoted to the study of the circular Wilson loop operator in a new and very stimulating context: a defect version of the usual $\mathcal{N} = 4$ SYM theory. The general study of defects is an important subject, which has relations with the physics of mostly every field theory. Spatial defects can be introduced into a CFT, reducing the total amount of symmetry. Of particular interest are dCFTs with holographic duals, of which a certain number of examples exist, following the original idea presented in [11–14]. In [15, 16] they consider the $\mathcal{N} = 4$ SYM theory with a codimension-one defect located at $x_3 = 0$ that separates two regions of space-time where the gauge group is respectively $SU(N)$ and $SU(N-k)$. In the field theory description, the difference in the rank of the gauge group is related to a non-vanishing vacuum expectation value (VEV) proportional to $1/x_3$, assigned to three of the $\mathcal{N} = 4$ SYM scalar fields in the region $x_3 > 0$

$$\phi^i_{cl} = -\frac{1}{x_3} t_i \oplus 0_{(N-k)\times(N-k)} \qquad\qquad i = 1, 2, 3$$

where t_i are the $SU(2)$ generators in a k-dimensional irreducible representation. The VEV originates from the boundary conditions on the defect that preserve part of the original supersymmetry. The field theory configuration is realized in string theory through a D5-D3 brane system involving a single probe D5 brane of profile $AdS_4 \times S^2$, in the presence of a background gauge field flux of k units through the S^2. The flux k controls the VEV of the scalar fields and represents a new parameter, compared to the usual $\mathcal{N} = 4$ SYM, which can be used to probe the theory in different regimes. Over the last few years, there has been a certain amount of work in studying such a system. In particular, the vacuum expectation value for a large class of scalar operators has been computed both at weak coupling [17], using perturbation theory, and at strong coupling, through the dual-brane set-up

[18–20]. The insertion of a defect at $x_3 = 0$ breaks translations, Lorentz and special conformal transformations along the x_3 direction while the generator of scale transformations preserves $x_3 = 0$. Thus, the conformal group in four dimensions $SO(2,4)$ is broken to the three-dimensional conformal group $SO(2,3)$. Due to this less conformal symmetry preserved by the system, one-point functions can be different from zero depending on the perpendicular direction to the defect, and this fact has been largely exploited in these investigations. More recently, a serious attempt to extend the integrability program in this context has been performed by the "Niels Bohr Institute" (NBI) group [21–23], leading to some interesting generalizations of the original techniques. Moreover, the presence of the extra-parameter k allows for an interesting double-scaling limit, able in principle to connect the perturbative regime in the field theory with the gauge-gravity computations. It consists in sending the 't Hooft coupling λ as well as k^2 to infinity while keeping fixed the ratio of the two parameters: the perturbative expansion organizes in power of the ratio, that can be considered small. At the same time, the 't Hooft coupling is still large, supporting the validity of the dual gravity calculations. Thus, in that regime, one could try to successfully compare gauge and gravity results, providing a new non-trivial verification of the AdS/CFT correspondence [20].

Less attention has been instead devoted to the Wilson loops. More recently circular Wilson loops, analog to the supersymmetric ones in ordinary $\mathcal{N} = 4$ SYM, have been examined in [24], producing some interesting results. There it was considered a circular Wilson loop of radius R placed at distance L from the defect and parallel to it, whose internal space orientation has been parameterized by an angle χ. Its vacuum expectation value has been computed both at weak and strong coupling, and, in the double scaling limit and for small χ and small L/R, the results appeared consistent. In this thesis, based on [25], we will investigate further the same circular Wilson loop in defect $\mathcal{N} = 4$ SYM theory, generalizing the computations presented in [24] both at strong and weak coupling. In particular, we will cover the full parameter space of the string solution of our system. Namely, we derive the exact solution for the minimal surface, describing the Wilson loop in the AdS/CFT setting, for any value of the flux k, angle χ and ratio L/R and we can explore the complicated structure of the solution in different regions of the parameter. Nicely we recover, in the limit of large k, the result of [24] without restrictions on L/R and χ. The main output of our analysis is the discovery of a first-order phase transition of Gross-Ooguri type [26]: for any flux k and any non-zero angle χ the disk solution

(describing the Wilson loop in the absence of defect) still, exist and dominates, as expected, when the operator is far from the defect. On the other hand, our cylindrical string solution, connecting the boundary loop with the probe D5-brane, is favorite below a certain distance (or equivalently for large radius of the circles). We can compare the classical actions associated with the solutions, by a mixture of analytical and numerical methods, finding the critical ratio L/R, at which the transition occurs, as a function of k and χ. A second important conclusion is that in the BPS case, that corresponds to $\chi = 0$, the cylindrical solution does not exist for any choice of the physical parameters, suggesting that light supergravity-mode exchanges with the disk solution always saturate the expectation value at strong coupling. This strongly resembles an analog result for correlators of relatively BPS Wilson loops in $\mathcal{N} = 4$ SYM [27], that can be also exactly computed through localization [28, 29]. The weak coupling analysis corroborates the exceptionality of the BPS case. The first non-trivial perturbative contribution is evaluated exactly in terms of generalized hypergeometric functions. Its large k expansion does not scale in a way to match the string solution. In the regime $L/R \to \infty$, we expect instead that the perturbative result could be understood in terms of the operator product expansion (OPE) of the Wilson loop. We reconstruct from the first two non-trivial terms of the expansion some known result for the one-point function of scalar operators.

The thesis will be organized as follows:

- Chapter 1: we will give a review of the AdS/CFT correspondence starting with introducing fundamental aspects of supersymmetry, conformal symmetry, and superconformal symmetry. Next, we will describe in some detail the $\mathcal{N} = 4$ SYM theory. Then, we will give some insights into the large N limit of gauge field theories and their relation to classical string theory. To enunciate what the correspondence states, we will introduce branes considering their two possible descriptions in terms of open and closed strings. At this point, we will give the dictionary for the mapping between the observables of the two theories.

- Chapter 2: we will describe the Wilson loop operators in both abelian and non-abelian gauge theories. Then, we will generalize to supersymmetric theories discussing the condition that allows us to preserve some fraction of the global symmetry. We will review the straight line and the circular Wilson loop cases,

focusing on the latter. Then, we will examine the holographic dual of the operator computing the expectation value, in the supergravity approximation, for the circular contour. The last section of this chapter will be devoted to the operator product expansion of the circular Wilson loop.

- Chapter 3: we will introduce dCFTs focusing on a defect version of $\mathcal{N} = 4$, which is the main point of our analysis. We will describe the symmetries preserved by the defect and the boundary conditions on the defect necessary to preserve a fraction of the original supersymmetry. Then, we will investigate the string theory realization of the field configuration. We will study the brane construction that realizes the D3-D5 probe system on which we focus our attention. In the last section we will introduce the double-scaling limit that will allow us to compare weak and strong coupling computations. Moreover, we will review also some results obtained for the one point function of chiral primaries operators in the defect theory.

- Chapter 4: We will consider the circular operator in the set-up described in chapter 3. We will focus on its computation at strong coupling, in the supergravity limit. We will find the solutions to the equation of motions for the minimal surfaces corresponding to the Wilson loop. Then, we will impose the boundary conditions for the fundamental string dual to the circular operator in the presence of a defect. We will analyze the allowed parameter space for the minimal surface and we will focus on the structure of the solution.

- Chapter 5: we will give the perturbative result for the expectation value of the circular Wilson loop. We will compare the perturbative and the strong coupling results thanks to the double-scaling limit. Then, we will focus on the BPS circle enlightening the peculiarity of this particular case. Finally, we will briefly discuss the OPE for the Wilson loop in the limit in which it is placed far away from the defect.

- Chapter 6: we will study the case in which two concentric circular Wilson loops are inserted in the defect theory. We will briefly review the results for the connected string solution between two circles without the defect. Then, we will comment on what we expect when the defect is present. Since the work is currently in progress, we will give only some preliminary comments and insights.

Both chapter 4 and 5 are based on [25]. In the conclusions we will discuss the main results of this thesis and we also suggest further developments and outlooks of our research. Technical aspects are summarized in appendices A, B, C, D, E, F and G.

Chapter 1

The ADS/CFT correspondence

This chapter contains the introductory material to the AdS/CFT conjecture, which is the first attempt to make quantitative the 't Hooft idea of a connection between string and field theory.

1.1 Supersymmetric gauge theories

Symmetries are one of the most important ingredients of theoretical physics and have served as a fundamental guiding principle in the construction of new theories. In particular, a central role among symmetries is played by supersymmetry (SUSY). It leads to massive cancellations between fermionic and bosonic degrees of freedom that allow us to compute analytically many quantities of interest. For this reason, although up to now there exists no-experimental evidence for supersymmetry, it still plays a central role in theoretical physics. For instance, supersymmetric theories have been used to try to understand the phenomenon of confinement in asymptotically free theories, and in a more recent vision they have a pivotal position in the context of the AdS/CFT correspondence.

A generic quantum field theory (QFT) that describes fundamental interactions has to exhibit the following symmetries

- **Poincaré invariance:** the theory is invariant under the Poincaré group which consists of translations, generated by P_μ, and Lorentz transformations, whose generators are $M_{\mu\nu}$. The Lie algebra of the Poincaré group contains $D(D+1)/2$ generators. The following commutation rules complete the specification of the

Lie algebra:

$$\begin{aligned}[M_{\mu\nu}, M_{\rho\sigma}] &= -i(\eta_{\mu\rho}M_{\nu\sigma} + \eta_{\nu\sigma}M_{\mu\rho} - \eta_{\mu\sigma}M_{\nu\rho} - \eta_{\nu\rho}M_{\mu\sigma}) \\ [M_{\mu\nu}, P_{\rho}] &= -i(\eta_{\mu\rho}P_{\nu} - \eta_{\nu\rho}P_{\mu}) \\ [P_{\mu}, P_{\nu}] &= 0\end{aligned} \tag{1.1.1}$$

where $\eta_{\mu\nu} = \text{diag}(-,+,+,+)$ is the metric of four-dimensional Minkowski space.

- **Internal symmetry invariance:** the theory is invariant under the action of a connected Lie group G generated by the T^a, which are Lorentz scalars. They are typically related to conserved quantum numbers like electric charge and isospin. The Lie algebra is given by the commutation relation

$$[T^a, T^b] = if_c^{ab}T^c \tag{1.1.2}$$

  where f_c^{ab} are the structure constants of G.

- **Invariance under discrete symmetries**: the theory is invariant under CPT, namely under the simultaneous charge conjugation (C), parity transformation (P), and temporal inversions (T).

In 1967 Coleman and Mandula [30] provided a theorem which states that in a generic QFT, under certain reasonable assumptions as causality, locality, unitarity, the most general symmetry group enjoyed by the S-matrix is the direct product

$$\text{Poincaré Group} \times \text{internal symmetries}. \tag{1.1.3}$$

Thus, the generators of the Poincaré group must commute with those of the internal group

$$[P_{\mu}, G] = 0 \qquad [M_{\mu\nu}, G] = 0. \tag{1.1.4}$$

The theorem can be bypassed by weakening the assumptions that the symmetry algebra only involves commutators, all generators being bosonic generators. This assumption can be relaxed allowing for fermionic generators which satisfy anti-commutation relations and in this way the set of allowed symmetries can be enlarged. In 1975 Haag, Lopuszanski and Sohnius [31] showed that SUSY is the only possibility to evade the theorem. The Poincaré algebra is extended to what is known as graded Lie algebra or supersymmetry algebra.

1.1.1 Supersymmetry

Supersymmetry is a space-time symmetry mapping bosons into fermions and vice versa. The SUSY generators are the Q^I_α, and $\bar{Q}^I_{\dot{\alpha}}$ are their hermitian conjugate, where $\alpha, \dot{\alpha} = 1, 2$ are space-time spinor indices, and $I = 1, ..., \mathcal{N}$ labels the number of supercharges, which are fermionic generators of spin 1/2. In a four-dimensional supersymmetric field theory the Q^I_α and $\bar{Q}^I_{\dot{\alpha}}$ are $2\mathcal{N}$ anticommuting fermionic generators transforming in the representations $(1/2, 0)$ and $(0, 1/2)$ of the Lorentz group, respectively. In four-component notation they constitute a set of $\mathcal{N}$ Majorana spinors

$$Q^I = \begin{pmatrix} Q^I_\alpha \\ \bar{Q}^{I\dot{\alpha}} \end{pmatrix} \qquad \bar{Q}^I = \left(Q^{I\alpha},\, \bar{Q}^I_{\dot{\alpha}}\right). \tag{1.1.5}$$

These generators act schematically as

$$Q\,|\text{boson}\,\rangle = |\text{fermion}\,\rangle \qquad Q\,|\text{fermion}\,\rangle = |\text{boson}\,\rangle\,, \tag{1.1.6}$$

since Q modifies the spin of a particle and hence its space-time properties, SUSY is not an internal symmetry but a space-time symmetry. If $\mathcal{N} = 1$, there is only a SUSY generator plus its hermitian conjugate, but if $\mathcal{N} > 1$ we have an extended version of SUSY. There is no algebraic reason to have a limit on $\mathcal{N}$, but increasing $\mathcal{N}$ the theory must contain particles of increasing spin. In particular, we require

- $\mathcal{N} \leq 4$ for theories without gravity (spin ≤ 1)

- $\mathcal{N} \leq 8$ for theories with gravity (spin ≤ 2).

The graded Lie algebra contains both fermionic and bosonic generators, which means that both commutators and anti-commutators are included in the pattern with the structure

$$[B, B] = B \qquad [B, F] = F \qquad \{F, F\} = B, \tag{1.1.7}$$

where B stands for a bosonic generator and F for a fermionic one. The resulting general super-Poincaré algebra is given by the relations

$$\begin{aligned}
[P_\mu, Q^I_\alpha] &= 0 \\
[P_\mu, \bar{Q}^I_{\dot\alpha}] &= 0 \\
[M_{\mu\nu}, Q^I_\alpha] &= i(\sigma_{\mu\nu})_\alpha{}^\beta\, Q^I_\beta \\
[M_{\mu\nu}, \bar{Q}^{I\dot\alpha}] &= i(\bar\sigma_{\mu\nu})^{\dot\alpha}{}_{\dot\beta}\, \bar{Q}^{I\dot\beta} \\
\left\{Q^I_\alpha, \bar{Q}^J_{\dot\beta}\right\} &= 2\sigma^\mu{}_{\alpha\dot\beta} P_\mu \delta^{IJ} \\
\left\{Q^I_\alpha, Q^J_\beta\right\} &= \epsilon_{\alpha\beta} Z^{IJ} \qquad\qquad Z^{IJ} = -Z^{JI} \\
\left\{\bar{Q}^I_{\dot\alpha}, \bar{Q}^J_{\dot\beta}\right\} &= \epsilon_{\dot\alpha\dot\beta}\, (Z^{IJ})^*
\end{aligned} \tag{1.1.8}$$

plus the standard commutation relations (1.1.1) and (1.1.2). Here, $\epsilon_{\alpha\beta}$ and $\epsilon_{\dot\alpha\dot\beta}$ are antisymmetric two-index tensors defined as

$$\epsilon_{\alpha\beta} = \epsilon_{\dot\alpha\dot\beta} = \begin{pmatrix} 0 & -1 \\ -1 & 0 \end{pmatrix} \tag{1.1.9}$$

which are used to lower spinorial indices. The matrices σ^μ are given by $(\sigma^\mu)_{\alpha\dot\alpha} = (\mathbb{1}, -\sigma_i)_{\alpha\dot\alpha}$ where the σ_i are the Pauli matrices, and the $\sigma_{\mu\nu}$ are particular combinations of σ_μ and $\bar\sigma_\nu$. The $Z^{IJ} = -Z^{JI}$ are bosonic operators called central charges since they commute with all generators of the full algebra and they are scalars under the Lorentz group.

In the simplest case corresponding to $\mathcal{N} = 1$, there are no indices I, J and there is no possibility of central charges ($Z = 0$). The SUSY algebra is invariant under a global phase rotation of all supercharges Q_α, forming the group $U(1)_R$. When $\mathcal{N} > 1$, the different supercharges may be rotated into one another under the unitary group $U(\mathcal{N})_R$. This automorphism symmetry of the graded algebra is called R-symmetry. The generators Q and $\bar{Q}$ will carry a representation under this internal symmetry group, while the generators of the Poincaré group commutes with them as state the Coleman-Mandula theorem

$$\begin{aligned}
[M_{\mu\nu}, T^a] &= 0 \\
[P_\mu, T^a] &= 0 \\
[Q^I_\alpha, T_a] &= (R_a)^I{}_J Q^J_\alpha \\
[\bar{Q}_{I\,\dot\alpha}, T_a] &= -\bar{Q}_{J\,\dot\alpha} (R_a)^J{}_I,
\end{aligned} \tag{1.1.10}$$

where the matrices $(R_a)^I{}_J$ provide unitary representation of the internal symmetry group, if $\mathcal{N} = 1$ the R_a are just real numbers.

This result is the most general one for a massive theory. In a massless theory, another set of fermionic charges, S^I_α and their conjugates may be present. Moreover, for a massless theory, the central charges Z_{IJ} are zero and thus the anticommutation relations between the Q and the $\bar{Q}$ become simpler.

Representations of SUSY algebra: a particle is an irreducible representation of the Poincaré algebra which is a subalgebra of the SUSY algebra. It follows that any irreducible representation of the supersymmetry algebra is a representation of the Poincaré algebra, which in general will be reducible. This means that instead of single-particle states, we have to deal with (super) multiplets that correspond to a collection of particles. The particles inside a supermultiplet are related by the action of the supersymmetric generators Q^I_α and $\bar{Q}^I_{\dot{\alpha}}$, and have spins that differ by 1/2 as reflected by the commutation relation $[Q, M_{\mu\nu}] \neq 0$. Inside the same supermultiplet we have both fermions and bosons which must have the same mass as stated by the commutation rule $[Q, P_\mu] = 0$. Moreover, a supermultiplet contains an equal number of bosonic and fermionic degrees of freedom.

1.1.2 Conformal symmetry

According to the Coleman-Mandula theorem, one possible bosonic extension of the Poincaré group is to consider also the symmetry under scale transformations. For instance, such symmetry naturally arises in critical systems where there is no length scale in the problem. A theory that shows scale invariance is typically invariant under the bigger group of conformal transformations that enlarges the Poincaré group to the conformal group. There are theories, as Yang-Mills, that are only classically invariant under scale transformations and others which preserve this symmetry also at the quantum level. One can think of UV complete QFT as characterized by a renormalization group (RG) flow from a UV to an IR fixed point both described by conformal field theories (CFTs). Thus, studying CFTs will let us map out the possible endpoints of RG flows and thus understand the space of QFTs. Another essential feature is that in principle, one can solve a CFT without even writing down a Lagrangian since only the knowledge of the spectrum and three-point functions of the theory is needed. Moreover, these theories are fundamental also in the study of the AdS/CFT correspondence, which allows us to explore different aspects of gauge theory and string theory. A conformal transformation is a transformation of coor-

dinates that preserves the angles and leaves the metric $g_{\mu\nu}$ invariant up to a local factor

$$g_{\mu\nu} \to g'_{\mu\nu}(x') = \Omega(x) g_{\mu\nu}(x)\,. \tag{1.1.11}$$

Isometries, that correspond to $\Omega(x) = 1$, are a subset of conformal transformations. When $g_{\mu\nu}$ is the flat space metric, the group of isometries is simply the Poincaré group. Instead, scale transformations correspond to $\Omega(x) = \text{const}$. On a d-dimensional Minkowski flat space, whose metric is $g_{\mu\nu} = \eta_{\mu\nu}$, infinitesimal conformal transformations are defined as the coordinate transformations

$$x^\mu \to x'^\mu = x^\mu + \epsilon^\mu(x), \tag{1.1.12}$$

and the variation of the metric is

$$\delta\eta_{\mu\nu} = -(\partial_\mu \epsilon_\nu + \partial_\nu \epsilon_\mu) + \mathcal{O}(\epsilon^2). \tag{1.1.13}$$

Under the requirement given in (1.1.11) with $\Omega(x) \simeq 1 - \omega(x)$, an infinitesimal conformal transformation has to satisfy the so called conformal Killinq equation

$$\partial_\mu \epsilon_\nu + \partial_\nu \epsilon_\mu = \omega(x)\eta_{\mu\nu}, \tag{1.1.14}$$

where $\mu = 0, ..., d-1$. In dimensions $d > 2$ the equation above has the general solution

$$\epsilon^\mu = \alpha^\mu + m^{[\mu\nu]}x_\nu + \lambda x^\mu + 2(b\cdot x)x^\mu - b^\mu x^2. \tag{1.1.15}$$

Each parameter corresponds to different transfromations:

- a^μ: constant parameter of an infinitesimal translation generated by $P_\mu = -i\partial_\mu$, this class of solutions has $\omega(x) = 0$
- $m^{[\mu\nu]}$: constant antisymmetric tensor that corresponds to infinitesimal Lorentz transformations generated by $M_{\mu\nu} = i\,(x_\mu\partial_\nu - x_\nu\partial_\mu)$.
  For these solutions $\omega(x) = 0$
- λ: constant parameter which corresponds to infinitesimal dilatations with the associated generator $D = -ix^\mu\partial_\mu$, this transformation has $\omega(x) = 2\lambda$
- b^μ: constant vector corresponding to the insfinitesimal special conformal transformations (SCT) generated by $K_\mu = -i\,(2x_\mu x^\nu\partial_\nu - x^2\partial_\mu)$, this type of solution is characterized by $\omega(x) = 4(b\cdot x)$.

The commutation relations defining the algebra are

$$\begin{aligned}
[D, P_\mu] &= iP_\mu \\
[D, K_\mu] &= -iK_\mu \\
[M_{\mu\nu}, K_\rho] &= -i\left(\eta_{\mu\rho}K_\nu - \eta_{\nu\rho}K_\mu\right) \\
[K_\mu, P_\nu] &= 2i\left(\eta_{\mu\nu}D - M_{\mu\nu}\right) \\
[M_{\mu\nu}, M_{\rho\sigma}] &= -i(\eta_{\mu\rho}M_{\nu\sigma} + \eta_{\nu\sigma}M_{\mu\rho} - \eta_{\mu\sigma}M_{\nu\rho} - \eta_{\nu\rho}M_{\mu\sigma}) \\
[M_{\mu\nu}, P_\rho] &= -i(\eta_{\mu\rho}P_\nu - \eta_{\nu\rho}P_\mu) \\
[P_\mu, P_\nu] &= 0 \\
[D, M_{\mu\nu}] &= 0 \\
[D, D] &= 0 \\
[K_\mu, K_\nu] &= 0.
\end{aligned} \tag{1.1.16}$$

The conformal algebra in d dimensions is isomorphic to $SO(1, d+1)$ in euclidean signature or $SO(2, d)$ in Minkowski space, which is also the algebra of Lorentz transformations in $\mathbb{R}^{(2,d)}$ space. The number of generators is

$$\begin{aligned}
&1 \text{ dilatation } + \ d \text{ translations } + \ d \text{ special conformal} + \\
&+\frac{d(d-1)}{2} \text{ Lorentz} = \frac{(d+2)(d+1)}{2}.
\end{aligned} \tag{1.1.17}$$

The $d = 2$ case is a special case since the conformal algebra has infinitely many generators. The conformal group in two dimensions is the set of all analytic maps, which is infinite-dimensional and the conformal algebra corresponds to the Virasoro algebra.

1.1.3 Representation of the conformal group

Mass and Lorentz quantum numbers, corresponding to the Casimirs of the Poincaré group, are usually used to identify particles. In the presence of conformal invariance, the mass operator $P^\mu P_\mu$ does not commute anymore with the other generators, for example, the commutator with D is different from zero. Since mass and energy can be rescaled by applying dilatations, field theories that show conformal symmetry do not have asymptotic states and the entire formalism of S matrix do not make sense. In order to find another way to label the states, we consider a specific representation of the conformal group in which our operators have a well-defined dimension Δ, namely they can be thought as eigenvectors of the dilatation

operator D. To find the action of the generators on the fields, we focus on the stability group, which is the subgroup that leaves the origin invariant [32]. In the case of the conformal group this is spanned by $M_{\mu\nu}$, D and K_μ. The action of D on a generic operator at the origin is

$$[D, \mathcal{O}_\Delta(0)] = i\Delta\mathcal{O}_\Delta(0). \tag{1.1.18}$$

If $\mathcal{O}_\Delta$ is a scalar operator, under the scale transformation $x \to \lambda x$ it transforms as $\mathcal{O}'(x') = \lambda^{-\Delta}\mathcal{O}(x)$. Using the relation $\mathcal{O}_\Delta(x) = e^{-iP\cdot x}\ \mathcal{O}_\Delta(0)\ e^{iP\cdot x}$ together with the conformal algebra one can work out the action of D at a generic point x

$$[D, \mathcal{O}(x)] = i(\Delta + x^\mu\partial_\mu)\mathcal{O}(x). \tag{1.1.19}$$

Notice that using (1.1.18) and the first two commutators in (1.1.16) it is easy to show that P_μ rises the scaling dimension of the operator $\mathcal{O}_\Delta(x)$ while K_μ lowers it

$$\begin{aligned}[D, [P_\mu, \mathcal{O}_\Delta(0)]] &= -\,[\mathcal{O}_\Delta(0), [D, P_\mu]] - [P_\mu, [\mathcal{O}_\Delta(0), D]] \\ &= +\,i(\Delta + 1)\,[P_\mu, \mathcal{O}_\Delta(0)]\end{aligned} \tag{1.1.20}$$

$$\begin{aligned}[D, [K_\mu, \mathcal{O}_\Delta(0)]] &= -\,[\mathcal{O}_\Delta(0), [D, K_\mu]] - [K_\mu, [\mathcal{O}_\Delta(0), D]] \\ &= +\,i(\Delta - 1)\,[K_\mu, \mathcal{O}_\Delta(0)]\ ,\end{aligned} \tag{1.1.21}$$

where we have used the Jacobi identities. Since $M_{\mu\nu}$ commutes with D, it does not modify the dimension of the operator. In unitary CFTs, there is a lower bound on the dimensions of the fields meaning that each representation of the conformal algebra must have some operators of lowest dimension Δ_0, which must be annihilated by K_μ at the origin and which are known as *conformal primaries*. Acting on a primary with P_μ, it is possible to construct an infinite tower of operators with scaling dimension greater than Δ_0 that are called conformal descendants of the primary field. In particular, a conformal primary is defined by the following commutation relations for the stability group

$$\begin{aligned}[D, \mathcal{O}_{\Delta_0}(0)] &= i\Delta_0\mathcal{O}_{\Delta_0}(0) \\ [M_{\mu\nu}, \mathcal{O}_{\Delta_0}(0)] &= iS_{\mu\nu}\mathcal{O}_{\Delta_0}(0) \\ [K_\mu, \mathcal{O}_{\Delta_0}(0)] &= 0,\end{aligned} \tag{1.1.22}$$

where $S_{\mu\nu}$ is a matrix that depends on the Lorentz spin of the field and is zero for scalars.

1.1.4 Correlation functions

Conformal symmetry imposes strong constraints on correlation functions through the Ward identities. The one-point functions are zero. In fact, invariance under translations implies that necessarily one-point functions have to be equal to a constant

$$\langle \phi_\Delta \rangle = c. \tag{1.1.23}$$

Invariance under scale transformations translates under the following condition

$$\langle \phi_\Delta(x) \rangle = \lambda^\Delta \langle \phi_\Delta(\lambda x) \rangle \quad \Rightarrow c = \lambda^\Delta c. \tag{1.1.24}$$

Namely, in a CFT the one-point function of an operator ϕ with scaling dimension Δ is zero unless $\Delta = 0$, which corresponds to consider the identity operator. Two-point functions are completely fixed up to a normalization factor that for scalar fields can be set to 1 in such a way that the correlators between two scalar primaries can be written as

$$\langle \phi_{\Delta_1}(x_1)\phi_{\Delta_2}(x_2) \rangle = \frac{\delta_{\Delta_1,\Delta_2}}{|x_1 - x_2|^{2\Delta}}, \tag{1.1.25}$$

where $\Delta_1 = \Delta_2 \equiv \Delta$ is the condition imposed by invariance under finite SCTs. There are similar results also for non scalar operators as the two-point functions of the current or the stress-tensor. Also the spatial dependence of three-point functions is fully determined by conformal invariance

$$\langle \phi_{\Delta_1}(x_1)\phi_{\Delta_2}(x_2)\phi_{\Delta_3}(x_3) \rangle = \frac{\lambda_{\Delta_1,\Delta_2,\Delta_3}}{|x_{12}|^{\Delta_1+\Delta_2-\Delta_3}\,|x_{13}|^{\Delta_1+\Delta_3-\Delta_2}\,|x_{23}|^{\Delta_2+\Delta_3-\Delta_1}}, \tag{1.1.26}$$

where $x_{ij} = x_i - x_j$ and $\lambda_{\Delta_1,\Delta_2,\Delta_3}$ are constant free parameters. This expression for three-point correlators is obtained using the same normalization choosen in (1.1.25). Coordinate dependence of higer-point functions is not completely fixed by conformal invariance since they depend on conformally invariant cross-ratios which are combinations of the x_i. The number of these factors increase as

$$\frac{n(n-3)}{2}, \tag{1.1.27}$$

where n is the number of the fields in the correlators. For instance, if we consider four-point functions we can construct two different cross-ratios while they are not present when $n = 2, 3$. A significant feature of CFT is that it is possible to determine the cross-ratios only in terms of the parameter $\lambda_{\Delta_1,\Delta_2,\Delta_3}$, the dimension of the

primary operators and quantities called conformal blocks which are fully determined by conformal invariance. This is a consequence of the operator product expansion (OPE) that allows expressing the product of two operators close to each other in terms of local operators at the middle point. Respect to QFT in which the OPE is used only in the asymptotic short-distance limit, in a CFT the OPE gives a convergent series expansion at finite point separation between the operators. The OPE can be schematically written as

$$\phi_{\Delta_1}(x)\phi_{\Delta_2}(0) = \sum_{primaries\ \phi} \mathcal{C}(x)\phi_{\Delta}(0)\,, \tag{1.1.28}$$

where $\mathcal{C}(x)$ are numerical coefficients. Thus, the remarkable fact is that in a CFT, any n-point correlation function can be expressed in terms of conformal dimensions and structure constants, that are called CFT data, using the OPE iteratively.

1.1.5 Superconformal symmetry

If a theory happens to be both supersymmetric and conformal, we can combine the two symmetries in the superconformal invariance. Using the Jacobi identity involving P, D and Q one can notice that to ensure the closure of the algebra it is necessary to introduce other spinorial generators denoted by S^I_α and $\bar{S}^I_{\dot\alpha}$ that are called special conformal supercharges. These are the fermionic superpartners of K_μ and play the same role of Q^I_α and $\bar{Q}^I_{\dot\alpha}$ for P_μ. The superconformal group in four dimensions is $SU(2,2\,|\,\mathcal{N})$ and corresponds to a conformal theory with the addition of $\mathcal{N}$ supercharges Q_α, $\mathcal{N}$ superconformal charges S_α and of the generators of a $U(\mathcal{N})_R$ global symmetry. Some of the relevant commutation relations are

$$\begin{aligned}
\left[D, Q^I_\alpha\right] &= \frac{i}{2}Q^I_\alpha & \left[D, \bar{Q}^I_{\dot\alpha}\right] &= \frac{i}{2}\bar{Q}^I_{\dot\alpha}\\
\left[K^\mu, Q^I_\alpha\right] &= 2i\sigma^\mu_{\alpha\dot\beta}\bar{S}^{I\dot\beta} & \left[K^\mu, \bar{Q}^{I\dot\alpha}\right] &= 2i\bar{\sigma}^{\mu\dot\alpha\beta}S^I_\beta\\
\left[D, S^I_\alpha\right] &= -\frac{i}{2}S^I_\alpha & \left[D, \bar{S}^I_{\dot\alpha}\right] &= -\frac{i}{2}\bar{S}^I_{\dot\alpha}\\
\left[P^\mu, S^I_\alpha\right] &= \sigma^\mu_{\alpha\dot\beta}\bar{Q}^{I\dot\beta} & \left[P^\mu, \bar{S}^{I\dot\alpha}\right] &= \bar{\sigma}^{\mu\dot\alpha\beta}Q^I_\beta\\
\left[K^\mu, S^I_\alpha\right] &= 0 & \left[K^\mu, \bar{S}^I_{\dot\alpha}\right] &= 0\\
\left[M_{\mu\nu}, S^I_\alpha\right] &= i(\sigma_{\mu\nu})_\alpha{}^\beta\, S^I_\beta & \left[M_{\mu\nu}, \bar{S}^{I\dot\alpha}\right] &= i(\bar{\sigma}_{\mu\nu})^{\dot\alpha}{}_{\dot\beta}\,\bar{S}^{I\dot\beta}\\
\left\{S^I_\alpha, S^J_\beta\right\} &= 0 & \left\{\bar{S}^I_{\dot\alpha}, \bar{S}^J_{\dot\beta}\right\} &= 0\\
\left\{S^I_\alpha, \bar{S}^J_{\dot\alpha}\right\} &= 2\sigma^\mu_{\alpha\dot\alpha}K_\mu\delta^{IJ}. &&
\end{aligned} \tag{1.1.29}$$

The other relations involving Q, S and T are given by

$$\begin{aligned}
\left\{Q^I_\alpha, S_{\beta J}\right\} &= \epsilon_{\alpha\beta}\left(\delta^I{}_J D + T^I_J\right) + \frac{1}{2}\delta^I{}_J(\sigma^{\mu\nu})^\gamma_\alpha \epsilon_{\gamma\beta}\, M_{\mu\nu} \\
\left\{\bar{Q}^I_{\dot\alpha}, \bar{S}_{\dot\beta J}\right\} &= \epsilon_{\dot\alpha\dot\beta}\left(\delta^I{}_J D + T^I_J\right) + \frac{1}{2}\delta^I{}_J \epsilon_{\dot\alpha\dot\gamma}(\bar\sigma^{\mu\nu})^{\dot\gamma}_{\dot\beta}\, M_{\mu\nu} \\
\left[\bar{S}^I_{\dot\alpha}, T_a\right] &= (R_a)^I{}_J \bar{S}^J_{\dot\alpha} & \left[S^I_\alpha, T_a\right] &= -(R_a)^I{}_J S^J_\alpha \\
[Q^I_\alpha, T_a] &= (R_a)^I{}_J Q^J_\alpha & [\bar{Q}_{I\,\dot\alpha}, T_a] &= -\bar{Q}_{J\,\dot\alpha}(R_a)^J{}_I \\
\left[Q^I_\alpha, T\right] &= -i\left(\frac{4-\mathcal{N}}{4\mathcal{N}}\right) Q^I_\alpha & \left[\bar{Q}^I_{\dot\alpha}, T\right] &= i\left(\frac{4-\mathcal{N}}{4\mathcal{N}}\right) \bar{Q}^I_{\dot\alpha} \\
\left[S^I_\alpha, T\right] &= i\left(\frac{4-\mathcal{N}}{4\mathcal{N}}\right) S^I_\alpha & \left[\bar{S}^I_{\dot\alpha}, T\right] &= -i\left(\frac{4-\mathcal{N}}{4\mathcal{N}}\right) \bar{S}^I_{\dot\alpha}\,,
\end{aligned} \tag{1.1.30}$$

where T^I_J are the generators associated to R-symmetry transformations ($I, J = 1, ..., \mathcal{N}$) which are now part of the algebra and do not act just as external automorphisms since they appear in the anti-commutator of the supersymmetry charges with the S^I_α. The operator T in these relations is the generator of the $U(1)_R$ factor of the R-symmetry group

$$U(N)_R = SU(N)_R \times U(1)_R \tag{1.1.31}$$

while T_a generates $SU(\mathcal{N})_R$. The $\mathcal{N} = 4$ case is special because T commutes with all the generators of the superconformal group. Thus, T has the same action on all the states of the same supermultiplet and the R-symmetry group for the $\mathcal{N} = 4$ case is $SU(4)$ instead of $U(4)$ as would be expected from general cases. Following this argument, the superconformal group of $\mathcal{N} = 4$ theory in four dimensions is $PSU(2, 2\,|\,4)$.

1.1.6 Representation of the superconformal algebra

Previously, we have defined a conformal primary as an operator that is at the base of an infinite tower of descendants, generated by the multiple action of the translation generator P_μ, and that is annihilated by K_μ at the origin. If the theory in addition to conformal invariance also exhibits supersymmetry, we can introduce *superconformal primary operators*. These operators are a subsector of conformal primaries and are defined by the relations

$$\left[S^I_\alpha, \mathcal{O}_{\Delta_0}(0)\right] = 0 \qquad \left[\bar{S}^I_{\dot\alpha}, \mathcal{O}_{\Delta_0}(0)\right] = 0. \tag{1.1.32}$$

From the superconformal algebra, one can easily realize that the operator S and its conjugate $\bar{S}$ lower the scaling dimension of $1/2$, while Q and $\bar{Q}$ increase it of $1/2$. Thus, the action of the Poincaré supercharges on a superconformal primary generates all the other states of the multiplet called *superconformal descendants*, which in turn are conformal primaries. Superconformal primary operators are always conformal primaries, but the vice versa is not true in general, and it may be that a primary is not a superconformal primary. Since the conformal algebra is a subalgebra of the superconformal algebra, representations of the latter split into several representations of the former. The superconformal algebra contains a set of special representations, called *short representations*, that are those constructed starting from a *chiral primary operator* Φ which is not only annihilated by $S, \bar{S}$ and K_μ, but also by some of the Q's. Since $\left[Q^I_\alpha, \Phi(0)\right] = 0$ for some $I = 1, ..., \mathcal{N}$, chiral primaries are BPS operators that do not receive quantum corrections to their scaling dimension Δ. A chiral primary satisfies the relation

$$\text{chiral primary } \Phi: \quad [\{Q', S\}, \Phi(0)] = 0\,, \tag{1.1.33}$$

where Q' stands for a subgroup of the Poincaré supercharges. Using Jacobi identities, the above relation implies that the conformal dimension is fixed in terms of the Lorentz and R-symmetry quantum numbers and in a unitarity representation, Δ is bounded from below by them.

1.1.7 $\mathcal{N} = 4$ Super Yang-Mills Theory

The $\mathcal{N} = 4$ SYM theory is a superconformal field theory (SCFT) with the maximal amount of rigid supersymmetry in four dimensions, namely sixteen real Poincarè supercharges. Any other four-dimensional gauge theory with $\mathcal{N} > 4$ would have to contain particles with spin bigger than one and would hence not be renormalizable. A convenient approach to derive the action of $\mathcal{N} = 4$ SYM theory is given by considering the dimensional reduction of the ten-dimensional $\mathcal{N} = 1$ SYM theory to four dimensions [33, 34]. The ten-dimensional gauge theory is the low energy effective theory coming from type I superstring theory. It consists in a vector multiplet that contains a gauge field A_M and a ten-dimensional Majorana-Weyl spinor Ψ with 16 real components. The gauge group is $SU(N)$, and all fields take values in the Lie algebra $\mathfrak{su}(N)$

$$A_M = A^a_M T^a \qquad\qquad \Psi = \Psi^a T^a\,. \tag{1.1.34}$$

The generators T^a are a basis of the Lie algebra and they satisfy the normalization condition $\mathrm{Tr}(T^a T^b) = \frac{1}{2}\delta^{ab}$. The action of $\mathcal{N}=1$ SYM theory in ten dimensions is

$$S_{\mathcal{N}=1} = -\frac{1}{g_{10}^2}\int d^{10}x\ \mathrm{Tr}\left(\frac{1}{2}F_{MN}F^{MN} - i\bar{\Psi}\Gamma_M D^M\Psi\right), \tag{1.1.35}$$

where $M,N = 0,....,9$ and Γ^M are ten dimensional Dirac matrices that obey the Clifford algebra for $\mathbb{R}^{(1,9)}$

$$\left\{\Gamma^M,\Gamma^N\right\} = -2\eta^{MN}\mathbb{1}\,, \tag{1.1.36}$$

where we are using the mostly positive flat metric $\eta^{MN} = \mathrm{diag}(-,+,...,+)$. The fields have classical mass dimensions $[A_M] = 1$ and $[\Psi] = 3/2$ whereas the ten dimensional Yang–Mills coupling constant has mass dimension $[g_{10}] = 3$. The non-abelian field strenght and the covariant derivative are given by

$$\begin{aligned} F_{MN} &= \partial_M A_N - \partial_N A_M - i\,[A_M, A_N] \\ D_M &= \partial_M - i\,[A_M,\quad]\,. \end{aligned} \tag{1.1.37}$$

The action (1.1.35) is gauge invariant and since the fields transform in the adjoint of $SU(N)$ the gauge transformations are

$$A_M \to U(x)A_M U(x)^\dagger - i\partial_M U(x)U(x)^\dagger \qquad \Psi(x)\to U(x)\Psi U(x)^\dagger, \tag{1.1.38}$$

where $U(x)$ is an element of $SU(N)$. Moreover, the action is also invariant under the following supersymmetry transformations

$$\begin{aligned} \delta_\epsilon A_M &= i\,\bar{\epsilon}\,\Gamma_M\Psi \\ \delta_\epsilon\Psi &= \frac{1}{2}F_{MN}\Gamma^{MN}\epsilon, \end{aligned} \tag{1.1.39}$$

where $\Gamma_{MN} = \frac{1}{2}\,[\Gamma_M,\Gamma_N]$ and ϵ, the supersymmetry parameter, is a ten-dimensional constant Majorana-Weyl spinor. The dimensional reduction to four dimensions is obtained by demanding that the fields only depend on the coordinates $x^\mu \in \mathbb{R}^{(1,3)}$. The remaining volume integrals in the action, $V = \int dx^4...dx^9$, are absorbed in a redefinition of the coupling constant that becomes dimensionless

$$g_{YM} = V^{-\frac{1}{2}}\,g_{10}. \tag{1.1.40}$$

If we consider the ten-dimensional gauge field, it can be decomposed into a four-dimensional gauge field A_μ and into the fields

$$\phi_i = A_{i+3} \qquad i = 1,2,..,6 \tag{1.1.41}$$

which are the last six components of A_M. The indipendence of the fields on the coordinates x^I, where $I = 4, ..., 9$, implies for the element of the gauge group

$$\partial_I U(x) = 0, \tag{1.1.42}$$

which means that also the gauge transformations depends only on the first four coordinates. Thus, it is easy to see that the fields ϕ_i are scalars under the four-dimensional Lorentz group $\mathbb{R}^{(1,3)}$ and transform in the adjoint of $SU(N)$ as

$$\phi_i \to U(x)\phi_i\, U(x)^\dagger. \tag{1.1.43}$$

Using the decomposition of A_M, it is straightforward to work out the components $F_{\mu,i+3}$ and$F_{i+3,j+3}$

$$F_{\mu,i+3} = \partial_\mu \phi_i - i\left[A_\mu, \phi_i\right] = D_\mu \phi_i \qquad F_{i+3,j+3} = -i\left[\phi_i, \phi_j\right]. \tag{1.1.44}$$

Thus, the F^2 term in the action (1.1.35) reads

$$-\frac{1}{2}\mathrm{Tr}\left(F_{MN}F^{MN}\right) = -\mathrm{Tr}\left(\frac{1}{2}F_{\mu\nu}F^{\mu\nu} + D_\mu\phi_i D^\mu\phi^i - \frac{1}{2}\left[\phi_i, \phi_j\right]\left[\phi^i, \phi^j\right]\right) \tag{1.1.45}$$

To reduce the fermionic kinetic part it is necessary to choose an appropriate representation of the ten-dimensional Clifford algebra, which discriminates naturally between the four and six-dimensional spinor indices. The details of the dimensional reduction are related to a particular choice of the representation of gamma matrices. We can leave them out using the ten-dimensional compact notation to deal with the fermionic part of the $\mathcal{N} = 4$ action. The four-dimensional theory has a unique multiplet that in components read

$$\mathcal{V}_{\mathcal{N}=4} = \left(A_\mu,\ \lambda^{\alpha=1,2}_{a=1,..,4},\ \phi_{i=1,..,6}\right), \tag{1.1.46}$$

where as explained before A_μ is the four-dimensional spin one gauge boson and ϕ_i are the six real scalars. The λ^α_a are four Weyl spinors that can be recast in the ten-dimensional Majorana-Weyl spinor Ψ of the $\mathcal{N} = 1$ theory. Thus, the action of the $\mathcal{N} = 4$ SYM theory in four dimensions is given by

$$\begin{aligned} S_{\mathcal{N}=4} = -\frac{1}{g^2_{YM}}\int d^4x\ \mathrm{Tr}\Big(&\frac{1}{2}F_{\mu\nu}F^{\mu\nu} + D_\mu\phi_i D^\mu\phi^i - \frac{1}{2}\left[\phi^i, \phi^j\right]^2 + \\ &-i\bar{\Psi}D_\mu\Gamma^\mu\Psi - \bar{\Psi}\Gamma^i\left[\phi_i, \Psi\right]\Big). \end{aligned} \tag{1.1.47}$$

Here the Γ are the ten dimensional Dirac matrices. The supersymmetry transformations under which the action is invariant are

$$\begin{aligned}\delta_\epsilon A_\mu &= i\bar{\epsilon}\,\Gamma_\mu\Psi \\ \delta_\epsilon \phi_i &= i\bar{\epsilon}\,\Gamma_i\Psi \\ \delta_\epsilon \Psi &= \frac{1}{2}F_{\mu\nu}\Gamma^{\mu\nu}\epsilon + D_\mu\phi_i\Gamma^{\mu i}\epsilon - \frac{i}{2}\left[\phi_i,\phi_j\right]\Gamma^{ij}\epsilon.\end{aligned} \tag{1.1.48}$$

Symmetries: performing the ten-dimensional reduction á la Kaluza–Klein on a six-dimensional torus T^6, the ten-dimensional Lorentz group breaks as follows

$$SO(1,9) \to SO(1,3) \times SO(6)_R, \tag{1.1.49}$$

where $SO(1,3)$ is the four-dimensional Lorentz group and $SO(6)_R \simeq SU(4)_R$ is the internal global R-symmetry group of the $\mathcal{N}=4$ theory. Under the R-symmetry group

- A_μ is a singlet of $SU(4)_R$
- ϕ_i transforms in the fundamental of $SO(6)_R$, but it can be rewritten as an antisymmetric tensor $\phi_{[ab]}$ in the **6** dimensional representation of $SU(4)_R$, where $a,b=1,..,4$
- λ_a^α transform in the fundamental representation of $SU(4)_R$, a is the R-symmetry index and α is the spinorial index of the $SL(2,\mathbb{C})$ universal cover of the Lorentz group.

The $\mathcal{N}=4$ action inherits the invariance under the supersymmetry transformations (1.1.16) of the ten-dimensional theory. Apart from Poincaré supersymmetry, the action (1.1.47) contains no dimensional parameters and is classically invariant under the scale transformations

$$x \to c\,x \qquad A \to c^{-1}\,A \qquad \phi \to c^{-1}\,\phi \qquad \Psi \to c^{-3/2}\,\Psi. \tag{1.1.50}$$

Thus, scale invariance and Poincaré invariance combine into conformal symmetry, forming the group $SO(2,4) \sim SU(2,2)$. Furthermore, the combination of $\mathcal{N}=4$ Poincaré supersymmetry and conformal invariance produces an even larger superconformal symmetry given by the supergroup $PSU(2,2|4)$, as explained in the previous section.

The conformal symmetry of a theory can be broken at the quantum level by the introduction of a renormalization scale μ that breaks scale invariance. The observables of the theory become scale-dependent through the dependence on μ of the parameters of the theory. In the $\mathcal{N}=4$ theory, fixing the rank of the gauge group N, the only independent parameter is the coupling constant g_{YM} which scale dependence is described by the β function

$$\beta = \mu \frac{dg_{YM}}{d\mu}. \tag{1.1.51}$$

Using superspace argument, the β function of $\mathcal{N}=4$ SYM theory was shown to be zero up to three loops [35–37]. Subsequently, it was argued that $\beta(g_{YM})$ it is zero also to all loop orders using the light-cone gauge [38, 39]. It is easy to see that the $\beta(g_{YM})$ it is zero at one loop using the formula [40]

$$\beta^{(1)}(g_{YM}) = -\frac{g_{YM}^3}{16\pi^2}\left(\frac{11}{3}C(A) - \frac{1}{6}\sum_k C(\text{scalar}) - \frac{2}{3}\sum_l C(\text{Weyl})\right), \tag{1.1.52}$$

where C denotes the quadratic Casimir of the representation of gauge fields, scalars, and fermions. Since all the fields transform in the adjoint representation of $SU(N)$, all the Casimir are equal to N, and fermions and scalars balance the contribution of the gauge fields in such a way that $\beta^{(1)}(g_{YM}) = 0$. Thus, $\mathcal{N}=4$ SYM is a superconformal theory also at the quantum level and it is a UV finite theory. Since g_{YM} does not run, the theory can be described by two freely tunable parameters: the coupling constant and the parameter N. These two parameters can be combined giving the 't Hooft coupling constant

$$\lambda = g_{YM}^2 N. \tag{1.1.53}$$

Furthermore, the theory exhbits an exact non-perturbative $SL(2,\mathbb{Z})$ duality, that interchanges electric and magnetic fields and charges. This invariance is expressed combining the theta-angle and the coupling constant to form the complex parameter

$$\tau \equiv \frac{\theta_i}{2\pi} + \frac{4\pi i}{g_{YM}^2}. \tag{1.1.54}$$

The quantum theory is invariant under $\theta_i \to \theta_i + 2\pi$, or $\tau \to \tau + 1$. The Montonen-Olive conjecture [41] states that the quantum theory is also invariant under the transformation $\tau \to -\frac{1}{\tau}$. The combination of both symmetries yields the S-duality group $SL(2,\mathbb{Z})$ generated by

$$\tau \to \frac{a\tau + b}{c\tau + d} \qquad \text{with} \quad ad - bc = 1, \quad a,\, b,\, c,\, d \in \mathbb{Z}. \tag{1.1.55}$$

Notice that when the theta angle vanishes the S duality corresponds to send g_{YM} in $1/g_{YM}$, namely to a weak/strong coupling exchange. Since this additional symmetry changes the electric degrees of freedom with the magnetic ones, it maps the Wilson loop, that describes an electric charge moving on a closed contour, in the 't Hooft loop that instead describes a monopole passing trough the same path. In the perspective of the Maldacena correspondence that we will describe later, the S-duality has a natural manifestation on the string side. In fact, type IIB superstring theory on a curved background is conjectured to have an identical $SL(2,\mathbb{Z})$ self-duality symmetry that exchanges the fundamental strings with D1-strings, D5-branes with NS5- branes and take the D3-branes into themselves.

Dynamical phase: To determine the moduli space of vacua of $\mathcal{N}=4$ theory we study the potential

$$\frac{1}{2g_{YM}^2}\int d^4x\,\mathrm{Tr}\left([\phi_i,\phi_j]^2\right). \tag{1.1.56}$$

The supersymmetric ground state of the theory corresponds to minimize the potential, namely to the condition

$$[\phi_i,\phi_j]=0 \qquad i,j=1,...,6. \tag{1.1.57}$$

There are two different classes of solutions to this equation:

- $\langle\phi_i\rangle=0$ for all $i=1,...,6$, this corresponds to the *superconformal phase*. The gauge symmetry and the superconformal group $PSU(2,2|4)$ are unbroken.
- At least one of the $\langle\phi_i\rangle$ is different from zero, this corresponds to the *Coulomb phase*. Conformal invariance is broken since the expectation value of the scalar field sets naturally a scale, and also the gauge symmetry may generically be broken to $U(1)^r$, where r is the rank of the gauge algebra.

Superconformal chiral primaries: In $\mathcal{N}=4$ SYM theory an important role is played by the single trace operators involving only scalars

$$\mathrm{Str}\left(\phi^{\{i_1}\phi^{i_2}...\phi^{i_n\}}\right)(x), \tag{1.1.58}$$

where "Str" denotes the symmetrized trace over the gauge algebra ensuring that the above operators are totally symmetric in the $SO(6)$ R-indices i_j. The curly brackets between the field indices indicate that all traces over $SO(6)$ are removed so that

they transform under an irreducible representation of the superconformal algebra $PSU(2,2\,|\,4)$. The operators (1.1.58) are superconformal chiral primary operators (CPOs) and one-half BPS states of the superconformal algebra. A simple example is given by the single trace operator with scaling simension $\Delta = 2$

$$\mathrm{Str}\left(\phi^{\{i}\,\phi^{j\}}\right) = \mathrm{Tr}\left(\phi^i\phi^j\right) - \frac{1}{6}\delta^{ij}\mathrm{Tr}\left(\phi^k\phi^k\right). \tag{1.1.59}$$

Since this is a protected operator, it does not receive an anomalous dimension. On the other hand the operator

$$\mathrm{Tr}\left(\phi^i\phi^i\right) \tag{1.1.60}$$

that is called *Konishi operator* is unprotected and acquires quantum corrections. The unitary representations of the superconformal algebra $PSU(2,2\,|\,4)$ are labelled by the quantum numbers of the maximal bosonic subalgebra

$$\begin{array}{cccc} SO(1,3) & \times SO(1,1) & \times SU(4)_R, \\ (s_+,s_-) & \Delta & [r_1,r_2,r_3] \end{array} \tag{1.1.61}$$

where $s_\pm$ are the spin quantum numbers for the Lorentz group. $SO(1,1)$ is the dilatations group whose representations are classified by Δ and $[r_1,r_2,r_3]$ are Dinkin labels for the R-symmetry group and

$$\dim([0,k,0]) = \frac{1}{12}(k+1)(k+2)^2(k+3). \tag{1.1.62}$$

The operator in (1.1.59) is characterized by $\dim([0,2,0]) = 20$ and it is known as the $20'$ chiral primary operator.

1.2 'T Hooft expansion of gauge theories and string theory

T'Hooft was the first who proposed the study of non-abelian gauge theories with gauge group $SU(N)$ in the limit in which the number of colors N was very large, namely $N \to \infty$. The Yang-Mills theory has two independent parameters, as we said in the previous section, that can be combined to form the t'Hooft coupling constant $\lambda = g_{YM}^2 N$. The 't Hooft expansion corresponds to keep λ fixed and performing an expansion of the observables in power of N. It turns out that different powers of N correspond to different topologies for the Feynman diagrams. This fact becomes

more clear by adopting the double line notation for both the gauge propagator and the vertices. Each gauge propagator carries a factor of $\frac{\lambda}{N}$ while each vertex gives a $\frac{N}{\lambda}$ contribution. Moreover, every loop in the diagram contributes to a power of N.

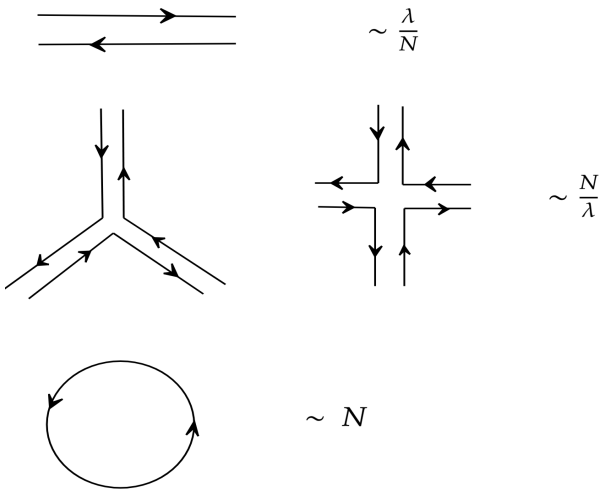

A diagram with no external legs, which thus contributes to the vacuum energy, with V vertices, E propagators and F loops gets a factor

$$D \sim \left(\frac{\lambda}{N}\right)^E \left(\frac{N}{\lambda}\right)^V N^F = N^{F-E+V}\, \lambda^{E-V} \tag{1.2.1}$$

Every Feynman diagram of this type, in the double line notation, can be associated with a closed surface with V vertices, F faces, and E edges. Thus, we can introduce the Euler characteristic

$$\chi = F - E + V \tag{1.2.2}$$

that only depends on the topology of the surface. For a closed surface, χ is connected to the genus h in the following way

$$\chi = 2 - 2h, \tag{1.2.3}$$

where h counts the number of holes of a closed surface. For instance, a sphere has $h = 0$ while for a torus $h = 1$. A further distinction between the type of diagrams can be made considering those which can be drawn on a plane without crossing any lines, which are called *planar diagrams*, and those, the *non-planar*, for which this is not possible. The planar diagrams correspond to $h = 0$ and contribute as $N^2\lambda^n$, where the power n depends on the specific diagram considered. The free energy can

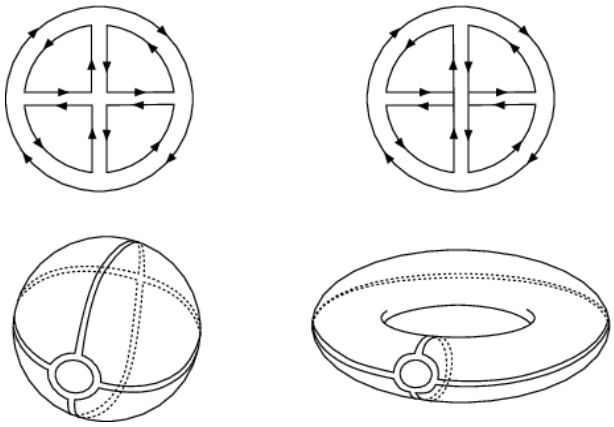

Figure 1.1: Two vacuum diagrams for a $U(N)$ theory. In the first line, we have the Feynman diagrams drawn with the double line notation, while in the second there are the corresponding closed surfaces. The first diagram corresponds to a planar diagram while the second is a non-planar example.

be written as an expansion in powers of $1/N$

$$F = \sum_{h=0}^{\infty} N^{2-2h} f_h(\lambda), \tag{1.2.4}$$

where $f_h(\lambda)$ is the sum of Feynman diagrams that can be drawn on a surface of genus h. From this formula, it is clear that the dominant diagrams in the large N expansion are those with $h = 0$. For this reason, the large N limit is also called the planar limit of the gauge theory.

A topological expansion of this kind can also be done in the context of closed oriented string theory. The worldsheet for interacting strings is just a two-dimensional surface with holes and boundaries. More holes are present on the worldsheet, and higher is the corresponding loop order in perturbation theory. Thus, the genus of the surface is just the number of string loops and string perturbation theory can be taught as an expansion of the type

$$\mathcal{A} = \sum_{h=0}^{\infty} g_s^{2h-2} F_h(\alpha'), \tag{1.2.5}$$

where g_s is the string coupling constant, α' is the square of the string length l_s and $\mathcal{A}$ is some string amplitude. Now it is quite evident that expression (1.2.4) and (1.2.5) can be identified if one sets

$$g_s \sim \frac{1}{N}. \tag{1.2.6}$$

Therefore, the large N expansion in gauge theory corresponds to a weak coupling expansion in g_s. The above procedure is not enough to be a proof because it is based on perturbative analysis on which we cannot have full control. It gives no direct information about the string theory that corresponds to a given gauge theory. Regardless, it represents an important argument in support of the existence of a gauge theory/strings duality. As we will see in the next sections, the AdS/CFT conjecture is a concrete realization of such a duality.

1.3 The $AdS_5 \times S^5$ correspondence

The AdS/CFT correspondence [3–5, 42], also referred to as gauge/gravity duality, is one of the most remarkable achievements of string theory in the last decade. The duality has its foundations on the holographic principle that argues that the information stored in a d-dimensional volume can be encoded in its boundary area. This idea arises from the study of black holes thermodynamics [43, 44]. In particular, the Bekenstein bound fixes the maximal amount of entropy in a volume to be proportional to the area $S_{max} = A/(4G_N)$, where A is measured in Planck units, and G_N is the Newton constant. If the gravity theory lives in d dimensions, the entropy is proportional to A_d, which in turn is the same as a volume in $d-1$ dimensions. Moreover, since the entropy is an extensive quantity, if we have a QFT in $d-1$ dimensions, it results that $S_{QFT} \propto V_{d-1}$. Thus, a theory of gravity has the same entropy of a QFT which lives in a less dimensional space. This is what also happens for a hologram in which the information on a 3d object is encoded in a 2d picture. The main message coming from the holographic principle is that a QFT on flat space-time can be viewed as a theory of gravity. One of the principal advantages of the duality is that strongly-coupled QFT can be investigated by studying classical gravitational theory. Thus, the correspondence represents the first attempt to make quantitative the idea formulated by 't Hooft. The AdS/CFT conjecture is a concrete realization of the holographic principle. It is founded on a duality map between ordinary QFTs and higher-dimensional models of gravity and strings on anti-De Sitter (AdS) background. The correspondence has profound consequences that go far beyond string theory. It finds applications in a lot of different domains as condensed matter physics, the study of non-equilibrium systems, the analysis of the strong coupling dynamics of QCD, the physics of black holes, and many other topics. The most established example of this correspondence is the

duality that connects $\mathcal{N} = 4$ SYM theory in four dimensions and type IIB string theory on $AdS_5 \times S^5$, where AdS_5 stands for a five-dimensional AdS space and S^5 is a five sphere. After that, many other examples of gauge/gravity dualities have been discovered and inspected as the duality between 3d superconformal field theories and string/M-theory.

1.3.1 AdS space

AdS space- time is of central importance for gauge/gravity duality. Therefore, we study Anti-de Sitter space-time in detail. AdS_{d+1} spaces are maximally symmetric solutions of Einstein's equations in $d+1$ dimensions with negative cosmological constant Λ and the same curvature everywhere. From

$$\begin{aligned} S_{EH} =& \frac{1}{16\pi G_N} \int d^{d+1}x \sqrt{-g}\,(R - 2\Lambda) \\ & R_{\mu\nu} - \frac{1}{2} g_{\mu\nu} R = -\Lambda g_{\mu\nu}, \end{aligned} \tag{1.3.1}$$

where G_N is the Newton constant and L is the AdS radius, we have that for AdS_{d+1} spaces

$$\Lambda = -\frac{d(d-1)}{2\,L^2} \quad \Rightarrow \quad R = -\frac{d(d+1)}{L^2}. \tag{1.3.2}$$

Moreover, since the Ricci tensor is proportional to the metric

$$R_{\mu\nu} = -\frac{d}{L^2}\, g_{\mu\nu} \tag{1.3.3}$$

this solution is an Einstein space. In Euclidean signature, the maximally symmetric solution with positive curvature is the sphere S^{d+1} with isometry group $SO(d+2)$ and the one with negative curvature is the hyperboloid H^{d+1} with isometry group $SO(1, d+1)$. In Minkowskian signature, the maximally symmetric solution with $\Lambda > 0$ is called de-Sitter space (dS) and the one with $\Lambda < 0$ is called Anti-de-Sitter (AdS). All of these spaces can be realized as the set of solutions of a quadratic equation in a $(d+2)$-dimensional flat space. If we consider a flat space with signature $\mathbb{R}^{2,d}$ which line element is

$$ds^2 = -du^2 - dv^2 + \sum_{i=1}^{d} dx_i^2, \tag{1.3.4}$$

AdS_{d+1} spaces are hyperboloids defined by the equation

$$u^2 + v^2 - \sum_{i=1}^{d} x_i^2 = -L^2. \tag{1.3.5}$$

From this definition, it is clear that the isometry group of AdS_{d+1} space is $SO(2,d)$. These considerations will be useful when we will explote the AdS/CFT correspondence considering the matching of the symmetries.
There are different set of coordinates that can be employed to parametrize AdS_{d+1}. For example, we may use the *global coordinates* defined as

$$\begin{aligned} u &= L\cosh\rho\cos\tau \\ v &= L\cosh\rho\sin\tau \\ x_i &= L\,\omega_i\sinh\rho \qquad i=1,2,...d\,, \end{aligned} \tag{1.3.6}$$

where $\sum_{i=1}^{d}\omega_i^2 = 1$ are the angular coordinates on the S^{d-1} sphere. The range of variation of the other coordinates is: $\rho\in\mathbb{R}^+$ and $\tau\in[0,2\pi]$. The name global is due to the fact that they cover the Minkowskian hyperboloid once and the line element is

$$ds^2 = L^2\left(-\cosh^2\rho\,d\tau^2 + d\rho^2 + \sinh^2\rho\,d\Omega_{d-1}^2\right). \tag{1.3.7}$$

Since the time coordinate τ is periodic, the AdS space is not simply connected because there are closed timelike curves that cannot be shrinked to a point, otherwise the manifold will be no well causal behaved. This problem can be avoided unwrapping the timelike circle, namely by taking $\tau\in\mathbb{R}$. This corresponds to consider the universal covering space to which we will refer with *global AdS*. Only time translations and rotations on the sphere, $SO(2)\times SO(d)$, are manifest in this parametrization and constitute a compact subgroup of the full isometry group $SO(2,d)$.
We can solve equation (1.3.5) also by considering the *Poincarè coordinates* that correspond to the following parametrization for the hyperboloid coordinates

$$\begin{aligned} u &= \frac{1}{2r}\left(1+r^2\left(L^2+\vec{y}^2-t^2\right)\right) \\ v &= L\,r\,t \\ x_j &= L\,r\,y_j \\ x_d &= \frac{1}{2r}\left(1-r^2\left(L^2-\vec{y}^2+t^2\right)\right), \end{aligned} \tag{1.3.8}$$

where $j=1,...,d-1$, $t\in\mathbb{R}$, $r>0$ and $\vec{y}\in\mathbb{R}^{d-1}$. The corresponding line element is

$$ds^2 = L^2\left(\frac{dr^2}{r^2} + r^2\left(-dt^2+d\vec{y}^2\right)\right). \tag{1.3.9}$$

In this case, the metric has slices, for fixed r, isomorphic to d-dimensional Minkowski space-time, hence the name Poincarè coordinates. Due to the restriction $r>0$, this

patch of coordinates cover only half of the hyperboloid. The plane $r = \infty$ can be interpreted as the conformal boundary of AdS_{d+1} which is $\mathbb{R}^{1,d-1}$, while $r = 0$ correponds to the Poincarè horizon since the Killing vector ∂_t has zero norm. Notice that $r = 0$ is only a coordinate singularity and for $r < 0$ there is another Poincarè patch.
There is a further form in which the metric of Poincaré coordinates is usually written. It is achieved by taking $r \to \frac{1}{z}$

$$ds^2 = \frac{L^2}{z^2}\left(dz^2 - dt^2 + d\vec{y}^2\right), \tag{1.3.10}$$

in this case the conformal boundary is located at $z = 0$ and the Poincarè horizon is at $z = \infty$.
In the Poincarè patch the manifest isometry group is $SO(1, d-1) \times SO(1, 1)$. The first symmetry group is the Lorentz group of the boundary while the second corresponds to dilatations on the boundary and it is realized as $t \to \lambda t,\ \vec{y} \to \lambda\vec{y},\ z \to \lambda z$.

1.3.2 Type IIB supergravity

Type IIB is a string theory for closed superstrings in ten dimensions. The low energy limit of this theory leads to type IIB supergravity whose field content reflects the massless part of the spectrum of the full superstring theory (see [42] and [45] for a short review)

$$\text{type IIB} \begin{cases} g_{\mu\nu} & \text{graviton} \\ \phi & \text{dilaton} \\ B_{\mu\nu} & \text{Kalb-Ramond field} \\ C_0, C_2, C_4 & \text{R-R forms} \\ 2\psi_{\mu\alpha} & \text{gravitinos} \\ 2\lambda_{\dot{\alpha}} & \text{dilatinos} \end{cases} \tag{1.3.11}$$

The NS-NS sector contains the symmetric traceless rank-two tensor $g_{\mu\nu}$ which has 35 components, the antisymmetric Kalb-Ramond field with 28 components and the dilaton which has 1 component because corresponds to the trace. The NS-R and the R-NS sectors contain two gravitinos $\psi_{\mu\alpha}$ (56 components each) with the same chirality and two spinors $\lambda_{\dot{\alpha}}$ (8 components each), called dilatini, which have also the same chirality but oppisite to that of gravitinos. The R-R sector contains a 0-form C_0 that is a scalar, a 2-form C_2 with 28 components and a 4-form C_4^+ with

35 components. Thus, the massless spectrum gives a total of 128 fermions and 128 bosons, as we expect thanks to the supersymmetry. The bosonic part of the type IIB supergravity action, in string frame, reads

$$\begin{aligned} S_{sugra} = \frac{1}{(2\pi)^7 \alpha'^4} \int d^{10}x \sqrt{-g} \Big(e^{-2\Phi} \Big(R + 4\partial_\mu \phi \partial^\mu \phi - \frac{1}{2} \left| H_{(3)} \right|^2 \Big) - \\ - \frac{1}{2} \left| F_{(1)} \right|^2 - \frac{1}{2} \left| \tilde{F}_{(3)} \right|^2 - \frac{1}{4} \left| \tilde{F}_{(5)} \right|^2 \Big) - \\ - \frac{1}{2(2\pi)^7 \alpha'^4} \int C_{(4)} \wedge H_{(3)} \wedge F_{(3)}. \end{aligned} \tag{1.3.12}$$

where $H_{(3)}$ is the field strength of $B_{\mu\nu}$ and

$$\begin{aligned} F_{(1)} &= dC_{(0)} \\ F_{(3)} &= dC_{(2)} \\ F_{(5)} &= dC_{(4)} \end{aligned} \tag{1.3.13}$$

$$\tilde{F}_{(3)} = F_{(3)} - C_{(0)} \wedge H_{(3)}$$

$$\tilde{F}_{(5)} = F_{(5)} - \frac{1}{2} C_{(2)} \wedge H_{(3)} + \frac{1}{2} B_{(2)} \wedge F_{(3)}. \tag{1.3.14}$$

In type IIB string theory the field strength $\tilde{F}_{(5)}$ is bound to be self-dual which means that $\tilde{F}_{(5)} = \star \tilde{F}_{(5)}$, where the star denotes the Hodge dual. This constraint is usually imposed at the level of the equations of motion.

1.3.3 D-branes and open strings perspective

A central role in the AdS/CFT conjecture is played by D-branes, which are non-perturbative extended objects introduced by Polchinski in [46]. We can say that the AdS/CFT correspondence is a consequence of the two possible ways in which Dp-branes can be described. They can be viewed as $(p+1)$-dimensional hypersurfaces (p spatial + time) where open strings can end or as solitonic solutions to the equations of motion of supergravity theories. If we consider the first description, Dp-branes are obtained when one discusses the dynamics of open string and has to impose Dirichlet and Neumann boundary conditions for the string endpoints. In particular, Dirichlet conditions correspond to the directions that are normal to the Dp-branes world-volume, while Neumann conditions coincide with the directions in which the hypersurfaces extend. The open strings are free to move only along Neumann directions, and the case of full Neumann conditions corresponds to a brane

whose world-volume fills the entire space. The presence of a Dp-brane breaks the original Lorentz symmetry group in d dimensions in such a way that the resulting symmetry is the Lorentz group in (p+1) dimensions and rotations invariance along the directions in which the Dp-brane does not extend

$$SO(1, d-1) \to SO(1, p) \times SO(d-p-1). \tag{1.3.15}$$

Dp-branes are not only simply hypersurfaces, but they are dynamical objects that can move and fluctuate. Their fluctuations are described by open strings, and there are two classes of excitations. The first one corresponds to deformations along the transverse coordinates to the $(p+1)$-dimensional world-volume in the ten-dimensional target space and can be parametrized by ϕ_i, where $i = 1, ..., 9-p$. These degrees of freedom are nothing but massless scalar fields that can be interpreted as collective transverse coordinates of the brane. Moreover, there are also internal excitations corresponding to the abelian massless gauge field A_a $(a = 0, ..., p)$ living on the world-volume of the brane. The Dirac-Born-Infeld (DBI) action describes the low-energy dynamics of a Dp-brane in flat space and its motion in a background created by closed string modes $g_{\mu\nu}$, $B_{\mu\nu}$ and Φ

$$S_{DBI} = -T_{D_p} \int d^{p+1}\xi \, e^{-\tilde{\Phi}} \sqrt{-\det\left(\gamma_{ab} + B_{ab} + 2\pi\alpha' F_{ab}\right)}. \tag{1.3.16}$$

The pullback of the metric and the Kalb-Ramond field are denoted as γ_{ab} and B_{ab}

$$\begin{aligned} \gamma_{ab} &= g_{\mu\nu} \frac{\partial X^\mu}{\partial \xi^a} \frac{\partial X^\nu}{\partial \xi^b} \\ B_{ab} &= B_{\mu\nu} \frac{\partial X^\mu}{\partial \xi^a} \frac{\partial X^\nu}{\partial \xi^b}, \end{aligned} \tag{1.3.17}$$

$a, b = 0, ..., p$ are indices on the world-volume and $\mu, \nu = 0, ..9$ are indices of the ten-dimensional target space, α' is equal to the square of the string length l_s. F_{ab} is the field strength of the $U(1)$ gauge field A_a, and $\Phi = \Phi_0 + \tilde{\Phi}$ is the decomposition of the dilaton in a constant piece Φ_0, which is related to the string coupling constant $(e^{\Phi_0} = g_s)$, and a varying piece $\tilde{\Phi}$. T_{D_p} is the tension of the brane and is given by

$$T_{D_p} = \frac{1}{(2\pi)^p \, l_s^{p+1} g_s}. \tag{1.3.18}$$

The way in which the tension depends on the string coupling, $T_{D_p} \sim 1/g_s$, reflects the non-perturbative nature of Dp-branes. Notice that they become very heavy at weak coupling $(g_s \to 0)$, and this justifies treating them as rigid objects in this limit.

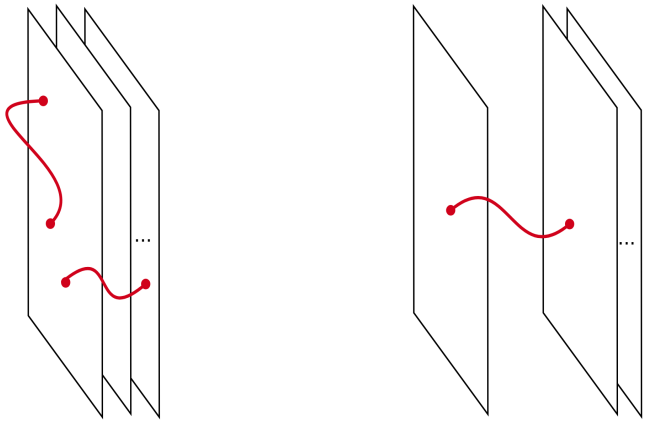

Figure 1.2: On the left, we have open strings ending on N coincident Dp-branes. The gauge theory living on the world-volume has a $U(N)$ gauge group, and the gauge fields are massless. On the right, we have $N-1$ coincident Dp-branes, and one put at a finite distance. The gauge group is broken to $U(N-1)\times U(1)$ and the string stretched between the stack of branes and the single one corresponds to a massive W-boson

Moreover, Dp-branes are charged under the R-R $(p+1)$-form (C_{p+1}) of string theory, which naturally couples to surfaces through the action

$$S_p = T_{D_p}\int_{\Sigma_{p+1}} C_{p+1}, \tag{1.3.19}$$

where Σ_{p+1} is the world-volume of the brane. Thus, the generalized action for a Dp-brane also involves a Wess-Zumino term

$$\begin{aligned} S_{D_p} &= S_{DBI} + S_{WZ} \\ S_{WZ} &= T_{D_p}\int \sum_q C_{q+1}\wedge e^{B_{ab}+2\pi\alpha' F_{ab}}. \end{aligned} \tag{1.3.20}$$

S_{WZ} takes into account the interaction of the R-R field C_{q+1} with the Kalb-Ramond field. We have seen that on a single Dp-brane lives an abelian gauge theory. In order to generalize to the non-abelian case, we need to introduce the Chan-Paton factors $m,n=1,...,N$ on a stack of N coincident Dp-branes. These non-dynamical degrees of freedom are assigned to the endpoints of the open strings, and they contain N^2 copies of the states arising in the presence of a single Dp-brane. Thus, the fields of the open strings spectrum can be arranged in hermitian matrices

$$(A_a)^m_n \qquad (\phi_i)^m_n\ . \tag{1.3.21}$$

They form the bosonic part of the vector multiplet of a Super Yang-Mills (SYM) theory in the world-volume of the branes, transforming in the adjoint representation of the gauge group $U(N)$. Since the $U(1)$ component of the $U(N)$ local symmetry can be decoupled, we can conclude that the low-energy theory arising from a stack of N coincident Dp-branes is a SYM theory with gauge group $SU(N)$ in $p+1$ dimensions. The relation between the SYM coupling constant and g_s is

$$g_{YM}^2 = 2(2\pi)^{p-2} l_s^{p-3} g_s. \tag{1.3.22}$$

If the branes are not coincident but separated by a finite distance, the effective theory becomes SYM with gauge group $U(1)^N$. Pulling the Dp-branes apart corresponds to a Higgs mechanism responsible for the spontaneous symmetry breaking $U(N) \to U(1)^N$ of the gauge group in the low-energy effective theory. The relative positions between the branes are given by the expectation values acquired by the scalar fields.

Focusing on D3-brane

D3-branes are especially important when we consider the AdS/CFT correspondence in its original formulation. When $p = 3$, we have a $3+1$ world-volume and $10-4 = 6$ scalar fields. In addition to the open strings that lives on the D3-branes, there can also be closed strings moving in the full ten-dimensional space-time. If we consider a stack of N coincident D3-branes, the open string sector is weakly coupled, and perturbative string theory gives an accurate description of this system only if $g_s N << 1$. This limit also guarantees that $g_s << 1$ to have small string loop corrections. The massive string states have masses $M^2 \sim 1/\alpha'$, and they decouple when we take the low energy limit. It can be realized in two different ways: we can fix the energy scale E and take $\alpha' \to 0$, or fix the characteristic string scale α' and take E very small. In the following, we will use the first approach. Thus, in the low energy limit, the closed string sector reduces to the massless field of supergravity. The corresponding effective theory living on the stack of N D3-branes can be identified with a four-dimensional SYM theory with gauge group $SU(N)$ and with sixteen Poincaré supercharges. From (1.3.22) the relation between the Yang-Mills and string coupling is

$$g_{YM}^2 = 4\pi g_s. \tag{1.3.23}$$

Since the interactions between open and closed strings are proportional to α', these two sectors do not interact in the low energy limit. Thus, we get two decoupled

systems

- free limit of type IIB supergravity in flat ten-dimensional space
- four-dimensional $\mathcal{N} = 4$ SYM theory on the D3-branes. The theory is weakly coupled ($\lambda << 1$), and one can use perturbation theory to do accurate calculations of quantities like correlation functions.

1.3.4 D3-branes and closed strings perspective

In the previous, we have considered D-branes from the point of view of open strings. In the closed strings perspective, D-branes are solitonic solutions to the classical equations of motion of the low energy limit of superstring theory. Moreover, extremal D-branes are 1/2 BPS objects; namely, they preserve half of the space-time supersymmetry. We concentrate now on D3-branes since, as said before, they are very important in the context of AdS/CFT correspondence. Smooth solutions to type IIB supergravity equation of motions are given by extremal black D3-branes which are characterized by [47]

$$\begin{aligned} ds^2 &= H(r)^{-\frac{1}{2}} dt^2 + H(r)^{-\frac{1}{2}} d\vec{x}^2 + H(r)^{\frac{1}{2}} \left(dr^2 + r^2 d\Omega_5^2 \right) \\ e^{\Phi} &= g_s H(r)^{\frac{3-p}{4}} \quad \underset{p=3}{\Longrightarrow} e^{\Phi} = g_s \\ F_5 &= dH(r)^{-1} \wedge dx^0 \wedge dx^1 \wedge dx^2 \wedge dx^3 \\ H(r) &= 1 + \frac{L^4}{r^4} \qquad \text{with} \qquad L^2 = 4\pi g_s N \alpha'^2, \end{aligned} \tag{1.3.24}$$

where $\vec{x} \in \mathbb{R}^3$, L is the D3-branes curavture radius and F_5 is the self-dual field strength of the R-R C_4-form which has N unit of flux through the S^5 sphere appearing in the metric above

$$\int_{S^5} F_5 = N. \tag{1.3.25}$$

The $p = 3$ case is special since the dilaton is constant. The background defined in (1.3.24) is derived solving the supergravity equations of motion, without the α' corrections due to massive string modes that should occur if the full string theory is taken into account. Supergravity is a reliable approximation of the full string theory when

$$L^2 >> \alpha'. \tag{1.3.26}$$

This condition, from the definition of L given above, implies that

$$g_s N >> 1. \tag{1.3.27}$$

It is possible to have $g_s << 1$, but it is necessary that $N >> 1$. Since we can rewrite L in terms of the 't Hooft coupling constant λ

$$L^4 = 4\pi g_s N \alpha'^2 = g_{YM}^2 N \alpha'^2 = \lambda \alpha'^2, \tag{1.3.28}$$

the condition (1.3.27) is equivalent to ask $\lambda >> 1$ for the supergravity approximation to hold. Moreover, quantum corrections are small if the characteristic scale of the geometry L is bigger than the Planck length $l_P \sim (g_s^2\, \alpha'^4)^{\frac{1}{8}}$

$$L >> l_P \quad \Rightarrow \quad N >> 1. \tag{1.3.29}$$

To study the geometry generated by the solution in (1.3.24), we consider the metric

$$ds^2 = H(r)^{-\frac{1}{2}} dt^2 + H(r)^{-\frac{1}{2}} d\vec{x}^2 + H(r)^{\frac{1}{2}} \left(dr^2 + r^2 d\Omega_5^2 \right) \tag{1.3.30}$$

and its limits in two different regimes:

- if $r >> L$, then $H(r) \sim 1$ and the metric (1.3.30) reduce to the flat one in ten-dimensional Minkowski space $\mathbb{R}^{(1,9)}$
- if $r << L$ we are in the region defined as *near-horizon region* or *throat*, in which $H(r)$ is given by $H(r) \sim \frac{L^4}{r^4}$ and the metric reads

  $$ds^2 = \frac{r^2}{L^2}(-dt^2 + d\vec{x}^2) + \frac{L^2}{r^2} \left(dr^2 + r^2 d\Omega_5^2 \right). \tag{1.3.31}$$

  If we use the coordinate redefinition $z \equiv \frac{L^2}{r}$, the metric has the following asymptotic form

  $$ds^2 = \frac{L^2}{z^2} \left(-dt^2 + d\vec{x}^2 + dz^2 \right) + L^2 d\Omega_5^2. \tag{1.3.32}$$

  This is clearly the metric of $AdS_5 \times S^5$ in the case in which both the five-dimensional AdS space and the five-sphere S^5 have the same radius of curvature L.

1.3.5 The Maldacena conjecture

We have seen that D-branes admit two equivalent descriptions. These two faces of the same object are what underlies the AdS/CFT correspondence. Since in (1.3.30) the g_{00} component is not constant, the energy will depend on r. In particular, the

energy E_r, measured by an observer at the position r, and E_∞, measured by an observer at infinity, are related by

$$E_\infty = H(r)^{-\frac{1}{4}} E_r. \tag{1.3.33}$$

For an observer located at infinity, an object moving towards $r = 0$ will have lower and lower energy. Thus, from his perspective, there are two different types of low energy closed strings modes:

- free limit of type IIB supergravity in the flat ten-dimensional Minkowski space. These low energy modes occupy the asymptotic flat region of the geometry generated by the D3-branes at $r \to \infty$
- modes confined in the near-horizon region. Due to the relation (1.3.33), for $r \to 0$, the modes in the throat can have arbitrary energy. Thus, we have the entire spectrum of type IIB string theory on $AdS_5 \times S^5$ background.

Since we are in the low energy limit, the two sectors do not interact. The correct way to take this limit when $r \to 0$ is to send also α' to zero keeping fixed the ratio r/α', performing the so-called Maldacena limit. In this way, the energy of the objects in the throat is arbitrary while the energy at infinity $E_\infty \sim \sqrt{\alpha'} E_r \, r/\alpha'$ is fixed.

We started with a background generated by considering only supergravity modes. Then, we recognize that for an observer at infinity, all the superstring states on this background are low energy modes, due to the red-shift of the energy. A backreaction may be expected since we are considering the whole superstring spectrum and particularly high energy excitations on a background derived only by considering supergravity modes. All the expected corrections vanish since $AdS_5 \times S^5$ is thought to be an exact solution not only for supergravity but for the entire type IIB string theory itself. We can now put together the open and closed strings perspectives. In both cases, we have free type IIB supergravity in ten-dimensional Minkowski space plus other two theories that should be the same thing. Thus, this identification leads to enunciate the AdS/CFT correspondence in its strongest form:

$\mathcal{N} = 4$ SYM theory with gauge group $SU(N)$ in four dimensions is equivalent to type IIB superstring theory on $AdS_5 \times S^5$.

This equivalence is conjectured to be valid for all λ and N but can also be formulated in a weaker form. As we have seen before, type IIB string theory can be

Strongest form	$\mathcal{N}=4$ SYM theory any N and λ $4\pi g_s = g_{YM}^2$	Full quantum type IIB theory on $AdS_5 \times S^5$ $L^4 = 4\pi g_s N \alpha'^2$
Strong form	't Hooft limit of $\mathcal{N}=4$ SYM λ fixed, $N \to \infty$ $1/N$ expansion	Classical type IIB string theory on $AdS_5 \times S^5$ g_s loop expansion
Weak form	Large λ limit of $\mathcal{N}=4$ SYM $N \to \infty$ $1/\sqrt{\lambda}$ expansion	Classical type IIB supergravity on $AdS_5 \times S^5$ α' expansion

Table 1.1: Differnt forms of the AdS/CFT correspondence in order of strength.

approximated to type IIB supergravity as long as

$$L^2 >> \alpha' \qquad \lambda >> 1 \qquad N >> 1, \tag{1.3.34}$$

implying that the supergravity regime corresponds to strongly coupled gauge theories. On the other hand, the perturbative field theory regime $\lambda << 1$ corresponds to strongly coupled string theory. Thus, the AdS/CFT is a weaker/strong duality. This statement makes the correspondence very fascinating since performing calculations in the supergravity regime, we can obtain information on the strong coupling dynamics of the gauge theory. Vice versa, perturbation theory on the field theory side gives insights into the non-perturbative string theory. At the same time, the duality is very hard to check since there is no overlap between the two domains in which we can do calculations with the standard tools. In order to check the correspondence, Wilson loops and protected operators as chiral primary operators will play a fundamental role. For instance, correlation functions of protected operators can be computed at tree level, and since radiative corrections are forbidden, the results still hold at strong coupling.

1.3.6 Comparing the symmetries and correlation functions

A first check that can be done for the AdS/CFT correspondence to hold is to see if the symmetries of the two theories involved in the duality are identical. The superconformal group of $\mathcal{N}=4$ SYM theory, as previously shown, is $PSU(2,2\,|\,4)$ and its bosonic subgroup arises as the product of the conformal group $SO(2,4)$

by the $SU(4)_R$ R-symmetry group. On the gravity side, the bosonic subgroup is immediately recognized as the isometry group of the $Ads_5 \times S^5$. The fermionic part of $\mathcal{N} = 4$ theory consists of 16 Poincaré supercharges and 16 superconformal supercharges, which is the same amount of supersymmetry that we have in type IIB string theory on $AdS_5 \times S^5$. Moreover, $\mathcal{N} = 4$ SYM theory also has Montonen-Olive or S-duality symmetry realized on the complex coupling constant τ. Type IIB string theory experiments also this global discrete symmetry. Matching global symmetries is a key ingredient but represents only the first step. We need a precise prescription to have a one-to-one mapping of all of the quantum states, operators, observables, processes, etcetera, between the two theories. For example, the vacuum state of the $\mathcal{N} = 4$ theory corresponds to the state of the string theory which is the empty $AdS_5 \times S^5$ geometry, without the excitation of gravitons or other modes in the spectrum. In 1998 Gubser, Klebanov and Polyakov [4] and Witten [5] proposed a prescription to compute n-point correlation functions on both side of the correspondence, making the the AdS/CFT duality much more useful and functional. The general idea is to match the generating functional of CFT correlation functions to the full partition function of type IIB string theory in $AdS_5 \times S^5$ with some specific boundary conditions

$$\left\langle e^{\int d^4x \phi_0(x)\mathcal{O}(x)} \right\rangle_{CFT} = Z_{string}\left[\phi(x,z) \mid_{z=0} = \phi_0(x)\right], \tag{1.3.35}$$

where $\phi_0(x)$ plays the role of a current and is the value of the AdS field $\phi(x,z)$ at the boundary, which is located at $z = 0$. The core of this prescription is that a field ϕ in AdS space is associated with an operator $\mathcal{O}$ in the CFT side. The two have the same quantum numbers and they know about each other via boundary couplings. Since correlation functions specify the dynamics of QFTs, the gauge theory living on the boundary is completely defined by bulk the gravitational theory. Actually, there are limits in applying the prescription (1.3.35). The first one is that the full partition function of type IIB superstring theory on $AdS_5 \times S^5$ is not known. Secondly, while taking functional derivatives on both side of (1.3.35), one runs into divergences which need to be regularized. The latter problem is solved by performing the so-called holographic renormalization [48, 49]. In the weak form of the duality, corresponding to $\lambda \to \infty$ and $N \to \infty$, the partition function on the r.h.s. of (1.3.35) is obteined from the on-shell action in classical supergravity

$$Z_{string}\left[\phi_0(x)\right] \simeq e^{-S_{sugra}[\phi_0(x)]}\,. \tag{1.3.36}$$

This equality has to be seen as a saddle point approximation allowing for predictions of the CFT correlation functions at strong coupling.

Chapter 2

Supersymmetric Wilson loop operators

2.1 Wilson loops in non-abelian gauge theories

The Wilson loop operator, introduced by Wilson in [50], is a very important non-local and gauge-invariant observable that describes the parallel transport for an external particle along a close path $\mathcal{C}$. This operator has a very central role in the study of gauge theories. In more mathematical terms, we can define it as the holonomy of the gauge field A_μ. Its physical meaning can be easily understood considering the motion of an external charge along a closed curve in QED. The action for this charge is

$$S_{\mathcal{C}} = \oint_{\mathcal{C}} A_\mu dx^\mu, \tag{2.1.1}$$

which gives in the path-integral the following contribution

$$e^{iS_{\mathcal{C}}} = e^{i\oint_{\mathcal{C}} A_\mu dx^\mu} \equiv \mathcal{W}(\mathcal{C}). \tag{2.1.2}$$

$\mathcal{W}(\mathcal{C})$ is the Wilson loop, and it is nothing but the Aharonov-Bohm phase factor picked up by the wave-function of a heavy quark along a closed path. The non-abelian definition of the operator involves the trace since we want a gauge-invariant object

$$\mathcal{W}(\mathcal{C}) = \frac{1}{\dim_{\mathcal{R}}} \mathrm{Tr}_{\mathcal{R}} \mathcal{P} \exp\left(i \oint_{\mathcal{C}} A_\mu(x) dx^\mu \right), \tag{2.1.3}$$

where A_μ is a matrix written in terms of the generators T^a of the gauge group, namely $A_\mu = A_\mu^a T^a$. We are considering a generic representation $\mathcal{R}$ of the gauge group over which the trace is taken, $1/\dim_{\mathcal{R}}$ is a normalization factor and $\mathcal{P}$ denotes

the path ordering of the integral. Since the A_μ are Lie algebra valued fields, in general, they do not commute. Thus, we have an exponential of non-commuting matrices that leads to an ambiguity in its definition in terms of the Taylor series. The cure to this problem is found by imposing the path ordering which is defined as

$$\begin{aligned}\mathcal{P}\exp\left(i\oint_{\mathcal{C}}A_\mu(x)dx^\mu\right) =& \mathbb{1} + i\int_a^b ds_1 A_\mu(x(s_1))\frac{dx^\mu}{ds_1} - \\ &- \int_a^b ds_1\int_a^{s_1} ds_2 A_\mu(x(s_1))\frac{dx^\mu}{ds_1}A_\nu(x(s_2))\frac{dx^\nu}{ds_2} + \ldots \ ,\end{aligned} \tag{2.1.4}$$

where $s \in [a,b]$ parametrize the contour $\mathcal{C}$ and $s_1 > s_2$ in such a way that higher values of the path parameter s stand to the left in every term. The non-local nature of this operator means that it depends only on the type of contour parametrized by s and not on a single point. The Wilson loops are of fundamental importance because they constitute a complete basis of gauge-invariant operators for the pure Yang-Mills theory, and all gauge invariant functions of A_μ can be derived from them by choosing appropriate paths. We are particularly interested in the situation in which the close path $\mathcal{C}$ is a rectangular loop in the Euclidean space-time and the trace in the definition of the Wilson loop is taken over the fundamental representation of the gauge group, such as the N-dimensional representation of $SU(N)$. In this situation we have the creation of a quark-antiquark pair $(q\bar{q})$ at $t = 0$ located at a spatial distance R. Since they are external sources, their masses are taken to infinity, so we may expect them to be static (no kinetic energy). After a long time T, we let them rejoin and annihilate. The expectation value of the rectangular Wilson loop encodes the static potential for this configuration, when $T >> R$ we have

$$\lim_{T\to\infty}\langle\mathcal{W}(\mathcal{C})\rangle \sim e^{-TE_I(R)}, \tag{2.1.5}$$

where E_I is the interaction energy of the pair at a distance R. The previous formula is obtained by taking a complete basis of eigenstates inserted into a quark correlator, in the limit in which T is very large, only the ground state with the lowest energy, which is precisely the potential, survives in the sum over states. In a confining theory, the quark-antiquark pair has binding energy that grows linearly with distance

$$E = m_q + m_{\bar{q}} + E_I(R) \qquad \text{with} \quad E_I(R) = \sigma R \ , \tag{2.1.6}$$

σ is the tension of the color flux tube connecting them. Thus, for the case in exam

$$\lim_{T\to\infty}\langle\mathcal{W}(\mathcal{C})\rangle \sim e^{-TE_I(R)} \sim e^{-\sigma TR}. \tag{2.1.7}$$

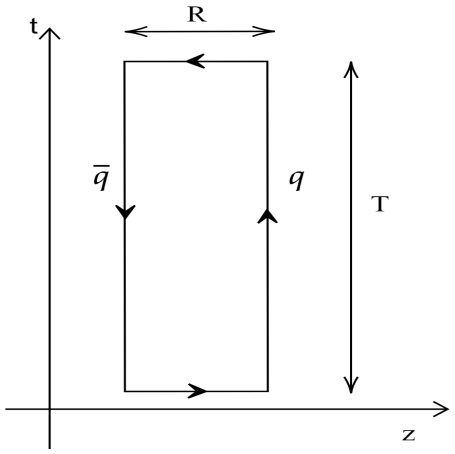

Figure 2.1: On a rectangular contour, the Wilson loop measures the potential of a pair of heavy quarks providing a tool to inspect the confinement of the theory.

TR is the area of the rectangular contour. In fact, in a confining theory the Wilson loop operator is expected to show the so-called *area low*

$$\lim_{T\to\infty} \langle \mathcal{W}(\mathcal{C}) \rangle \sim e^{-\sigma \mathcal{A}(\mathcal{C})}, \tag{2.1.8}$$

where $\mathcal{A}(\mathcal{C})$ is the area encoded by the loop. The behavior that characterized the deconfined phase of a gauge theory follows the *perimeter low*

$$\lim_{T\to\infty} \langle \mathcal{W}(\mathcal{C}) \rangle \sim e^{-\delta M \text{ (perimeter of } \mathcal{C})}. \tag{2.1.9}$$

The coefficient δM can be interpreted as contributing to the renormalization of the quark mass due to interaction of the quark with quantized gauge fields. Thus, the expectation value of the Wilson loop plays the role of the order parameter for confinement, allowing to distinguish between the confining and deconfining phase according to the so-called "Wilson criterion."

2.2 BPS Wilson loops in $\mathcal{N} = 4$ SYM theory

A generalization of the Wilson loop operator (2.1.4) in $\mathcal{N} = 4$ SYM theory was proposed by Maldacena in [6] and it is known as the *Maldacena Wilson loop*. In Euclidean signature, it reads

$$\mathcal{W}(\mathcal{C}) = \frac{1}{N} \mathrm{Tr} \mathcal{P} \exp \left[\oint_{\mathcal{C}} ds \left(i A_\mu(x) \dot{x}^\mu + |\dot{x}| \, \theta^i \phi_i \right) \right], \tag{2.2.1}$$

where $\dot{x}^\mu = \partial_s x^\mu(s)$, $x^\mu(s)$ parametrize the contour $\mathcal{C}$ and θ^i is a six-vector ($\theta^i\theta_i = 1$) that specifies a point on S^5 and in general it can depend on s. We are now considering the Wilson loop associated with a particle that transforms in the fundamental representation of the gauge group. In $\mathcal{N} = 4$ SYM theory, all the fields transform in the adjoint since they belong to the same vector multiplet of the gauge field A_μ. Thus, we need to introduce naturally a very massive particle transforming in the fundamental representation. With this aim, we consider $N+1$ coincident D3-branes whose world-volume effective theory is $\mathcal{N} = 4$ SYM with gauge group $SU(N+1)$. Then, we separate one of these branes in at least one of the six transverse directions. One of the six scalars of the theory gets an expectation value, breaking the $SU(N+1)$ gauge group to $SU(N) \times U(1)$ via Higgs-like mechanism. The open strings stretched between the stack of N D3-branes and the separated one have a mass proportional to the D-branes separation. Moreover, the low energy excitation of these string states behaves as a W-boson. The end-point of this string acts in the $SU(N)$ gauge theory as a quark in the fundamental representation of the gauge group, and in the large N limit the $U(1)$ group decouples. Since the scalars of the $SU(N+1)$ theory are valued in the Lie algebra of this group, they can be written as $(N+1) \times (N+1)$ matrices that contain the scalars of $SU(N)$ that remain massless, whereas the $(N+1, N+1)$ element is the vacuum expectation value $M\theta^i$. Since M, which corresponds to the separation distance in the flat six-dimensional space-time, is proportional to the mass of the heavy W-boson, its value has to be large. The $SO(6)$ R-symmetry is reduced to $SO(5)$ symmetry by choosing which scalar gets a vacuum expectation value, and θ^i parametrizes the direction of the symmetry breaking. The Wilson loop (2.2.1) corresponds to the traced holonomy of the heavy W-Boson. As one can notice, respect to the standard Wilson loop (2.1.4), the Maldacena operator couples not only to the gauge field but also to the six scalars of the theory. More arguments justify this additional coupling, for instance, the fact that the scalars are in the same supermultiplet of the gauge field. Another way to derive it is to consider the operator in four dimensions as obtained via dimensional reduction from a Wilson loop in the ten-dimensional $\mathcal{N} = 1$ SYM theory. Following the same strategy used to get $\mathcal{N} = 4$ SYM from the ten-dimensional theory, we obtain a bigger class of Wilson loops characterized by an arbitrary coupling $\dot{y}^i$ to the scalars. The loops that satisfy the condition

$$\dot{x}^2 = \dot{y}^2 \qquad \dot{y}^i = |\dot{x}|\,\theta^i \tag{2.2.2}$$

belong to the Maldacena Wilson loops class and show significant and nice properties, as we will review.

2.2.1 Supersymmetry variation of the Wilson loop

The presence of the scalars with the right coupling in the definition (2.2.1) is also fundamental to have an object that is supersymmetric. Under the supersymmetry transformations

$$\begin{aligned} \delta_\epsilon A^\mu &= i\bar{\epsilon}\,\Gamma^\mu \Psi \\ \delta_\epsilon \Phi^i &= i\bar{\epsilon}\,\Gamma^i \Psi \end{aligned} \tag{2.2.3}$$

the Maldacena Wilson loops transform as

$$\begin{aligned} \delta_\epsilon \mathcal{W}(\mathcal{C}) = \frac{1}{N}\mathrm{Tr}\,\mathcal{P}\left[i \oint_{\mathcal{C}} ds\, \bar{\epsilon}\left(i\dot{x}^\mu \Gamma_\mu + |\dot{x}|\,\Gamma^i \theta_i \right)\Psi \times \right. \\ \left. \times \exp\left(\oint_{\mathcal{C}} ds' \left(i\dot{x}^\mu A_\mu + |\dot{x}|\,\theta^i \phi_i \right) \right) \right], \end{aligned} \tag{2.2.4}$$

where we have used the ten-dimensional notation in which Ψ and the susy parameter ϵ are sixteen components Majorana-Weyl spinors. $\Gamma^M = (\Gamma^\mu, \Gamma^i)$ are the ten-dimensional Dirac matrices. Some fraction of the total supersymmetry is preserved if

$$\bar{\epsilon}\left(i\dot{x}^\mu \Gamma_\mu + |\dot{x}|\,\Gamma^i \theta_i \right)\Psi = 0\,, \tag{2.2.5}$$

where the number of linearly independent solutions determines the amount of conserved supercharges. It is possible to have a non-trivial result if

$$\left(i\dot{x}^\mu \Gamma_\mu + |\dot{x}|\,\Gamma^i \theta_i \right)^2 = |\dot{x}|^2 \left(1 - \theta^i \theta_i \right) = 0. \tag{2.2.6}$$

Thus, the condition $\theta^i \theta_i = 1$ is necessary to preserve some amount of supersymmetry. Moreover, if $\theta^i \theta_i = 1$, the above combination of Γ-matrices results to be nilpotent and the equation (2.2.5) has eight independent solutions that in general can depend on s and thus can be different at every point of the loop. The important consequence is that a Maldacena Wilson loop with an arbitrary closed contour is only locally supersymmetric. Local supersymmetry is not a symmetry of the action. If we want real supersymmetric invariant operators, rigid supersymmetry must be preserved. This translates in the requirement that $\bar{\epsilon}$ has to be constant. It is possible to

introduce the projectors

$$\begin{aligned} \mathcal{P}^{\pm} &= \frac{1}{\sqrt{2}}\left(\mathbb{1} \pm i\,\frac{\dot{x}^{\mu}}{|\dot{x}|}\gamma_{\mu}\gamma^{5}\rho_{i}\theta^{i}\right) \\ \mathcal{P}^{+}\mathcal{P}^{-} &= \mathcal{P}^{-}\mathcal{P}^{+} = 0 \\ \left(\mathcal{P}^{\pm}\right)^{2} &= 1\,, \end{aligned} \tag{2.2.7}$$

where we choose a particular representation of the gamma matrices in ten dimensions, namely

$$\Gamma^{M} = \begin{cases} \Gamma^{\mu} = \mathbb{1}_{8\times 8} \otimes \gamma^{\mu} \\ \Gamma^{i} = \gamma^{5} \otimes \rho^{i}\,. \end{cases} \tag{2.2.8}$$

Here γ^{μ} and ρ^{i} are respectively the gamma matrices of $SO(4)$ and $SO(6)$, the Poincaré and R-symmetry groups, and they commute with each-other. Thus, γ^{μ} only acts on four-dimensional spinor indices whereas ρ^{i} only acts on the R-symmetry ones. Moreover, $\gamma^{5} = -\gamma^{1}\gamma^{2}\gamma^{3}\gamma^{4}$ is the four-dimensional chirality matrix. We can rewrite the equation (2.2.5) in a more compact form

$$\bar{\epsilon}\left(i\dot{x}^{\mu}\Gamma_{\mu} + |\dot{x}|\,\Gamma^{i}\theta_{i}\right)\Psi = i\,\bar{\epsilon}\,\mathcal{P}^{+}\dot{x}^{\mu}\gamma_{\mu}\Psi = 0. \tag{2.2.9}$$

Choosing

$$\bar{\epsilon} = \bar{\epsilon}_{0}\mathcal{P}^{-} \tag{2.2.10}$$

with $\bar{\epsilon}_{0}$ a constant ten-dimensional Majorana-Weyl spinor, ensures that the SUSY variation vanishes thanks to the property of the projectors ($\mathcal{P}^{-}\mathcal{P}^{+} = 0$). Since the requirement to achieve global supersymmetry induces constraints on both $x^{\mu}(s)$ and $\theta^{i}(s)$, in the following we will consider different types of contours for which supersymmetry is not only locally preserved.

2.2.2 Straight line

A single infinite straight line in four dimensions is described by

$$\begin{aligned} x^{\mu} &= (0,0,0,s) \\ \dot{x}^{\mu} &= (0,0,0,1) \\ \theta^{i} &= (1,0,0,0,0,0)\,, \end{aligned} \tag{2.2.11}$$

and with this choiche the Wilson loop reads

$$\mathcal{W}(\mathcal{C}_{\text{line}}) = \frac{1}{N}\mathrm{Tr}\,\mathcal{P}\,\exp\left[\oint_{\mathcal{C}} ds\,(iA_{4} + \phi_{1})\right]. \tag{2.2.12}$$

The projectors

$$\mathcal{P}^{\pm} = \frac{1}{\sqrt{2}}\left(\mathbb{1} \pm i\,\gamma_4\gamma^5\rho_1\right) \tag{2.2.13}$$

are constant implying that $\bar{\epsilon}$ is indipendent on s. As a result, the straight line preserves half of the total supersymmetry and it is called a 1/2 BPS object [9]. Consistent with this property, the expectation value of this operator is protected from radiative corrections, and it is independent of the coupling constant

$$\langle \mathcal{W}(\mathcal{C})\rangle_{\text{line}} = 1. \tag{2.2.14}$$

Moreover, the 1/2 BPS straight line is related to the circular Wilson loop by an inversion. The circle shares several common features with the straight line, but its quantum expectation value is non-trivial as we will see in the following sections.

2.2.3 The circular Wilson loop

The circular Wilson loop operator in four dimensions can be parametrized by

$$\begin{aligned} x^{\mu}(s) &= (0, 0, \cos s, \sin s) \\ \dot{x}^{\mu}(s) &= (0, 0, -\sin s, \cos s) \\ \theta^{i} &= (1, 0, 0, 0, 0, 0), \end{aligned} \tag{2.2.15}$$

where $s \in [0, 2\pi]$. Since scale invariance tells us that the expectation value of the operator cannot depend on the value of the radius, we can consider an unit circle. The circular operator can be written as

$$\mathcal{W}(\mathcal{C}_{\text{circle}}) = \frac{1}{N}\text{Tr}\,\mathcal{P}\,\exp\left[\oint_{\mathcal{C}} ds\ (-iA_2\sin s + iA_3\cos s + \phi_1)\right]. \tag{2.2.16}$$

Since we are considering a circle in the $(3, 4)$ plane, it holds that

$$\begin{aligned} x^{\mu}\gamma_{\mu} &= x^{a}\gamma_{a} & \dot{x}^{\mu}\gamma_{\mu} &= \dot{x}^{a}\gamma_{a} \\ \dot{x}^{a} &= \epsilon^{ab}x_{b} & \gamma_{a}\gamma^{5} &= -\epsilon_{ab}\gamma^{1}\gamma^{2}\gamma^{b} \\ \text{with } a, b = 3, 4 & & \text{and} \quad \epsilon^{ab} &= \begin{pmatrix} 0 & -1 \\ 1 & 0 \end{pmatrix}. \end{aligned} \tag{2.2.17}$$

Using the above identities, we have that $\dot{x}^{\mu}\gamma_{\mu}\gamma^5 = \gamma_1\gamma_2 x_a\gamma^a$, and thus the projectors take the form

$$\mathcal{P}^{\pm} = \frac{1}{\sqrt{2}}\left(\mathbb{1} \pm i\gamma_1\gamma_2\rho_1 x^{a}\gamma_{a}\right). \tag{2.2.18}$$

It turns out that the supersymmetry parameter is given by

$$\bar{\epsilon} = \bar{\epsilon}_0 \left(\mathbb{1} - i\gamma_1\gamma_2\rho_1 x^a \gamma_a\right) = \bar{\epsilon}_Q + \bar{\epsilon}_S x^\mu \gamma_\mu \,, \tag{2.2.19}$$

meaning that $\bar{\epsilon}$ generates a superconformal transformation in $\mathbb{R}^4$, where $\bar{\epsilon}_Q$ and $\bar{\epsilon}_S$ are arbitrary, coordinate-independent ten-dimensional Majorana-Weyl spinors

$$\begin{aligned} \bar{\epsilon}_Q &= \bar{\epsilon}_0 \\ \bar{\epsilon}_S &= -i\bar{\epsilon}_0\gamma_1\gamma_2\rho_1 . \end{aligned} \tag{2.2.20}$$

In particular, $\bar{\epsilon}_Q$ is responsible for the Poincaré part, while $\bar{\epsilon}_S$ for the conformal part. Respect to the straight line, which preserves separately Poincaré and superconformal supercharges, the circle is is still a 1/2 BPS operator, but it is invariant under a combination of them. Moreover, its expectation value is not independent of the coupling constant λ. Since it commutes with some of the supercharges, many cancellations happen between the diagrams that contribute to the perturbative calculation.

2.2.4 Zarembo construction

For a general loop with varying θ^i and contour $\mathcal{C}$, the supersymmetry condition (2.2.5) corresponds to an infinite set of algebraic equations for sixteen unknown quantities. In [51] Zarembo proposed a simple ansatz to solve (2.2.5) for a generic contour $\mathcal{C}$ in $\mathbb{R}^4$. The construction is based on the requirement that the position of the loop on S^5 defined by the vector $\theta^i(s)$ follows the tangent vector $\dot{x}^\mu$ of the contour $\mathcal{C}$. Thus, we can choose the following condition for the scalar coupling

$$\theta^i(s) = M^i_\mu \frac{\dot{x}^\mu}{|\dot{x}|}, \tag{2.2.21}$$

where M^i_μ is a 6×4 rectangular matrix satisfying $M^i_\mu M^i_\nu = \delta_{\mu\nu}$. With this choice of θ^i, the Wilson loop becomes

$$\mathcal{W}_Z(\mathcal{C}) = \frac{1}{N}\mathrm{Tr}\mathcal{P}\mathrm{exp}\left[\oint_{\mathcal{C}} ds\, \dot{x}^\mu \left(iA_\mu + M^i_\mu \phi_i\right)\right]. \tag{2.2.22}$$

The supersymmetry equation (2.2.5) reduces to four algebraic equations

$$\left(\Gamma_\mu - iM^i_\mu \Gamma_i\right)\epsilon = 0\,. \tag{2.2.23}$$

A general curve in $\mathbb{R}^4$ preserves 1/16 of the original supersymmetry, but we can have an enhancement of the preserved supercharges if the loop contour lies in a

lower-dimensional subspace of $\mathbb{R}^4$. Thus, a curve in $\mathbb{R}^1$ is 1/2 BPS, in $\mathbb{R}^2$ it is 1/4 BPS, and in $\mathbb{R}^3$ it is 1/8 BPS. The vacuum expectation value of this class of Wilson loops is trivial

$$\langle \mathcal{W}_Z(\mathcal{C}) \rangle = 1. \tag{2.2.24}$$

In the original work of Zarembo, this has been checked at weak coupling for a general curve, considering the diagrams contributing up to λ^2 order. The basic ingredient in this calculation is the equality of the scalar and the vector propagators in Feynman gauge. For the circle and the line, this result was also corroborated from an AdS calculation in the original work (minimal surface vanishes). In [51], it was conjectured that planar Wilson loops, which are 1/4 BPS, do not receive quantum corrections. This conjecture was proven in [52] and [53]. The absence of quantum corrections for the case of a general Wilson loop in the Zarembo construction was proven in [54] on the string theory side of the duality.

2.2.5 DGRT construction

In [27, 55] Drukker, Giombi, Ricci and Trancanelli presented a family of operators, called DGRT Wilson loops, that follows an arbitrary curve on S^3. They can be thought as a generalization of the circular operator, and their expectation values, in general, are complicated functions of g_{YM} and N. The basic ingredient in the construction is to transform the scalars into a self-dual tensor

$$\phi_{\mu\nu} = \sigma^I_{\mu\nu} M^I_i \phi^i \tag{2.2.25}$$

with the modified gauge connection

$$A_\mu \to A_\mu + i\phi_{\mu\nu} x^\nu. \tag{2.2.26}$$

The M^I_i are 3×6 rectangular matrix with $M^1 M_1 = 1$, $M^2 M_2 = 1$, $M^3 M_3 = 1$ and all the other entries zero. The tensors $\sigma^I_{\mu\nu}$ are related to the invariant one-forms on S^3 which, in terms of flat coordinates x^μ satisfying the condition $x^2 = 1$, read

$$\begin{aligned}
\sigma_1^{R,L} &= 2\left[\pm(x^2dx^3 - x^3dx^2) + (x^4dx^1 - x^1dx^4)\right] \\
\sigma_2^{R,L} &= 2\left[\pm(x^3dx^1 - x^1dx^3) + (x^4dx^2 - x^2dx^4)\right] \\
\sigma_3^{R,L} &= 2\left[\pm(x^1dx^2 - x^2dx^1) + (x^4dx^3 - x^3dx^4)\right],
\end{aligned} \tag{2.2.27}$$

where σ_i^R are the right one-forms and σ_i^L are the left one-forms. Choosing the scalar coupling to rely on the right-forms

$$\sigma_I^R = 2\sigma_{\mu\nu}^I x^\mu dx^\nu \,, \tag{2.2.28}$$

the Wilson loop can be rewritten as

$$\begin{aligned} \mathcal{W}_{DGRT}(\mathcal{C}) = \frac{1}{N}\mathrm{Tr}\,\mathcal{P}\mathrm{exp}\left[\oint_{\mathcal{C}} dx^\mu \left(iA + \frac{1}{2}\sigma_I^R M_i^I \phi^i\right)\right] = \\ = \frac{1}{N}\mathrm{Tr}\,\mathcal{P}\mathrm{exp}\left[\oint_{\mathcal{C}} dx^\mu \left(iA_\mu - \sigma_{\mu\nu}^I x^\nu M_i^I \phi^i\right)\right] . \end{aligned} \tag{2.2.29}$$

The supersymmetry condition for the loop is

$$\delta_\epsilon \mathcal{W}_{DGRT}(\mathcal{C}) = \left(i\dot{x}^\mu \gamma_\mu - \sigma_{\mu\nu}^I \dot{x}^\mu \dot{x}^\nu M_i^I \rho^i \gamma^5\right) = 0 \,, \tag{2.2.30}$$

where we have used the gamma matrices decomposition (2.2.8). Solving (2.2.30), one finds that an arbitrary Wilson loop on S^3 preserves 1/16 of the original supersymmetries and it is called 1/16 BPS. The two preserved supercharges are combined Poincaré-superconformal charges. For special curves, the operator will preserve more supersymmetries. Restricting the Wilson loop to lie on an S^2 inside S^3, the equation (2.2.30), has more solutions and a generic Wilson loop on S^2 preserves 1/8 of the supersymmetries. The 1/2 BPS circular Wilson loop is included in the DGRT construction as a special example, this is simply a great circle on the S^2 (in the S^3 case is the same). We can also take the loop to be a non-maximal circle, namely a latitude of the S^2 with angle θ_0. The loop preserves 1/4 of the supersymmetries and it reduces to the maximal circle when $\theta_0 = \pi/2$.

2.3 The circular Wilson loop at weak coupling

Let us consider now the vacuum expectation value of the circular operator at weak coupling. It can be computed performing a Taylor expansion of the path ordered exponential

$$\begin{aligned} \langle \mathcal{W}(\mathcal{C}) \rangle = 1 - \frac{1}{N}\int ds_1 \int ds_2\, \mathrm{Tr}\Big(\dot{x}_1^\mu \dot{x}_2^\nu \langle \mathcal{P} A_\mu(x_1) A_\nu(x_2)\rangle_0 - \\ - |\dot{x}_1|\,|\dot{x}_2|\,\theta^i\theta^j \langle \mathcal{P}\phi_i(x_1)\phi_j(x_2)\rangle_0\Big) + \dots \,, \end{aligned} \tag{2.3.1}$$

where we have used the shorter notation $x_1 = x(s_1)$ and $x_2 = x(s_2)$. Notice that the trace over a single field is zero since the T^a are matrices of $\mathfrak{su}(N)$, with $a, b =$

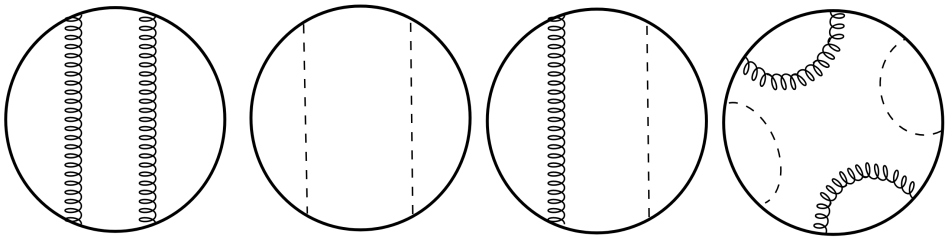

Figure 2.2: Examples of ladder and rainbow diagrams that can contribute to the circular Wilson loop expectation value.

$1, ..., N^2 - 1$. Since the gauge field and the scalars are valued in the lie algebra, we get

$$\begin{aligned}\langle \mathcal{W}(\mathcal{C})\rangle = 1 - \frac{1}{N}\int_0^{2\pi} ds_1 \int_0^{s_1} ds_2 \, \Big[\dot{x}_1^\mu \dot{x}_2^\nu \left\langle A_\mu^a(x_1) A_\nu^b(x_2)\right\rangle_0 \mathrm{Tr}(T^a T^b) - \\ - |\dot{x}_1|\,|\dot{x}_2|\,\theta^i\theta^j \left\langle \phi_i^a(x_1)\phi_j^b(x_2)\right\rangle_0 \mathrm{Tr}(T^a T^b)\Big] + \dots .\end{aligned} \tag{2.3.2}$$

In the Feynman gauge, the free-field propagators are

$$\begin{aligned}\left\langle A_\mu^a(x_1) A_\nu^b(x_2)\right\rangle_0 &= \frac{g_{YM}^2}{4\pi^2}\,\frac{\delta_{\mu\nu}\delta^{ab}}{|x_1 - x_2|^2} \\ \left\langle \phi_i^a(x_1)\phi_j^b(x_2)\right\rangle_0 &= \frac{g_{YM}^2}{4\pi^2}\,\frac{\delta_{ij}\delta^{ab}}{|x_1 - x_2|^2}.\end{aligned} \tag{2.3.3}$$

Using also the normalization

$$\mathrm{Tr}(T^a T^b) = \frac{1}{2}\delta^{ab} \tag{2.3.4}$$

of the generators of the gauge group we obtain [1]

$$\langle \mathcal{W}(\mathcal{C})\rangle = 1 - \frac{g_{YM}^2 N}{8\pi^2}\int_0^{2\pi} ds_1 \int_0^{s_1} ds_2 \,\frac{\dot{x}_1\cdot\dot{x}_2 - |\dot{x}_1|\,|\dot{x}_2|}{|x_1 - x_2|^2} + \dots . \tag{2.3.5}$$

Since for the circle

$$\frac{\dot{x}_1\cdot\dot{x}_2 - |\dot{x}_1|\,|\dot{x}_2|}{|x_1 - x_2|^2} = \frac{\dot{x}_1\cdot\dot{x}_2 - 1}{|x_1 - x_2|^2} = -\frac{1}{2}\,, \tag{2.3.6}$$

[1] In the prefactor, we have replaced $(N^2-1)/N$ by N in view of the large N limit. This would be the right result, if we were considering a $\mathfrak{u}(N)$ Lie algebra.

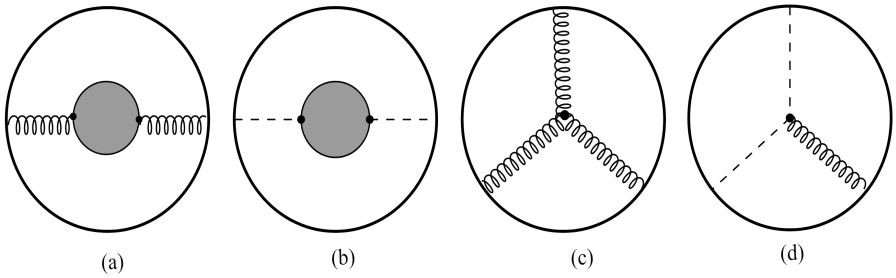

Figure 2.3: Diagrams with internal vertices that contribute at order λ^2. (a) and (b) give one-loop corrections to the gluon and the scalar exchange, (c) and (d) take into account the three-vertex diagrams.

the final risult for the expectation value of the Wilson loop at the first order in $\lambda = g_{YM}^2 N$ is

$$\langle \mathcal{W}(\mathcal{C}) \rangle = 1 + \frac{\lambda}{16\pi^2} \int_0^{2\pi} ds_1 \int_0^{s_1} ds_2 = 1 + \frac{\lambda}{8}. \tag{2.3.7}$$

It would be interesting to go further investigating the next orders in perturbation theory. At two-loop order, there are two different families of Feynman diagrams that contribute: the so-called ladder and rainbow diagrams, and the interacting graphs. The former does not contain any interaction vertices, but only the gluon and scalars propagators. The latter ones consist of diagrams with three-vertices and the self-energy corrections to the scalars and gluon propagators. As was firstly shown in [56], in the case of the circular Wilson loop in four dimensions interacting graphs cancel each other at order λ^2. In [56], it was also conjectured that this cancellation extended at all orders in perturbation theory, and only ladder and rainbow diagrams contribute to the perturbative series. This assumption was justified by the fact that the resummation of this type of diagrams in the gauge theory agrees with the strong coupling behavior obtained by a calculation in the gravity side, as we will analyze in the next section. In [57] was given a subsequent argument based on the conformal relation between the circle and the straight line. The contribution coming from the ladder and rainbow diagrams simplifies if one considers the planar limit (N very large) in which the propagators do not cross each other. Drukker and Gross [57] then extended this result to include all non-planar corrections. Moreover, in [56]

was observed that the combined vector-scalar propagator

$$\left\langle \left(iA^a_\mu(x_1)\dot{x_1}^\mu + \phi^a(x_1)\right)\left(iA^b_\nu(x_2)\dot{x_2}^\nu + \phi^b(x_2)\right)\right\rangle_0 = \frac{g^2_{YM}\,\delta^{ab}}{4\pi^2}\,\frac{1-\dot{x}_1\cdot\dot{x}_2}{|x_1-x_2|^2} = \\ = \frac{g^2_{YM}\,\delta^{ab}}{8\pi^2}\,, \tag{2.3.8}$$

is effectively constant, leading to the idea that the behavior of ladder and rainbow diagrams could be encoded in a zero-dimensional field theory, namely a matrix model

$$\langle \mathcal{W}\rangle_{\text{circle}} = \left\langle \frac{1}{N}\text{Tr }\exp(M)\right\rangle = \frac{1}{Z}\int \mathcal{D}M\,\frac{1}{N}\text{Tr}\,[\,\exp(M)]\exp\left(-\frac{2N}{\lambda}\text{tr}M^2\right), \tag{2.3.9}$$

where

$$Z = \int \mathcal{D}M\,\frac{1}{N}\exp\left(-\frac{2N}{\lambda}\text{tr}M^2\right), \tag{2.3.10}$$

and M is an hermitian $N\times N$ matrix. This matrix model can be solved analytically, and in the planar limit we get

$$\langle \mathcal{W}\rangle_{\text{circle}} = \frac{2}{\sqrt{\lambda}} I_1\left(\sqrt{\lambda}\right) \tag{2.3.11}$$

with I_1 the modified Bessel function of the first kind. The asymptotic expansion for large λ is given by

$$\langle \mathcal{W}\rangle_{\text{circle}} \overset{\lambda>>1}{=} \sqrt{\frac{2}{\pi}}\,\frac{e^{\sqrt{\lambda}}}{\lambda^{3/4}} \tag{2.3.12}$$

which shows the same exponential behavior that is found from the AdS/CFT prediction. However, this result is achieved by assuming an astonishing cancelation between the interacting diagrams. This conjecture was correctly proved in [10] by Pestun using supersymmetric localization which is a very powerful tool that allows to exactly compute the partition function and the expectation value of certain operators in supersymmetric theories. The key point is that the path integral of some protected observables "localizes" to the saddle-points of the classical action and reduces to a matrix integral. Using localization techniques, Pestun proved that $\mathcal{N}=4$ theory can be formulated on S^4, and the circular Wilson loop, being an object that preserves a fraction of the original superconformal symmetry, can be computed through a gaussian matrix model that encodes the full perturbative series. Thus, the circle operator in $\mathcal{N}=4$ SYM theory has great relevance because its expectation value can be computed exactly and allows to interpolate results between weak and strong coupling.

2.4 The holographic Wilson loop

The strong coupling description of the Wilson loop operator was proposed in [6, 7]. In the gauge theory side, the Wilson loop operator can be interpreted as the phase factor associated with a W-boson. From the closed strings point of view, we have a stack of N D3-branes whose near-horizon limit generates the $AdS_5 \times S^5$ background and a single brane separated from the others. The endpoint of the open string stretched between the coincident branes and the single one is dual to a quark. Since we want it to be an external source, the open string has to be infinitely massive. The mass of the string is proportional to the distance between the separated branes, pushing the single D3 at the boundary of AdS_5 it becomes infinitely massive. Thus, in string theory, the Wilson loop is represented by an open string whose worldsheet Σ ends on the contour $\mathcal{C}$ at the boundary of AdS_5 where the loop is defined. In general, to compute the Wilson loop expectation value we should consider the full partition function of type IIB string theory on $AdS_5 \times S^5$

$$\langle \mathcal{W}(\mathcal{C}) \rangle = Z_{\text{string}}\left[\mathcal{C}\right] \tag{2.4.1}$$

satisfying the boundary condition that Σ ends on the contour $\mathcal{C}$ and lies along $\theta^I(s)$ on S^5. In the supergravity limit $\lambda \to \infty$, the string partition function can be computed using a saddle point approximation and the Wilson loop expectation value is described by the area $A(\mathcal{C})$ of a minimal surface bounded by $\mathcal{C}$

$$\langle \mathcal{W}(\mathcal{C}) \rangle \sim e^{-A(\mathcal{C})}. \tag{2.4.2}$$

Due to the curvature of AdS_5, the minimal surface goes deep into the interior of space. The minimal area can be computed using the Nambu-Goto action on-shell

$$A(\mathcal{C}) = S_{\text{NG}} = \frac{1}{2\pi\alpha'} \int_\Sigma d\sigma d\tau \sqrt{\det\left(g_{MN} \partial_\alpha X^M \partial_\beta X^N\right)}\,, \tag{2.4.3}$$

where g_{MN} is the ten-dimensional background metric with $M, N = 0, ..., 9$. The $X^M(\tau, \sigma)$ are the coordinates that describe the embedding of the worldsheet of the fundamental string into the target space-time, and $\partial_\alpha X^M = \partial X^M / \partial \sigma^\alpha$ with $\sigma^\alpha = \{\tau, \sigma\}$. The minimal surface is embedded in AdS_5 and sits at a particular point on S^5. Since the AdS metric (1.3.10) is divergent at the boundary located at $z = 0$, also the minimal area experiments this divergence. We know from field theory computations that $\langle \mathcal{W}(\mathcal{C}) \rangle$ has to be not divergent. A finite result is produced if one considers the Legendre transform of the area [9]. This fact can be understood

as follows: the Wilson loop imposes six Neumann and four Dirichlet boundary conditions, which are complementary to those imposed by the D3-branes, but the area is not an appropriate action functional for the Neumann problem. In fact, this kind of condition fixes the string momentum, rather than the location of the loop at the boundary. Thus, the area for the minimal surface is not well-defined, and it is necessary to use its Legendre transformation. From the physical point of view, this transformation corresponds to subtract the divergent piece from the area due to the infinite mass of the W-boson [6]

$$-\ln\langle\mathcal{W}(\mathcal{C})\rangle = A(\mathcal{C}) - ML(\mathcal{C})\,, \tag{2.4.4}$$

where M is the mass of the W-boson and $L(\mathcal{C})$ is the perimeter of the loop. To regularize the divengent area, we introduce a cut-off ϵ in the z coordinate ($\epsilon \to 0$) such that the regularized area is given by an integral in the region $z \geq \epsilon$. The divergent part of the area results to be

$$\frac{\sqrt{\lambda}}{2\pi\epsilon}\oint ds\,|\dot{x}| = \frac{\sqrt{\lambda}}{2\pi\epsilon}\,L(\mathcal{C}). \tag{2.4.5}$$

Since the mass of the W-bosn is expressible as $M = \frac{\sqrt{\lambda}}{2\pi\epsilon}$, the Legendre transformation $\tilde{A}$ is defined as

$$\tilde{A} = A(\mathcal{C}) - \frac{\sqrt{\lambda}}{2\pi\epsilon}L(\mathcal{C}). \tag{2.4.6}$$

It precisely cancels this linear divergence in $A(\mathcal{C})$ given by (2.4.5). An important remark is that the regularized area for a minimal surface that extends only in AdS, is strictly negative because of the subtraction of the boundary divergence. Therefore, in the strong 't Hooft coupling limit the Wilson loop expectation value exponentiates and the exponent is positive. The α' expansion of the sigma model, obtained by expanding around the classical solution and integrating out fluctuations, yields $1/\sqrt{\lambda}$ corrections to the Wilson loop expectation value which are suppressed in the supergravity limit.

2.4.1 Minimal surface for the circular Wilson loop

The calculation of the minimal surface ending on a circle was presented in [9] and [8]. Since the circle couples only to one scalar and lives on a two-dimensional subspace of $\mathbb{R}^4$, we can consider the loop frozen on the S^5 and the minimal surface only extends in AdS_3 with the metric

$$\frac{L^2}{z^2}\left(dz^2 + dr^2 + r^2 d\varphi^2\right)\,, \tag{2.4.7}$$

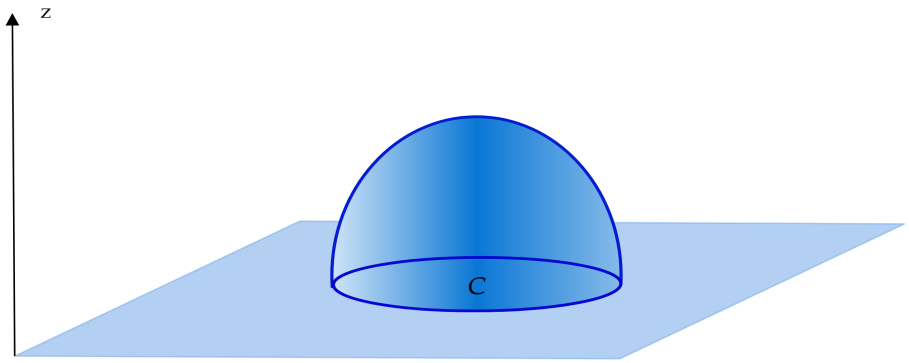

Figure 2.4: Minimal surface dual to the circular Wilson loop operator bounded to end on the contour $\mathcal{C}$ on the boundary of AdS.

where (r, φ) are the polar coordinate describing the plane in $\mathbb{R}^4$ in which the circle lies. We can make the following ansatz for the coordinates

$$r = r(\sigma) \qquad z = z(\sigma) \qquad \varphi = \tau\,, \tag{2.4.8}$$

where the choice for φ corresponds to select the static gauge. The range spanned by the worldsheet coordinates (σ, τ) is: $0 \leq \tau \leq 2\pi$ and $0 \leq \sigma < \infty$. We can compute the minimal area with the on-shell Polyakov action, since it is classically equivalent to the Nambu-Goto action

$$S_{Pol} = \frac{1}{4\pi\alpha'} \int d\tau d\sigma \sqrt{h} h^{\alpha\beta} \partial_\alpha X^M \partial_\beta X^N g_{MN}\,, \tag{2.4.9}$$

where $h_{\alpha\beta}$ is the metric on the worldsheet and $h = \sqrt{\det(h_{\alpha\beta})}$. Choosing the conformal gauge for $h_{\alpha\beta}$, in which the metric has signature $(+,+)$, the action becomes

$$S_{Pol} = \frac{1}{4\pi\alpha'} \int d\tau d\sigma \left(\partial_\tau X^M \partial_\tau X^N + \partial_\sigma X^M \partial_\sigma X^N\right) g_{MN} \tag{2.4.10}$$

with the Virasoro constraints given by

$$\begin{aligned} \partial_\tau X \cdot \partial_\sigma X &= 0 \\ (\partial_\tau X^M)^2 - (\partial_\sigma X^M) &= 0\,. \end{aligned} \tag{2.4.11}$$

The first constraint is automathically satisfied by the ansatz for the coordinates, while the second one becomes

$$z'^2 + r'^2 = r^2\,, \tag{2.4.12}$$

where the prime symbol denotes the derivative taken respect to σ. The action reads

$$S_{\rm Pol} = \frac{\sqrt{\lambda}}{4\pi}\int d\sigma d\tau\, \frac{z'^2 + r'^2 + r^2}{z^2}\,. \tag{2.4.13}$$

The equation of motions

$$\begin{aligned} z''z - z'^2 + r'^2 + r^2 &= 0 \\ r'' - r - \frac{2r'\,z'}{z} &= 0 \end{aligned} \tag{2.4.14}$$

are solved by

$$r(\sigma) = \frac{R}{\cosh\sigma}\,, \qquad z(\sigma) = R\tanh\sigma \tag{2.4.15}$$

which satisfy also the Virasoro constraint (2.4.12). Geometrically, this solution represents a hemisphere $r^2 + z^2 = R^2$ in the bulk of AdS. In the end, we get the following expression for the action

$$S_{\rm Pol} = \sqrt{\lambda}\int d\sigma\,\frac{r^2}{z^2} = \sqrt{\lambda}\int_{\sigma_\epsilon}^{\infty}\frac{d\sigma}{\sinh^2\sigma} = \sqrt{\lambda}\,(-\coth\sigma)\Big|_{\sigma_\epsilon}^{\infty}\,, \tag{2.4.16}$$

where we have performed the trivial integration over τ. In the integration over σ, we have introduced to regularize the action a cut-off σ_ϵ satisfying the boundary condition

$$z(\sigma_\epsilon) = \epsilon \tag{2.4.17}$$

that leads to $\sigma_\epsilon = \frac{\epsilon}{R} + \mathcal{O}(\epsilon^3)$. Thus, following the procedure illustrated in (2.4.6) to remove the divergent piece from the action, we finally get

$$S_{\rm Pol} = -\sqrt{\lambda} \quad \Rightarrow \quad \langle \mathcal{W}(\mathcal{C})\rangle_{\rm circle} \simeq e^{-S} = e^{\sqrt{\lambda}} \tag{2.4.18}$$

This behavior essentially reproduces the strong coupling expansion of the matrix model achieved using localization. The factor $\lambda^{-3/4}$ in (2.3.12) is recovered by taking into account string fluctuations around the minimal surface [57].

2.5 Operator product expansion expansion of the Wilson loop

When the Wilson loop is probed from a distance much larger than the size of the loop itself, it can approximated by an expansion of local operators [8, 58]

$$\frac{\mathcal{W}(\mathcal{C})}{\langle \mathcal{W}(\mathcal{C})\rangle} = \mathbb{1} + \sum_k c_k R^{\Delta_k}\,\mathcal{O}^{(k)}(x)\,, \tag{2.5.1}$$

where R is the radius of the loop, the $O^{(k)}$ are composite operators with conformal weights Δ_k evaluated at the center of the loop, and c_k are the OPE coefficients that depend on λ. For the Maldacena Wilson loop operator we use the definition

$$\mathcal{W}(\mathcal{C}) = \mathrm{Tr}\,\mathcal{P}\exp\left[\oint_{\mathcal{C}} ds(iA_\mu(x)\dot{x}^\mu + |\dot{x}|\,\theta^i\phi_i(x)\right] . \tag{2.5.2}$$

In perturbation theory the scaling dimension of an operator can be represented as

$$\Delta = \Delta^{(0)} + \Delta^{(1)} + \Delta^{(2)} + \dots , \tag{2.5.3}$$

where $\Delta^{(0)}$ is the free field dimension, and $\Delta^{(1)}, \Delta^{(2)}$ are anomalous dimensions at order g^2, g^4 and so on. Since the symmetries of a CFT constraint the one-point functions of operators that are not the identity to be zero, the expectation value of the Wilson loop corresponds to the coefficient of the identity. The OPE coefficients can be computed perturbatively, but the result cannot be extrapolated to strong coupling. The operators appearing in (2.5.1) must have the same properties as the Wilson loop. Thus, the $\mathcal{O}^{(k)}$ should be bosonic and gauge invariant. Let us analyze the possible contributions to the OPE for some value of the scaling dimension.

- $\Delta = 0$: the only possible contribution comes from operators proportional to the identity;

- $\Delta = 1$: the only elementary fields with scaling dimension one are the scalars. The trace of a single scalar is the only gauge-invariant operator, but since the ϕ_i's are valued in the Lie algebra $\mathfrak{su}(N)$ this contribution vanishes;

- $\Delta = 2$: the only two types of gauge-invariant operators are the chiral primary operators $\mathcal{O}^a$ and the Konishi scalar $\mathcal{K}$. They are canonically normalized as

$$\mathcal{O}^a(x) = \frac{4\sqrt{2}\pi^2}{\lambda} C^a_{ij} :\mathrm{Tr}(\phi^i\phi^j): , \qquad \mathcal{K}(x) = \frac{4\pi^2}{\sqrt{3}\lambda} : \mathrm{Tr}(\phi^i\phi^i) : . \tag{2.5.4}$$

  Here the traceless symmetric tensor C^a_{ij} obeys $C^a_{ij}C^b_{ij} = \delta^{ab}$ with $a, b = 1, ..., 20$. The operators $\mathcal{O}^a$ lie in a short supermultiplet and transform in the **20** irreducible representation of the R-symmetry group $SO(6)_R$. They have vanishing anomalous dimension. The Konishi scalar is the lowest component of the long supermultiplet [59], and it acquires an anomalous dimension in perturbation theory. Its one-loop anomalous dimension is $\Delta^{(1)} = \frac{3\lambda}{4\pi^2}$ [60–67];

- $\Delta = 3$: among the classical operators we must have to consider

$$: \mathrm{Tr}(\phi^i\phi^j\phi^k) :, \qquad : \mathrm{Tr}(\phi^{\{i}\phi^j\phi^{k\}}) :, \qquad J^i_{\mu\nu} =: \mathrm{Tr}(\phi^i F_{\mu\nu}) :, \tag{2.5.5}$$

  where the second one is the chiral primary operator transforming in the **50** of $SO(6)_R$.

Given the expansion (2.5.3) for the scaling dimension, every term R^Δ in (2.5.1) produces logarithmic terms as

$$R^\Delta = R^{\Delta^{(0)}}\left(1 + \Delta^{(1)}\log R + \Delta^{(2)}\log R + \frac{1}{2}\Delta^{(1)^2}\log^2 R + ...\right), \tag{2.5.6}$$

in the limit $R \to 0$ the coefficients of the divergent logarithms $\log R$ is proportional to the one-loop anomalous dimensions of the non-protected operators appearing in the Wilson loop OPE, as the Konishi operator.
The OPE coefficients can be read off from the correlation functions of the Wilson loop with local operators. For instance, we consider CPOs with scaling dimension $\Delta \equiv k$ defined as

$$\mathcal{O}^I_k(x) = \frac{(8\pi^2)^{k/2}}{\sqrt{k}\lambda^{k/2}} C^I_{i_1...i_k} : \mathrm{Tr}(\phi^{i_1}...\phi^{i_k}) :, \tag{2.5.7}$$

where $C^I_{i_1..i_k}$ are totally symmetric and traceless tensors in the indices $i_1...i_k$ normalized as $C^I_{i_1..i_k}C^J_{i_1..i_k} = \delta^{IJ}$. If $k = 2$, we obtain the chiral primary operator $\mathcal{O}^a$ with $\Delta = 2$. One can choose a basis where the two-point correlators of the chiral primaries are unit normalized as

$$\left\langle \mathcal{O}^I_k(x)\mathcal{O}^J_k(y)\right\rangle = \frac{\delta^{IJ}}{|x-y|^{2k}}, \tag{2.5.8}$$

they are protected by supersymmetry and do not receive radiative corrections [68–75]. An expression for correlators of the circular Wilson loop with CPOs (2.5.7) valid for any λ was found in [76] and is given by

$$\frac{\left\langle \mathcal{W}(\mathcal{C})\mathcal{O}^I_k(L)\right\rangle}{\langle \mathcal{W}(\mathcal{C})\rangle} = \frac{2^{k/2-1}}{N}\sqrt{k\lambda}\,\frac{I_k(\sqrt{\lambda})}{I_1(\sqrt{\lambda})}\,\frac{R^k}{L^{2k}}Y^I(\theta), \tag{2.5.9}$$

where I_k and I_1 are modified Bessel functions and $Y^I(\theta)$ are spherical harmonics

$$Y^I(\theta) = C^I_{i_1...i_k}\theta^{i_1}...\theta^{i_k} \tag{2.5.10}$$

with the index I running over all the spherical harmonics of $SO(6)$ Casimir [77]. In the supergravity description, the correlation function of the Wilson loop with

a local operator is determined by an exchange of supergravity modes between the classical string worldsheet and the point of operator insertion on the boundary of AdS. The duals of CPOs are particular linear combinations of spin-zero Kaluza-Klein modes on S^5 of the metric and the anti-symmetric four form. In the $\lambda \to \infty$ limit, expression (2.5.9) reproduces the supergravity result [8]

$$\frac{\left\langle \mathcal{W}(\mathcal{C})\mathcal{O}_k^I(L)\right\rangle}{\langle \mathcal{W}(\mathcal{C})\rangle} = \frac{2^{k/2-1}}{N}\sqrt{k\lambda}\frac{R^k}{L^{2k}}Y^I(\theta). \tag{2.5.11}$$

In the $\lambda \to 0$ limit, (2.5.9) at the leading order reduces to

$$\frac{\left\langle \mathcal{W}(\mathcal{C})\mathcal{O}_k^I(L)\right\rangle}{\langle \mathcal{W}(\mathcal{C})\rangle} = \frac{2^{-k/2}}{N}\frac{\sqrt{k}}{k!}\lambda^{k/2}\frac{R^k}{L^{2k}}Y^I(\theta). \tag{2.5.12}$$

Perturbatively, the leading contribution to the correlation functions of the circular Wilson loop with the chiral primary with the smallest conformal dimension and the Konsishi operator is given by

$$\frac{\langle \mathcal{W}(\mathcal{C})\mathcal{O}^a(L)\rangle}{\langle \mathcal{W}(\mathcal{C})\rangle} = \frac{\lambda}{2\sqrt{2}N}\frac{R^2}{L^4}Y^a(\theta)\,, \qquad \frac{\langle \mathcal{W}(\mathcal{C})\mathcal{K}(L)\rangle}{\langle \mathcal{W}(\mathcal{C})\rangle} = \frac{\lambda}{4\sqrt{3}N}\frac{R^2}{L^4}. \tag{2.5.13}$$

From here we can read the first term in λ that contribute to the OPE coefficents of $\mathcal{O}^a$ and $\mathcal{K}$. Summarizing the lower dimensional content of the local operator expansion, we have

$$\begin{aligned}\frac{\mathcal{W}(\mathcal{C})}{\langle \mathcal{W}(\mathcal{C})\rangle} =& \mathbb{1} + R^{\Delta_\mathcal{K}}\left(\frac{\lambda}{4\sqrt{3}N} + \lambda^2\frac{C_2}{N} + ...\right)\mathcal{K}(x) + \\ &+ R^{\Delta_\mathcal{O}}\left(\frac{\lambda}{2\sqrt{2}N} - \frac{\lambda^2}{48\sqrt{2}N} + ...\right)Y_a(\theta)\mathcal{O}^a(x) + \text{higher scaling dimension}\,,\end{aligned} \tag{2.5.14}$$

the dots indicate higher order terms in λ of the corresponding operator expansion coefficients. The value of C_2 for the Konishi operator is not known, while the OPE coefficient at order λ^2 for the chiral primary operator with $k = 2$ is obtained expanding for small λ the r.h.s of (2.5.9). The scaling dimension of $\mathcal{O}^a$ is $\Delta_\mathcal{O} = 2$ and this operator does not get an anomalous dimension, whereas $\Delta_\mathcal{K}$ receives perturbative corrections and following (2.5.6) one can write

$$R^{\Delta_\mathcal{K}} = R^2\left(1 + \Delta_\mathcal{K}^{(1)}\log R + ...\right)\,. \tag{2.5.15}$$

Chapter 3

$\mathcal{N} = 4$ SYM theory with the insertion of a defect

Many properties of the AdS/CFT correspondence rely heavily on the large amount of supersymmetry or conformal symmetry, making difficult the application to the real world. Thus, any attempt to extend its validity to less symmetric situations is certainly welcome. A quite general possibility to reduce the number of symmetries in a QFT is to introduce a defect or an interface into the game: starting from some (super)conformal theory we can introduce, for example, a domain-wall preserving a subset of the original invariance. In this case, one generally obtains a defect Conformal Field Theory (dCFT), in which new degrees of freedom living on the defect interact non-trivially with the theory in the full space-time. Of central role are dCFT with holographic duals, of which a certain number of examples are known [11–14]. In particular, there exist a certain defect version of $\mathcal{N} = 4$ SYM theory, which possesses a holographic dual [15, 16] given by a D3-D5 system with flux. This chapter is devoted to the description of this system.

3.1 $\mathcal{N} = 4$ dCFT: field theory construction

We consider a defect version of $\mathcal{N} = 4$ SYM theory in which a codimension-one defect is introduced in the game and placed at $x_3 = 0$. It separates the whole space-time into two gauge theories with different gauge groups and central charges. For a positive value of x_3, the gauge group is $SU(N)$ whereas for $x_3 < 0$ we have $SU(N-k)$. The defect is defined by the boundary conditions between the two gauge

theories, and it preserves only a fraction of the total amount of supersymmetry. In addition to the usual action of $\mathcal{N} = 4$ SYM theory, which we will refer to as "bulk" or "ambient" theory, the system has a three-dimensional action describing a hypermultiplet of fundamental fields living on the defect. So far, this action has only been explicitly written down for the case in which $k = 0$ [13]. These defect fields besides self-interactions, are also coupled with the bulk fields [13, 14]. Since this coupling must occur in a supersymmetric way, the four-dimensional supermultiplet must be broken up into sets of fields that, when restricted to the defect, transform like three-dimensional supermultiplets. Under the reduced supersymmetry preserved by the defect, the vector multiplet of the bulk $\mathcal{N} = 4$ theory decomposes into a three-dimensional $\mathcal{N} = 4$ vector multiplet and adjoint hypermultiplet. The bosonic components of the vector multiplet are $(A_j, \phi_7, \phi_8, \phi_9)$, where $j = 0, 1, 2$, while the hypermultiplet consists of $(A_3, \phi_4, \phi_5, \phi_6)$. Since the R-symmetry group is broken down by the defect to $SO(3) \times SO(3) \sim SU(2)_H \times SU(2)_V$, the scalars of the vector multiplet will transform as the **3** of $SU(2)_V$, while those in the hypermultiplet as a triplet of $SU(2)_H$.

3.1.1 Symmetries

The defect breaks several of the original symmetries of the usual $\mathcal{N} = 4$ theory. The unbroken symmetries constitute a subgroup of the conformal group in four dimensions preserving $x_3 = 0$. This condition is preserved by the translations $P_{\hat{\mu}}$ and the Lorentz transformations $M_{\hat{\mu}\hat{\nu}}$, with $\hat{\mu}, \hat{\nu} = 0, 1, 2$, but not by P_3 and $M_{\hat{\mu}3} = -M_{3\hat{\mu}}$. Thus, the four-dimensional Poincaré group is reduced by the presence of the defect to the three-dimensional one. The generator of scale transformations D preserves $x_3 = 0$ as well as the special conformal transformations $K_{\hat{\mu}}$ but not K_3. Thus, the four-dimensional conformal group $SO(2, 4)$ of $\mathcal{N} = 4$ SYM theory is reduced to the three-dimensional conformal group $SO(2, 3)$ by the presence of the defect. The preserved symmetry group does not only act on the directions along the defect, the scale transformation, for example, rescales x_3 as well as the defect directions. Since the supercharges anticommute to translations, and the latter are partially broken, some fraction of supersymmetry has to be broken as well. In particular, we will impose suitable boundary conditions to have a defect which is an half-BPS domain-wall interpolating between $SU(N)$ and $SU(N - k)$. The R-symmetry group is reduced from $SO(6)$ to $SO(3) \times SO(3)$. The full symmetry group

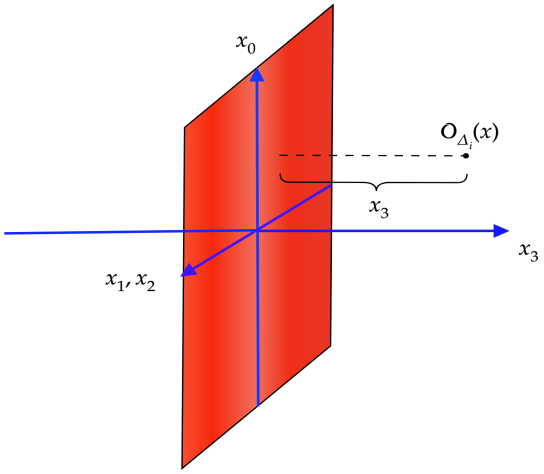

Figure 3.1: Insertion of an operator in the bulk $\mathcal{N} = 4$ theory at a distance x_3 from the defect.

of the system, including both bosonic and fermionic symmetries, is $OSp(4\,|\,4)$.

3.1.2 Correlation functions

In a dCFT correlation functions are less constrained than for a usual CFT since the defect breaks part of the conformal symmetry. In particular, the reduced conformal group allows a non-zero one-point function for composite operators $\mathcal{O}_i$ of the four-dimensional ambient theory. The remaining symmetries fix it up to a constant C [78]

$$\langle \mathcal{O}_{\Delta_i}(x) \rangle = \frac{C}{x_3^{\Delta_i}}, \tag{3.1.1}$$

where x_3 is the distance of the operator from the defect and $x \in \mathbb{R}^4$. Clearly, since translations are broken in the perpendicular direction to the defect, the one-point function depends only on this coordinate. Correlators involving only the operators on the defect have the properties expected from standard 3-dimensional conformal invariance. Another novel features of the dCFT is that two-point functions of operators with unequal scaling dimension can be non-vanishing and are fixed to be of the form

$$\left\langle \mathcal{O}_{\Delta_i}(x) \mathcal{O}_{\Delta_j}(y) \right\rangle = \frac{f(\xi)}{x_3^{\Delta_i} y_3^{\Delta_j}}, \tag{3.1.2}$$

where $f(\xi)$ is a function of the conformal ratio $\xi = \frac{|x-y|^2}{4x_3 y_3}$. If the distance from the defect is large respect to the separations between insertion points of the operators,

the correlation functions in a dCFT should reduce to the corresponding ones in the absence of the defect. Also two-point functions involving a bulk field $\mathcal{O}$ and a defect field $\hat{\mathcal{O}}$ are present

$$\left\langle \mathcal{O}_{\Delta_i}(x)\hat{\mathcal{O}}_{\Delta_j}(\vec{y})\right\rangle = \frac{\mu_{ij}}{x_3^{\Delta_1-\Delta_j}\,|x-(\vec{y},0)|^{2\Delta_j}}, \tag{3.1.3}$$

where $\vec{y}$ is a three-dimensional vector that denotes points along $\mathbb{R}^3$, and μ_{ij} is a bulk-to- boundary coupling.

3.1.3 Vacuum expectation values

A situation where the defect separates two regions of space with different ranks of the gauge group is realised by letting three of the scalar fields of the theory acquiring an expectation value for $x_3 > 0$. For $x_3 < 0$, all classical fields are vanishing. Since Poincaré transformations are broken along x_3, the vacuum expectation value of the scalar fields will depend only on the perpendicular direction to the defect. Thus, we consider the following non-trivial classical vacuum solution [16]

$$A_\mu = 0 \qquad \phi_i = \phi_i(x_3),\ (i=1,2,3) \qquad \phi_m = 0,\ (m=4,5,6). \tag{3.1.4}$$

As we have seen before, preserving all supersymmetries would imply preserving all translation symmetries but it is incompatible with having a boundary at $x_3 = 0$. If we want the defect to be an half-BPS domain-wall, interpolating between the two different gauge groups, we have to impose that the supersymmetry variation of the fermions vanishes. The supersymmetry transformations of the fermionic fields in the usual $\mathcal{N}=4$ SYM theory is

$$\delta_\epsilon \Psi = \frac{1}{2}F_{\mu\nu}\Gamma^{\mu\nu}\epsilon + D_\mu\phi_i\Gamma^{\mu i}\epsilon - \frac{i}{2}\left[\phi_i,\phi_j\right]\Gamma^{ij}\epsilon. \tag{3.1.5}$$

Thus, on a supersymmetric vacuum with the ansatz (3.1.4), one gets the equation

$$\partial_3\phi_i\Gamma^{3i}\epsilon = \frac{i}{2}\left[\phi_i,\phi_j\right]\Gamma^{ij}\epsilon. \tag{3.1.6}$$

It can be rewritten as Nahm's equations that arise frequently as conditions for supersymmetry

$$\frac{\partial\phi_i}{\partial x_3} = -\frac{i}{2}\epsilon_{ijk}\left[\phi_j,\phi_k\right]. \tag{3.1.7}$$

The supersymmetry parameter ϵ has to satisfy the condition

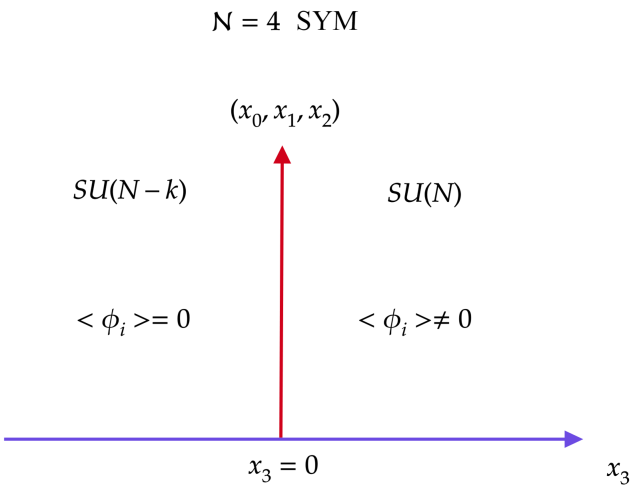

Figure 3.2: Field theory configuration of the set-up.

$$(1 - \Gamma_3\tilde{\Gamma}_{456})\epsilon = 0\,, \tag{3.1.8}$$

where $\tilde{\Gamma}_{i+3} = \Gamma_i$. The Nahm's equations have been introduced in the context of BPS monopoles [79] and they were originally related to D-branes in [80]. Equations (3.1.7) admit a "fuzzy funnel" solution [81] for the vacuum expectation value

$$\langle\phi_i\rangle_{\text{tree}} = \phi_i^{\text{cl}} = -\frac{1}{x_3}t_i \oplus 0_{(N-k)\times(N-k)} \qquad i = 1,2,3\,, \tag{3.1.9}$$

where t_i are the $SU(2)$ generators in a k-dimensional irreducible representation. They satisfy the commutation relations

$$[t_i, t_j] = i\epsilon_{ijk}t_k \qquad i,j,k = 1,2,3\,, \tag{3.1.10}$$

where ϵ_{ijk} is the totally anti-symmetric tensor. An expression for the representation matrices can be found in app. A.

3.2 D3-D5 brane system

The dCFT described in the previous sections is realized in string theory through a D3-D5 branes system [11, 12, 82, 83]. In general, the presence of Dp-branes in addition to the stack of N D3-branes could give rise to source terms in the equation of motions of type IIB supergravity, so that $AdS_5 \times S^5$ is no longer a solution.

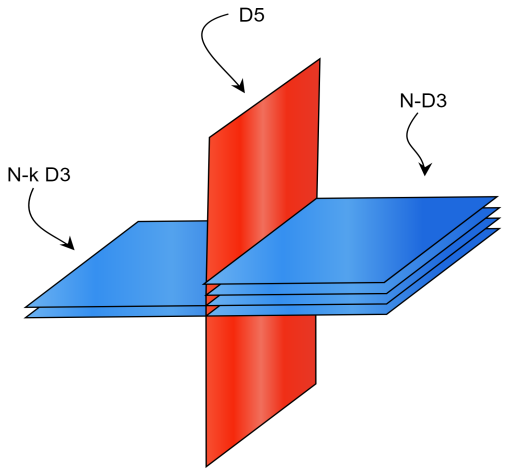

Figure 3.3: D3-D5 system: k of the D3-branes end on the probe D5-brane.

This means that the Dp-branes are backreacting on the geometry generated by the D3-branes and the backreaction may cause a running of the dilaton. The simplest way to analyse the D3-Dp system on the gravity side is to consider the limit where the Dp-branes are treated as probes. Namely, only a small number of Dp-branes is added (usually one or two), while the number N of D3-branes is taken to infinity. To analyze the string realization of the interface gauge theory, we put a single probe D5-brane, whose backreaction can be neglected, on the D3-brane background as realization of the defect. In the D3-D5 probe-system that we are considering, a stack of N D3 branes is intersected by a single probe-D5 and k of the D3 that get dissolved into the D5. Moreover, to ensure the stability of the system we have to require that

$$N >> k >> 1. \tag{3.2.1}$$

3.2.1 Brane construction and near horizon limit

The N D3-branes fill the 0123 directions, while the D5-brane spans 012456, and all the branes sit at the origin of the transverse coordinates. The branes share three directions and their intersection introduces the codimension-one domain wall that separates the vacua of the two different $\mathcal{N} = 4$ theories in the field theory description. Considering the D3-D5 dual system, we can better understand the singular behavior that arises at $x_3 = 0$ in the solution to the Nahm's equations for

	x_0	x_1	x_2	x_3	x_4	x_5	x_6	x_7	x_8	x_9
D3	•	•	•	•						
D5	•	•	•		•	•	•			

Figure 3.4: D3-D5 configuration in the ten dimensional space-time

ϕ_i (3.1.9). This pole comes from the fact that the D3-branes join the D5 exerting a pull on it. Thus, the D5 get distorted into *spikes* or *funnels*. The D3-branes acquire two extra dimensions in the shape of a noncommutative two-sphere, topologically $S^2 \simeq SU(2)$, whose radius goes like $1/x_3$. At the origin, $x_3 = 0$, S^2 decompactifies and the D3 open up into the D5.

If the D5-brane is not present, the D3 system has 16 unbroken supercharges, and $SO(1,3)$ Lorentz symmetry acting on the four coordinates (x_0, x_1, x_2, x_3) and an additional $SO(6)$ acting on the remaining $(x_4, x_5, x_6, x_7, x_8, x_9)$. Introducing the D5-brane, the full D3-D5 system preserves 8 supersymmetries, reduces the four-dimensional Lorentz symmetry to $SO(1,2)$ on (x_0, x_1, x_2) and breaks $SO(6)$ to $SO(3) \times SO(3)$ acting on (x_4, x_5, x_6) and (x_7, x_8, x_9). If we take the perturbative limit

$$g_s << 1 \qquad N >> 1 \quad \text{and} \quad g_s N << 1, \tag{3.2.2}$$

D-branes can be described as hyperplanes where open strings can end. In the D3-D5 system, we have different types of open strings. There are 3-3 open strings that have both the extrema on the stack of D3-branes, which give rise to the degrees of freedom of $\mathcal{N} = 4$ SYM theory. Besides, we find also 3-5 and 5-3 strings stretching between the stack of D3-branes and the single D5-brane, as well as 5-5 strings. In the Maldacena limit, $\alpha' \to 0$, the 5-5 strings living on the D5 decouple from the others. In fact, comparing the 't Hooft coupling λ_{D5} of the probe D5-brane to that of the D3-branes, we obtain the ratio

$$\frac{\lambda_{D5}}{\lambda_{D3}} = \frac{1}{N} 4\pi^2 \alpha' \tag{3.2.3}$$

that vanishes in the $\alpha' \to 0$ limit. The endpoints of 3-5 and 5-3 strings correspond, on the world-volume of the D3-branes, to pointlike excitations in the N or $\bar{N}$ of $SU(N)$. Thus, they transform in the fundamental representation of $SU(N)$. The effective field theories living on the D3-branes are the two $\mathcal{N} = 4$ theories with gauge

groups $SU(N)$ and $SU(N-k)$ separated by a $(2+1)$ defect. The low-energy limit of the 3-5 and 5-3 strings is an interacting hypermultiplet, localized at the intersections of the branes, namely on the defect. If we take into account the opposite regime

$$g_s N >> 1, \qquad g_s << 1, \tag{3.2.4}$$

we can view D3-branes as solutions to type IIB supergravity and in their near-horizon limit generates the $AdS_5 \times S^5$ background. The probe D5-brane, which can still be described as a hypersurface with propagating open 5-5 strings, wraps an equatorial S^2 inside the S^5 and lives on an AdS_4 inside the AdS_5. Thus, the probe-brane is realized as an $AdS_4 \times S^2$ submanifold inside the geometry generated by the D3-branes. The parameter k, which in the field theory is the difference between the ranks of the gauge groups of the two $\mathcal{N}=4$ theories, corresponds to the units of magnetic flux of the gauge field on the D5 through the S^2 sphere. The closed strings and open 5-5 strings living on the D5 describe the gravity side, while the low-energy limit of the 3-3 and 3-5 open strings produces the field theory, and the two systems are dual to each other.
The D5 is embedded in $AdS_5 \times S^5$ as follows: in the near-horizon geometry generated by the D3-branes, the useful coordinates are $(t,\, x_1,\, x_2,\, x_3)$, the radial coordinate r and the angles $\Omega_5 = (\theta, \alpha_1, \beta_1, \alpha_2, \beta_2)$ defined by the relations

$$\begin{aligned} &x_4 = r\, \sin\theta \sin\alpha_1 \cos\beta_1 \quad x_5 = r\, \sin\theta \sin\alpha_1 \sin\beta_1 \quad x_6 = r\, \sin\theta \cos\alpha_1 \\ &x_7 = r\, \cos\theta \sin\alpha_2 \cos\beta_2 \quad x_8 = r\, \cos\theta \sin\alpha_2 \sin\beta_2 \quad x_9 = r\, \cos\theta \cos\alpha_2. \end{aligned} \tag{3.2.5}$$

The metric for the near-horizon geometry in this coordinate system is

$$ds^2_{AdS_5\times S^5} = g_{MN} dx^M dx^N = \frac{r^2}{L^2}(-dt^2 + dx_1^2 + dx_2^2 + dx_3^2) + \frac{L^2}{r^2}(dr^2 + r^2 d\Omega_5^2) \tag{3.2.6}$$

with

$$d\Omega_5^2 = d\theta^2 + \sin^2\theta (d\alpha_1^2 + \sin^2\alpha_1\, d\beta_1^2) + \cos^2\theta (d\alpha_2^2 + \sin^2\alpha_2\, d\beta_2^2). \tag{3.2.7}$$

One can always change coordinates to $r = L^2 u$, such that the metric takes the standard AdS form

$$ds^2_{AdS_5\times S^5} = L^2 \left(\frac{du^2}{u^2} + u^2(-dt^2 + dx_1^2 + dx_2^2 + dx_3^2) + d\Omega_5^2 \right). \tag{3.2.8}$$

The D5-brane sits at $x_3 = 0$ and $\theta = \pi/2$, filling the AdS_4 defined by the coordinates $(t,\, x_1,\, x_2,\, u)$ and wrapping the S^2 parameterized by the angles $(\alpha_1,\, \beta_1)$. The isometry group of the metric (3.2.8) preserved by the D5-brane is $SO(2,3) \times SO(3) \times$

$SO(3)$. The group $SO(2,3)$ acts on the coordinates $(t,\, x_1,\, x_2,\, u)$ and from a field theory perspective is the three-dimensional conformal group. $SO(3) \times SO(3)$ rotates $(\alpha_1,\, \beta_1)$ and $(\alpha_2,\, \beta_2)$, respectively, in the field theory corresponds to the unbroken R-symmetry group.

3.2.2 D5 probe brane

We have seen that the probe D5-brane warps an $AdS_4 \times S^2$ geometry inside $AdS_5 \times S^5$. Considering the metric given in (3.2.8), we can perform another change of variable, $u = 1/y$, to get the following expression for the line element

$$ds^2_{AdS_5 \times S^5} = \frac{1}{y^2}\left(-dt^2 + dx_1^2 + dx_2^2 + dx_3^2 + dy^2\right) + d\Omega_5^2, \tag{3.2.9}$$

where we employ the unit in which the radii of AdS_5 and S^5 are 1. In this unit $\alpha' = 1/\sqrt{\lambda}$. The action of the D5-brane is given by

$$S = -T_5 \int d^6\xi \sqrt{-\det\left(\gamma + \mathcal{F}\right)} + T_5 \int \mathcal{F} \wedge C_4 \,. \tag{3.2.10}$$

The the first term is the Dirac-Born-Infeld action with γ the induced metric and $\mathcal{F} = 2\pi\alpha' F$. The Kalb-Ramond field B is switched to zero, F is the field strength associated to the gauge field on the D5-brane and the ξ's are the world-volume coordinates. The second term is the Wess-Zumino part of the action containing that couples $\mathcal{F}$ with the R-R 4-form

$$C_4 = -\frac{1}{y^4} dx^0 \wedge dx_1^2 \wedge dx_2^2 \wedge dx_3^2 \,. \tag{3.2.11}$$

The D5-brane tension is

$$T_5 = \frac{1}{(2\pi)^5 \alpha'^3 g_s}. \tag{3.2.12}$$

We consider the following ansatz for the solution of the probe D5-brane in the background (3.2.9)

$$y = y(x_3), \qquad \mathcal{F} = -\kappa \sin\alpha_1 d\alpha_1 d\beta_1 \,, \tag{3.2.13}$$

with a constant κ. Focusing on the DBI part of the action, since $\mathcal{F}$ is only turned on along the sphere, $\gamma + \mathcal{F}$ is block diagonal and the determinant factorize. Thus, we can isolate the contribution coming from the S^2 which gives

$$\int_{S^2} d^2\xi \sqrt{\det(\gamma + \mathcal{F})} = 4\pi\sqrt{1 + \kappa^2}. \tag{3.2.14}$$

For the AdS_4 part we just have the contribution coming from the induced metric and following the ansatz (3.2.13) for the radial coordinate y we get

$$\int d^4\xi\sqrt{-\det(\gamma)} = V\int dx_3\frac{1}{y^4}\sqrt{1+(\partial_3 y)^2}, \tag{3.2.15}$$

where V is the volume of the three-dimensional subspace $(t,\ x_1,\ x_2)$, and $\partial_3 = \partial/\partial x_3$. Thus, the full DBI action for the D5-brane reads

$$S_{DBI} = -4\pi T_5 V\int dx_3\frac{1}{y^4}\sqrt{\left(1+(\partial_3 y)^2\right)(1+\kappa^2)}. \tag{3.2.16}$$

The Wess-Zumino part contributes as

$$T_5\int \mathcal{F}\wedge C_4 = 4\pi T_5 V\int dx_3\ \frac{\kappa}{y^4}. \tag{3.2.17}$$

We can now write the full action

$$S_{D_5} = -4\pi T_5 V\int dx_3\frac{1}{y^4}\left(\sqrt{\left(1+(\partial_3 y)^2\right)(1+\kappa^2)}-\kappa\right). \tag{3.2.18}$$

The equations of motion

$$\partial_3\left(\frac{\partial_3 y}{y^4}\sqrt{\frac{1+\kappa^2}{1+(\partial_3 y)^2}}\right)+\frac{4}{y^5}\left(\sqrt{\left(1+(\partial_3 y)^2\right)(1+\kappa^2)}-\kappa\right)=0 \tag{3.2.19}$$

are solved by

$$y=\frac{x_3}{\kappa}, \tag{3.2.20}$$

which fixes the position of the probe-brane inside AdS_5. Thus, the D5-brane intersects AdS_5 along the AdS_4 hyperplane, tilted with respect to the boundary $y=0$ at an angle that depends on κ [11, 16, 84]. Since the D3-branes and the D5 are linked through the fuzzy funnel solutions, we can associate the constant κ appearing in the field strength of the world-volume gauge field to k, the number of D3-branes that get dissolved into the D5

$$k=-\frac{T_5}{T_3}\int_{S^2}\mathcal{F}=\frac{\kappa}{4\pi^2\alpha'}\int_0^{2\pi}d\beta_1\int_0^{\pi}d\alpha_1\sin\alpha_1=\frac{\kappa}{\pi\alpha'}. \tag{3.2.21}$$

Thus, we can write the following relation involving the 't Hooft coupling constant and the flux

$$\kappa=\pi k\alpha'=\frac{\pi k}{\sqrt{\lambda}}. \tag{3.2.22}$$

3.3 Quantum check of AdS/CFT

The parameter k represents a novelty respect to the usual $\mathcal{N}=4$ theory without the defect. It is of central importance since we can take both λ and k large defining the ratio

$$\frac{\lambda}{k^2} \quad \text{fixed}\,, \qquad \lambda \to \infty\,, \quad k \to \infty \tag{3.3.1}$$

which remains small and fixed [16]. The limit $\lambda \to \infty$ makes reliable the supergravity approximation on the string theory side, whereas the assumption of λ/k^2 being small might bring one to the realm of perturbation theory for the field theory side. If both in gauge theory and the gravity theory the observables of interest organize into expansions in powers of λ/k^2, one could try to compare gauge and string results in a situation where both supersymmetry and conformal symmetry are partially broken providing a non-trivial check of the AdS/CFT correspondence.

3.3.1 Tree level one-point functions

One- and two-point functions involving both bulk and defect fields have been analysed in the $k=0$ case [13, 85–88], but the study of correlation functions in the presence of flux is more recent. In [18] was computed the one-point function of the CPOs as defined in (2.5.9)

$$\mathcal{O}_\Delta(x) = \frac{(8\pi^2)^{\Delta/2}}{\sqrt{\Delta}\lambda^{\Delta/2}} C^{i_1\dots i_\Delta} \mathrm{Tr}\left(\phi^{i_1}\dots\phi^{i_\Delta}\right) \tag{3.3.2}$$

at tree level both in the gauge and gravity side. Here Δ is an integer which counts the number of fields and it is also equal to the scaling dimension of the operator which does not depend on the coupling constant. We recall that $C^{i_1\dots i_\Delta}$ is a traceless symmetric tensor such that $C^{i_1\dots i_\Delta} C_{i_1\dots i_\Delta} = 1$. The normalization of $\mathcal{O}_\Delta(x)$ is determined so that the two-point function without the defect is

$$\langle \mathcal{O}_\Delta(x)\mathcal{O}_\Delta(y)\rangle = \frac{1}{|x-y|^{2\Delta}}. \tag{3.3.3}$$

Since the defect preserves the $SO(3)\times SO(3)$ R-symmetry group, only operators that are invariant under $SO(3)\times SO(3)$ can have non-vanishing expectation values and $\Delta \equiv L$ must be even [18]. At tree level in the gauge theory side, using the fuzzy-funnel solution (3.1.9), the one-point function for the chiral primary operator

(3.3.2) inserted at $x_3 = \xi$ reads

$$\langle \mathcal{O}_L(\xi) \rangle = \frac{(2\pi^2)^{L/2}}{\lambda^{L/2}\sqrt{L}} \frac{C_{L/2}}{\xi^L} (k^2-1)^{L/2} k, \tag{3.3.4}$$

where $C_{L/2}$ is a coefficient that changes by the quantum corrections, while the dependence $1/\xi^L$ is fixed by conformal invariance and does not change. The same one-point function can be performed in supergravity approximation, where the scalar fields which correspond to the CPOs come from the fluctuation of the metric and the R-R 4-form. The string configuration dual to a one-point function is that of a string stretching from the insertion point of the dual gauge-theory operator at the AdS_5 boundary and ending on the D5-brane in the interior of $AdS_5 \times S^5$. In the case of a chiral primary, the string can be considered point-like and the one-point function can be computed using a variant of the Witten prescription [5, 18, 21]. Thanks to the double scaling limit, the two quantities can be matched taking $k >> 1$, and they completely agree in the leading order of λ/k^2 series.

3.3.2 Higgsing problem and one loop one-point functions

In order to calculate quantum corrections in the dCFT, the action of $\mathcal{N}=4$ SYM theory (1.1.47) has to be expanded around the classical solution

$$\phi_i = \phi_i^{cl} + \tilde{\phi}_i. \tag{3.3.5}$$

This expansion gives masses to the fields in the action. The mass terms that one finds involve mixing between fields of different flavour as well as mixing between colour components of the same field. This mixing problem was solved in [17, 20], the key point is to use $SU(2)$ representation theory. Moreover, since the VEVs of the scalar fields are proportional to the inverse distance to the defect, the mass terms are unconventional and depend on $1/x_3$. This dependence invalidates many of the traditional tools of QFT in Minkowski space. The problem is solved considering an auxiliary AdS_4 space whose radial coordinate is x_3 with the defect located at its boundary. Via a Weyl transformation, the x_3-dependence can be absorbed to obtain standard AdS_4 propagators, more details are given in app. B. At this point one has all the ingredients to calculate one loop-corrections to the one point functions of chiral primaries operators. In [17, 20] was considered the one-point function of the chiral primary operator

$$\mathcal{O}(\xi) = \mathrm{Tr}\left(Z^L\right)(\xi)\,, \qquad Z(\xi) = \phi_3 + i\phi_6\,. \tag{3.3.6}$$

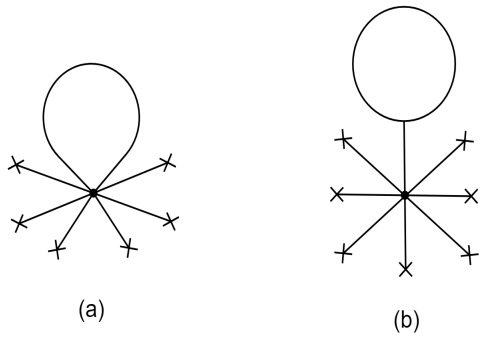

Figure 3.5: Tadpole (a) and lollipop (b) diagrams which contribute to the one-point functions of scalar fields at one-loop order. The operator is represented by a dot and the cross stands for the insertion of the classical solution.

At tree level, the one-point function of $\mathcal{O}$ has been obtained through integrability techniques [21] and is given by

$$\langle \mathcal{O}(\xi) \rangle_{\text{tree}} = -\frac{2}{\xi^L (L+1)} B_{L+1}\left(\frac{1-k}{2}\right), \tag{3.3.7}$$

where L has to be even and $B_{L+1}(u)$ are the Bernoulli polynomials. At one-loop order, there are two possible Feynman diagrams contributions: the tadpole and the lollipop diagram. The latter vanishes if one consider a supersymmetry-preserving renormalisation scheme. The former gives the following contribution

$$\langle \mathcal{O}(\xi) \rangle_{\text{tad.}} = -\frac{\lambda}{16\pi^2} \frac{2L}{\xi^L (L-1)} B_{L-1}\left(\frac{1-k}{2}\right). \tag{3.3.8}$$

The supergravity result found in [18] provides a prediction also for the one-loop correction to the one-point function that in the double scaling limit (3.3.1) and for $\mathcal{O}(\xi) = \text{Tr}(Z^L)(\xi)$ gives

$$\left.\frac{\langle \mathcal{O} \rangle_{\text{1-loop}}}{\langle \mathcal{O} \rangle_{\text{tree}}}\right|_{\text{sugra}} = \frac{\lambda}{4\pi^2 k^2} \frac{L(L+1)}{L-1}. \tag{3.3.9}$$

In the field theory side, using (3.3.7) and (3.3.8), the result is

$$\left.\frac{\langle \mathcal{O} \rangle_{\text{1-loop}}}{\langle \mathcal{O} \rangle_{\text{tree}}}\right|_{\text{gauge}} = \frac{\lambda}{4\pi^2 k^2} \left(\frac{L(L+1)}{L-1} + \mathcal{O}(k^{-2})\right), \tag{3.3.10}$$

where we have used

$$\frac{B_{L-1}\left(\frac{1-k}{2}\right)}{B_{L+1}\left(\frac{1-k}{2}\right)} \underset{k>>1}{\to} \frac{4}{k^2}. \tag{3.3.11}$$

The two computations perfectly matches in the double scaling limit. This result is particularly important since provides a first highly non-trivial check of the gauge-gravity duality in the case of partially broken supersymmetry as well as conformal symmetry. Further investigations are necessary to understand if the gauge theory computation continues to organise into a power series in λ/k^2 at higher loop order or not. Moreover, if one goes to higher loop field on the defect will enter in the computations introducing further challenges.

Chapter 4

Circular Wilson loop in defect $\mathcal{N} = 4$: strong coupling

We have seen in in Chapter 3 that respect to the standard $\mathcal{N} = 4$ SYM theory, the presence of the defect introduces naturally an extra-parameter k. It can be used to define the double-scaling limit. Taking both the 't Hooft coupling constant and k very large, one could try to successfully compare gauge and gravity results, providing a new non-trivial verification of the AdS/CFT correspondence [20]. One-point functions of local operators, both at tree-level and one-loop, match the AdS/CFT predictions accurately in the double-scaling limit. Further studies on the two-point functions, OPE and boundary OPE has been recently performed in [89]. Less attention has been instead devoted to other natural observables that AdS/CFT correspondence can explore in this context, namely Wilson loops. At strong coupling, these operators are evaluated by evaluating the area of the minimal surface spanned by the fundamental string in the supergravity dual with boundary conditions dictated by the contour and the scalar couplings [6, 7]. Their supersymmetric version [90] can be often evaluated exactly through localization techniques, allowing a precise interpolation between weak and strong coupling [10, 56, 57]. In the presence of defects, Wilson loop operators were first considered in [16]: their expectation values have been studied in the double-scaling limit, allowing to compare perturbation theory successfully to the string calculation in the case of quark-antiquark potential [16, 91, 92]. More recently, circular Wilson loops, analog to the supersymmetric ones in ordinary $\mathcal{N} = 4$ super Yang-Mills, have been examined in [24], producing some interesting results. There it was considered a circular Wilson loop of radius R

placed at distance L from the defect and parallel to it, whose internal space orientation has been parameterized by an angle χ. Its vacuum expectation value has been computed both at weak and strong coupling, and, in the double scaling limit and for small χ and small L/R, the results appeared consistent. In this thesis, based on [25], we investigate further the same circular Wilson loop in defect $\mathcal{N} = 4$ SYM theory, generalizing the computations presented in [24] both at strong- and weak-coupling. This chapter and the next one are based on [25].

4.1 Prelude

We would like to study the expectation value of circular Maldacena-Wilson loops in the vacuum configuration described in (3.1.4) and solved by the fuzzy funnel solution (3.1.9) . A natural choice is to center the circle along the x_3 axis at a distance L from the defect, i.e. $\mathcal{C} = (0, 0, 0, L)$. The radius of the circle is R and it extends only along the transverse directions x_1 and x_2, namely

$$x^\mu(\tau) = (0, R\cos\tau, R\sin\tau, L). \tag{4.1.1}$$

The residual $SO(3) \times SO(3)$ symmetry suggests to couple only two scalars to the Wilson loop: one massless ϕ_6 and one massive ϕ_3 and we get

$$\mathcal{W} = \mathrm{Tr}\,\mathcal{P}\exp\left(i\oint d\tau(A_\mu\dot{x}^\mu + i|\dot{x}|(\phi_3\sin\chi + \phi_6\cos\chi))\right), \tag{4.1.2}$$

where the angle χ parametrizes the strength of the coupling with the two scalars. Because of the conformal invariance $\langle\mathcal{W}\rangle$ does not depend separately by L and R but only through the ratio R/L. Moreover the explicit analysis performed in [24] shows that in the absence of the defect our observable is always 1/2 BPS, but in its presence all the supercharges are broken unless $\chi = 0$.

4.1.1 Setting-up the geometric description

As we have seen in section 3.2.1, The AdS_5 is parametrized in Poincarè coordinates where the metric takes the form

$$ds^2_{AdS_5} = \frac{1}{y^2}(-dt^2 + dy^2 + dr^2 + r^2 d\phi^2 + dx_3^2). \tag{4.1.3}$$

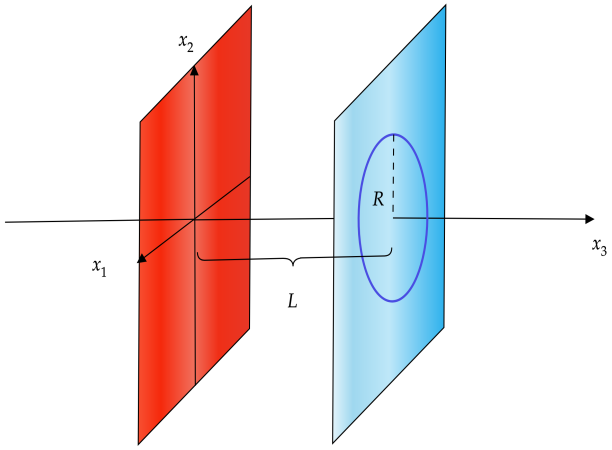

Figure 4.1: Circular Wilson loop of radius R placed on a plane planeparallel to the defect at a distance L from it.

and for the sphere S^5 we write

$$ds^2 = d\theta^2 + \sin^2\theta d\Omega^2_{(1)} + \cos^2\theta d\Omega^2_{(2)}, \tag{4.1.4}$$

where $d\Omega^2_{(i)} = d\alpha_i^2 + \sin^2\alpha_i d\beta_i^2$ denotes the metric of the two S^2 inside the S_5. In these coordinates the $D5$-brane solution wraps the sphere $\Omega_{(1)}$ and its embedding in the target space is given by [16]

$$y = \frac{1}{\kappa}x_3, \qquad \theta = \frac{\pi}{2}, \qquad \alpha_2 = \alpha_2^{(0)} \qquad \text{and} \qquad \beta_2 = \beta_2^{(0)}, \tag{4.1.5}$$

where $\alpha_2^{(0)}$ and $\beta_2^{(0)}$ are two constant values. For a single circular Wilson loop of radius R (parallel to the defect) we expect to find two competing classical string solutions. One is the usual *spherical* dome anchored to the circle on the boundary of AdS_5,

$$y^2(\sigma) + r^2(\sigma) = R^2 \qquad \phi = \tau, \tag{4.1.6}$$

which, however, does not move in the S^5. Alternatively we can consider a second extremal surface stretching from the boundary to the D5-brane. This former is supposed to control the strong coupling behavior of this observable when $\frac{L}{R} \gg 1$, while the latter is expected to dominate the dynamics in the opposite regime, $\frac{L}{R} \ll 1$. To determine the second class of extremal surfaces, following [24], we shall postulate the following ansatz

$$y = y(\sigma), \qquad r = r(\sigma), \qquad \phi = \tau, \qquad x_3 = x_3(\sigma) \quad \text{and} \quad \theta = \theta(\sigma), \tag{4.1.7}$$

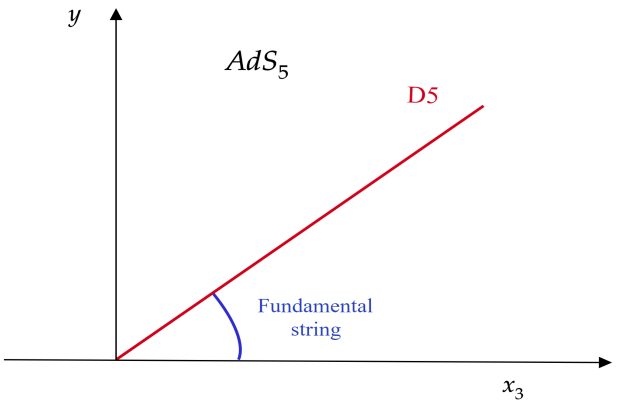

Figure 4.2: The probe D5-brane and the fundamental string in the AdS_5. The probe brane is tilted with respect to the boundary $y = 0$ at an angle that depends on κ.

for which the usual Polyakov action in conformal gauge reduces to

$$S = \frac{\sqrt{\lambda}}{4\pi} \int d\tau d\sigma \frac{1}{y^2}(y'^2 + r'^2 + r^2 + x_3'^2 + y^2\theta'^2). \tag{4.1.8}$$

The Eulero-Lagrange equations of motion for the action (4.1.8) must be paired with the Virasoro constraint

$$y'^2 + r'^2 + x_3'^2 + y^2\theta'^2 = r^2. \tag{4.1.9}$$

At the boundary of AdS_5, which is approached when $\sigma \to 0$, the usual Dirichlet boundary conditions must be imposed:

$$y(0) = 0, \qquad r(0) = R, \qquad x_3(0) = L \quad \text{and} \quad \theta(0) = \chi. \tag{4.1.10}$$

We have also a second set of boundary conditions to be obeyed where the surface intersects the *probe* $D5$ brane. We must require that

$$C_1 \equiv y(\tilde{\sigma}) - \frac{1}{\kappa} x_3(\tilde{\sigma}) = 0, \qquad \theta(\tilde{\sigma}) = \frac{\pi}{2}, \tag{4.1.11a}$$

$$C_2 \equiv y'(\tilde{\sigma}) + \kappa x_3'(\tilde{\sigma}) = 0, \qquad C_3 \equiv r'(\tilde{\sigma}) = 0, \tag{4.1.11b}$$

where $\tilde{\sigma}$ is the maximum value of σ. Eqs. (4.1.11a) and (4.1.11b) simply state that the extremal surface intersects orthogonally the boundary brane.
Since the coordinates x_3 and θ are ciclic variables in the action (4.1.8), their equations of motion immediately translate into two conservation laws

$$x_3'(\sigma) = -cy^2(\sigma) \qquad \text{and} \qquad \theta'(\sigma) = j, \tag{4.1.12}$$

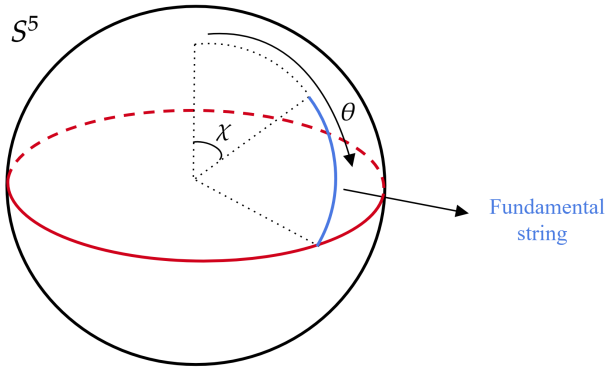

Figure 4.3: The D5-brane and the fundamental string configuration on the S^5.

where j and c are two integration constants to be determined. The equations for $y(\sigma)$ and $r(\sigma)$ are instead

$$yy'' + r'^2 + r^2 - y'^2 + c^2 y^4 = 0 \qquad yr'' - 2r'y' - yr = 0, \tag{4.1.13}$$

where we have used eqs. (4.1.12) to eliminate the dependence on x_3. The conservation laws (4.1.12) also allow us to eliminate the dependence on θ and x_3 in the Virasoro constraint. We get

$$\mathcal{V}(\sigma) \equiv \frac{r^2 - y'^2 - r'^2}{y^2} - c^2 y^2 = j^2. \tag{4.1.14}$$

4.2 General solution for the connected extremal surface

First, we solve the equation (4.1.12) for θ, we find that

$$\theta(\sigma) = j\sigma + \chi, \tag{4.2.1}$$

where we used the b.c. $\theta(0) = \chi$. The second boundary conditions $\theta(\tilde{\sigma}) = \frac{\pi}{2}$ determine the maximum value $\tilde{\sigma}$ of the world-sheet coordinate σ:

$$\tilde{\sigma} = \frac{1}{j}\left(\frac{\pi}{2} - \chi\right). \tag{4.2.2}$$

Next, we focus our attention on the AdS *radial* coordinate $y(\sigma)$ and on $r(\sigma)$ which are determined by the system of coupled eqs (4.1.13). To solve it we find convenient

to introduce the auxiliary function $g(\sigma) \equiv \frac{r(\sigma)}{y(\sigma)}$. Then, with help of eqs. (4.1.13) and the Virasoro constraint $\mathcal{V}(\sigma)$, we find

$$\frac{g''(\sigma)}{g(\sigma)} = 1 - j^2 + 2g^2(\sigma), \tag{4.2.3}$$

a second order differential equation containing only $g(\sigma)$, which can be easily integrated to get the first integral

$$g'(\sigma)^2 + (j^2-1)g(\sigma)^2 - g(\sigma)^4 = -\varepsilon_0 - j^2, \tag{4.2.4}$$

where the arbitrary integration constant has been parameterized as $-\varepsilon_0 - j^2$ for future convenience. This equation can be solved explicitly by quadratures through the method of separation of variables; but for the time being, we will not need the specific form of $g(\sigma)$.

To determine $y(\sigma)$, we can use the Virasoro constraint (4.1.14) where we have eliminated $r(\sigma)$ in favor of $g(\sigma)$ and performed the change of variable

$$y(\sigma) = \frac{1}{\sqrt{1+g^2(\sigma)}z(\sigma)}. \tag{4.2.5}$$

We find that the unknown function $z(\sigma)$ satisfies the differential equation

$$\left(g^2(\sigma)+1\right)^2 z'^2(\sigma) - \varepsilon_0 z^2(\sigma) + c^2 = 0. \tag{4.2.6}$$

Since the first and the last term in the l.h.s. of (4.2.6) are strictly positive this equation can admit real solutions if and only if $\varepsilon_0 \geq 0$. We can now easily integrate (4.2.6) by the method of separation of variables and get

$$z(\sigma) = \frac{c}{\sqrt{\varepsilon_0}}\cosh[v(\sigma)-\eta]. \tag{4.2.7}$$

where the function $v(\sigma)$ is defined by

$$v'(\sigma) = \frac{\sqrt{\varepsilon_0}}{1+g^2(\sigma)}, \tag{4.2.8}$$

combined with the boundary condition $v(0) = 0$. When deriving eq. (4.2.7) we have taken $c > 0$ because $x_3(\sigma)$ must decrease while σ grows (see eq. (4.1.12)).

The parameter η is an arbitrary integration constant. Then the expressions for the original coordinates (y and r) in terms of $g(\sigma)$ and $v(\sigma)$ are given by

$$y(\sigma)=\frac{\sqrt{\varepsilon_0}}{c}\frac{1}{\sqrt{1+g^2(\sigma)}}\text{sech}[v(\sigma)-\eta] \quad \text{and} \quad r(\sigma)=\frac{\sqrt{\varepsilon_0}}{c}\frac{g(\sigma)}{\sqrt{1+g^2(\sigma)}}\text{sech}[v(\sigma)-\eta]. \tag{4.2.9}$$

Finally, the coordinate x_3 is obtained by integrating eq. (4.1.12) with respect to σ. This can be done only in terms of the function $v(\sigma)$ and we obtain In fact if we use the explicit for $y(\sigma)$, we find that the derivative of x_3 can be cast into the following form

$$x_3'(\sigma)=-cy^2(\sigma)=-\frac{\sqrt{\varepsilon_0}}{c}v'(\sigma)\text{sech}^2[v(\sigma)-\eta], \tag{4.2.10}$$

from which we can easily determine the primitive with respect to σ:

$$x_3(\sigma)=x_0-\frac{\sqrt{\varepsilon_0}}{c}\tanh[v(\sigma)-\eta], \tag{4.2.11}$$

where x_0 is another arbitrary integration constant.

Next, we can exploit the boundary conditions in $\sigma=0$ and $\sigma=\tilde{\sigma}$ to determine the different integration constants. Since $g(\sigma)\simeq 1/\sigma$ close to $\sigma=0$, the condition $r(0)=R$ becomes

$$\frac{\sqrt{\varepsilon_0}}{c}\text{sech}\eta=R \qquad \Rightarrow \qquad c=\frac{\sqrt{\varepsilon_0}}{R}\text{sech}\eta \tag{4.2.12}$$

Instead $x_3(0)=L$ translates into

$$L=x_0+R\cosh\eta\tanh\eta \qquad \Rightarrow \qquad x_0=L-R\sinh\eta. \tag{4.2.13}$$

A suitable combination of the remaining three boundary conditions C_i given in (4.2.11) can be used to determine η in terms of L:

$$0=\kappa cC_1+\frac{1}{y(\tilde{\sigma})}C_2+\frac{r(\tilde{\sigma})}{y^2(\tilde{\sigma})}C_3=c(R\sinh\eta-L)=0 \qquad \Rightarrow \qquad \eta=\text{arcsinh}\frac{L}{R}. \tag{4.2.14}$$

Then we are left with two independent boundary conditions in $\sigma=\tilde{\sigma}$ to impose, for instance C_1 and C_3, which can be equivalently written as follows

$$\tanh\left(\eta-v\left(\tilde{\sigma}\right)\right)=\kappa\frac{\text{sech}\left(\eta-v\left(\tilde{\sigma}\right)\right)}{\sqrt{g^2\left(\tilde{\sigma}\right)+1}} \quad \text{and} \quad \tanh\left(\eta-v\left(\tilde{\sigma}\right)\right)=-\frac{g'\left(\tilde{\sigma}\right)}{\sqrt{\varepsilon_0}g\left(\tilde{\sigma}\right)}. \tag{4.2.15}$$

The latter can be solved to determine L/R as function of the two integration constant j^2 and ϵ_0[1]:

$$\operatorname{arcsinh}\frac{L}{R}=\eta=v(\tilde{\sigma})+\tanh^{-1}\left(-\frac{1}{\sqrt{\varepsilon_0}}\frac{g'(\tilde{\sigma})}{g(\tilde{\sigma})}\right). \tag{4.2.16}$$

Then the remaining boundary condition expresses the geometric flux κ in terms of the same variables

$$\kappa=-\frac{g'\left(\tilde{\sigma}\right)}{\sqrt{j^2+\epsilon_0-g^2\left(\tilde{\sigma}\right)}}. \tag{4.2.17}$$

The solution of the boundary conditions can be used to simplify the form of the parametric representation (4.2.9) and (4.1.11) of the extremal surface. We find

$$\begin{gathered}y(\sigma)=\frac{R\cosh\eta}{\sqrt{1+g^2(\sigma)}}\operatorname{sech}[v(\sigma)-\eta]\qquad r(\sigma)=R\cosh\eta\frac{g(\sigma)}{\sqrt{1+g^2(\sigma)}}\operatorname{sech}[v(\sigma)-\eta]\\ x_3(\sigma)=-R\cosh\eta\tanh[v(\sigma)-\eta].\end{gathered} \tag{4.2.18}$$

Finally, we can integrate eq. (4.2.4) to construct the explicit form[2] of the function $g(\sigma)$:

$$g(\sigma)=\sqrt{\frac{j^2-1}{m+1}}\operatorname{ns}\left(\sqrt{\frac{j^2-1}{m+1}}\sigma,m\right), \tag{4.2.19}$$

where

$$m\equiv\frac{j^2-1-\sqrt{\left(j^2+1\right)^2+4\varepsilon_0}}{j^2-1+\sqrt{\left(j^2+1\right)^2+4\varepsilon_0}}. \tag{4.2.20}$$

Since $\varepsilon_0>0$, the modular parameter m is real and spans the interval $(-\infty,0]$. More specifically, from the definition (4.2.20) we get two ranges for m according the value of j^2:

$$(a):\ -\infty<m<-1\quad\text{and}\quad j^2<1\qquad(b):\ -1\leq m\leq 0\quad\text{and}\quad j^2\geq 1. \tag{4.2.21}$$

For $j^2=1$, we obtain $m=-1$ independently of the value of ϵ_0. In the following we find more convenient to replace ϵ_0 with m as a free parameter by solving eq. (4.2.20). We get

$$\varepsilon_0=-\frac{\left(j^2+m\right)\left(j^2m+1\right)}{(m+1)^2}. \tag{4.2.22}$$

[1]Recall that $\tilde{\sigma}=\frac{1}{j}\left(\frac{\pi}{2}-\chi\right)$ is not an independent variable

[2]We are using Wolfram notation for the elliptic functions, e.g. $\operatorname{sn}(\sigma,m)$, $\operatorname{cn}(\sigma,m)$, $\operatorname{dn}(\sigma,m)\ldots$. Next to sn, cn, dn, we can define their inverse $\operatorname{ns}=\frac{1}{\operatorname{sn}}$, $\operatorname{nc}=\frac{1}{\operatorname{cn}}$, $\operatorname{nd}=\frac{1}{\operatorname{dn}}$ and their ratios $\operatorname{sc}=\frac{\operatorname{sn}}{\operatorname{cn}}$, $\operatorname{cs}=\frac{\operatorname{cn}}{\operatorname{sn}}$, ...

The positivity of the integration constant ε_0 combined with the bounds (4.2.21) translates into the following ranges for the new couple of free parameters (m, j^2):

$$\begin{aligned} &\text{REGION (A):}\ -1 \leq m \leq 0 \text{ and } j^2 \geq -\frac{1}{m} \quad \text{or} \\ &\text{REGION (B):}\ m \leq -1 \text{ and } j^2 \leq -\frac{1}{m}. \end{aligned} \tag{4.2.23}$$

4.2.1 Allowed regions for the parameters j, m and $\tilde{\sigma}$

To complete our task, we have to evaluate the integration constants m, j and the maximal value $\tilde{\sigma}$ of the world-sheet coordinate σ, given the distance L from the defect, the angle χ and the flux κ. The latter is easily obtained in terms of χ and j through eq. (4.2.2). Therefore the next natural step would be to solve the highly non-linear system of equations (4.2.16) and (4.2.17) and to compute m and j as functions of $L/R, \chi$ and κ. To begin with, we shall try to solve eq. (4.2.17) for j, or equivalently for the combination

$$x = \sqrt{\frac{j^2-1}{j^2(m+1)}}, \tag{4.2.24}$$

as a function of m, κ and χ. Since $\kappa = \frac{\pi k}{\sqrt{\lambda}} \geq 0$ and $g(\sigma) \geq 0$ (being the ratio of two positive coordinates), eq. (4.2.17) is solved for real values of the parameters if only if $g'(\tilde{\sigma}) < 0$ and

$$g^2(\tilde{\sigma}) \leq -m\frac{(j^2-1)^2}{(m+1)^2}\,. \tag{4.2.25}$$

The bound (4.2.25) ensures that the quantity under the square root in the denominator of (4.2.17) is non-negative. If we use the explicit expression (4.2.19) for $g(\sigma)$, its positivity and the requirement $g'(\tilde{\sigma}) < 0$ can be translated in the following bounds for $\tilde{\sigma}$

$$0 \leq \tilde{\sigma} \leq \sqrt{\frac{m+1}{j^2-1}}\mathbb{K}(m). \tag{4.2.26}$$

Since $\tilde{\sigma}$ can be expressed in terms of χ and j (see eq. (4.2.2)) the inequalities (4.2.26) can be also viewed as constraint on the admissible value of the auxiliary variable x, which replace j in our analysis. We get

$$0 \leq x \leq \frac{\mathbb{K}\,(m)}{\left(\frac{\pi}{2}-\chi\right)}. \tag{4.2.27}$$

The bounds (4.2.23) for j^2 translate into $x \geq 1$ independently of the region. Thus we have the following range of possible values of x:

$$1 \leq x \leq \frac{\mathbb{K}(m)}{\left(\frac{\pi}{2}-\chi\right)}. \tag{4.2.28}$$

Actually the variable x in the region (A) is always less or equal to $\frac{1}{\sqrt{1+m}}$ by construction, therefore in this region the bounds (4.2.28) become

$$1 \leq x \leq \text{Min}\left(\frac{1}{\sqrt{1+m}}, \frac{\mathbb{K}(m)}{\left(\frac{\pi}{2}-\chi\right)}\right). \tag{4.2.29}$$

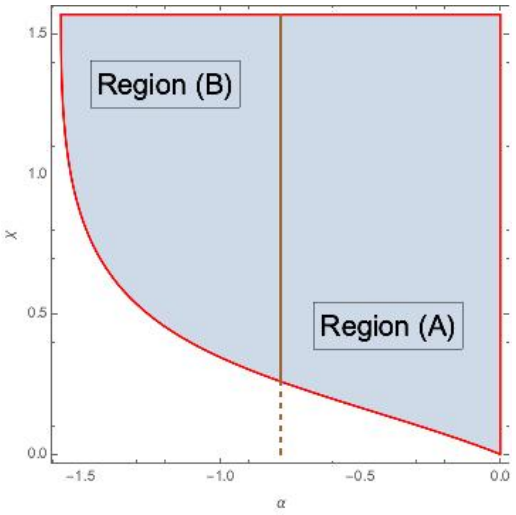

Figure 4.4: The light-blue region with the red boundary defines the allowed region in the (α, χ)-plane.

A necessary condition for the existence of solutions of eq. (4.2.17) is that the admissible intervals (4.2.28) and (4.2.29) for x are not empty, i.e. that the lower bound is smaller or equal to the upper one. If we set $m = \tan\alpha$ with $\alpha \in [-\frac{\pi}{2}, 0]$, we can solve this requirement numerically. The allowed region in the (α, χ)-plane is the area coloured in light blue in fig.4.4 bounded by the red line. The curved boundary in fig.4.4 corresponds to the pairs (α, χ) for which the two extrema either in (4.2.28) or in (4.2.29) coincide.This curve is given by

$$\chi = \frac{\pi}{2} - \mathbb{K}(m) = \frac{\pi}{2} - \mathbb{K}(\tan\alpha). \tag{4.2.30}$$

We have still to impose the constraint (4.2.25), which can be rewritten as follows

$$\text{cn}^2\left(x\left(\frac{\pi}{2}-\chi\right)\middle| m\right) \leq -\frac{1}{m}\left(1-\frac{1}{x^2}\right). \tag{4.2.31}$$

In both the allowed regions the r.h.s. of eq. (4.2.31) takes values between 0 and 1. Therefore the inequality (4.2.31) yields a further (non-trivial) restriction on the range of x. In particular it implies the existence of stronger lower bound $x_0 \geq 1$ for the unknown x that saturates the above inequality

$$-m\,\text{cn}^2\left(x_0\left(\frac{\pi}{2}-\chi\right)\middle| m\right) = 1 - \frac{1}{x_0^2}, \tag{4.2.32}$$

and obeys the bounds (4.2.29) in region (A) and (4.2.28) in region (B). Therefore we have the following two ranges for x

$$\begin{aligned} &\text{REGION (A):} \quad x_0 \leq x \leq \text{Min}\left(\frac{1}{\sqrt{1+m}}, \frac{\mathbb{K}(m)}{\left(\frac{\pi}{2}-\chi\right)}\right) \\ &\text{REGION (B):} \quad x_0 \leq x \leq \frac{\mathbb{K}(m)}{\left(\frac{\pi}{2}-\chi\right)}. \end{aligned} \tag{4.2.33}$$

However these stronger bounds for x does not affect the allowed region in the $(\alpha,\chi)-$plane[3] depicted in fig. 4.4.

We now give a closer look at the eq. (4.2.17) and its solutions when we vary the flux κ. We find more convenient to square it and to write

$$\frac{x^2 \text{cn}\left(\frac{1}{2}x(\pi-2\chi)\middle|m\right)^2 \text{dn}\left(\frac{1}{2}x(\pi-2\chi)\middle|m\right)^2}{\left(m\, x^2\, \text{cn}\left(\frac{1}{2}x(\pi-2\chi)\middle|m\right)^2 + x^2 - 1\right)\text{sn}\left(\frac{1}{2}x(\pi-2\chi)\middle|m\right)^2} = \kappa^2. \tag{4.2.34}$$

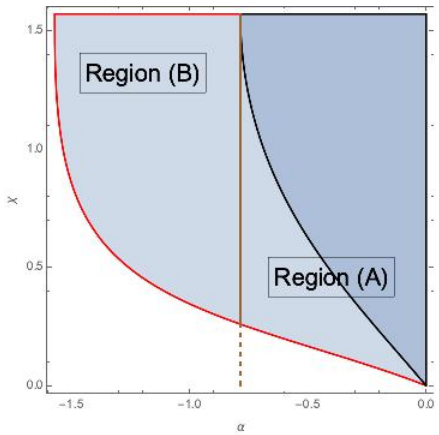

Figure 4.5: The inequality (4.2.35) holds in the region bounded by the black-line.

We can easily argue that this equation cannot be solved for a generic choice of the parameters in the region (A). Given m and χ, eq. (4.2.34) is solved for $\kappa = 0$ if we take $x = \frac{\mathbb{K}(m)}{\frac{\pi}{2}-\chi}$ (namely the value for which $g'(\tilde{\sigma}) = 0$). However, in the region (A) this x is an acceptable solution if and only if

$$\frac{\mathbb{K}(m)}{\frac{\pi}{2}-\chi} \leq \frac{1}{\sqrt{1+m}}. \tag{4.2.35}$$

The inequality (4.2.35) is obeyed in the ligth-blue region on the left of the black curve in fig. 4.5. In the darker region on the right of the black curve we cannot solve eq. (4.2.34) for arbitrary small value of κ. We can equivalently reformulate this obstruction as follows. We fix the flux κ and the angle χ and we increase m starting from its lower bound -1 in the region (A). We will reach a critical value m_c such that (4.2.34) is solved by the largest acceptable value for x, i.e. $x_c = \frac{1}{\sqrt{1+m_c}}$. Then, for $m \geq m_c$, there is no solution of eq. (4.2.34) in the interval (4.2.33).

[3]Requiring that these new intervals are not empty yields the same constraints on χ and α.

Therefore, given κ and χ, the set of allowed parameters is further restricted by the requirement the l.h.s. of (4.2.34) must be less than κ when $x=\frac{1}{\sqrt{1+m}}$:

$$\mathrm{sn}\left(\frac{(\pi-2\chi)}{2\sqrt{m+1}}|m\right)\geq\frac{\sqrt{2}}{\sqrt{m+1+\sqrt{(m-1)^2-4m\kappa^2}}}, \tag{4.2.36}$$

m_c is the value of m that saturates the inequality (4.2.36). In fig. 4.6 we have plotted the curve defined by the equality in (4.2.36) for different value of κ^2. Given a specific value of κ^2, the allowed region is the ligth-blue one below the corresponding curve. This region increase when κ^2 grows and we recover entire region (A) when $\kappa^2=\infty$.

The presence of this critical value m_c has a very simple and nice geometrical interpretation: the distance $L/R=\sinh\eta$ vanishes as $m\to m_c$, namely the Wilson loop touches the defect at $m=m_c$ (see sec. 4.3.1). Thus, for value of m bigger than the critical one there is no physical solution. The red curve separating the allowed region from the forbidden one corresponds to $m=-1/j^2$, namely to choose the integration constant c to vanish. Our family of solutions then coincides with the class of exact solutions discussed by [24]. In fact for this choice parameters our functions can be also written as:

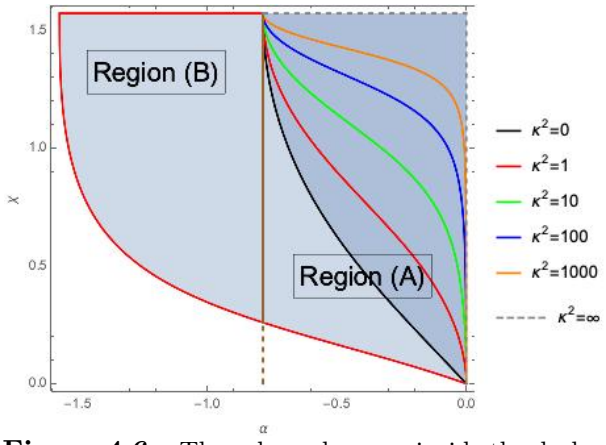

Figure 4.6: The coloured curves inside the darker region correspond to different values of κ^2 . The allowed region for m for fixed value of κ^2 is the one on the left of the relevant coloured curve. The region becomes larger when we increase the flux.

$$\begin{aligned} g(\sigma) =& j\ \mathrm{ns}\left(j\sigma\left|-\frac{1}{j^2}\right.\right)=\sqrt{1+j^2}\,\mathrm{ds}\left(\sqrt{1+j^2}\sigma\left|\frac{1}{1+j^2}\right.\right)\\ h(\sigma) =& \frac{1}{R}g(\sigma)\sqrt{1+\frac{1}{g(\sigma)^2}}=\frac{\sqrt{1+j^2}}{R}\mathrm{ns}\left(\sqrt{1+j^2}\sigma\left|\frac{1}{1+j^2}\right.\right), \end{aligned} \tag{4.2.37}$$

where we use the modular properties of the elliptic trigonometric functions. The solutions (4.2.37) are easily seen to be identical to the ones constructed in [24].

Some specific comments are in order for the two extremal points $\chi=0$ (BPS configuration) and $\chi=\frac{\pi}{2}$.

$\chi = 0$ case: for this choice of the angle governing the coupling of the scalars, the admissible region for m shrinks to a point, $m = 0$ (see fig. 4.6). Consequently the integration constant j^2, which must be always greater than $-1/m$, diverges and $\tilde{\sigma} = \frac{\pi}{2j}$ vanishes. In other words, the space of parameters collapses to a point and no regular connected solution exists for the BPS configuration.

$\chi = \frac{\pi}{2}$ case: at variance with the other values of χ the disconnected solution cannot exist for all distances: in fact when $\frac{L}{\kappa R} = 1$ the disconnected solution touches the brane. If this occurs before the connected solution starts dominating, the phase transition from the disconnected to the connected solution becomes of order 0. Nevertheless, we have checked that the connected solution becomes dominant always before the spherical dome touches the defect.

4.3 The structure of the solutions

4.3.1 The distance from the defect

Once we solved eq. (4.2.34) to obtain x (and thus j) in terms of χ, κ and m, the distance from the defect can be computed through eq. (4.2.16). An analytic expression of this quantity in terms of elliptic integral of the third kind is given in appendix C.

The goal of this section is to determine when we can invert eq. (4.2.16) and determine the last integration constant m as a function of the dimensionless distance L/R, χ and κ. If we keep fixed the angle and the flux, the dependence of $\frac{L}{R} = \sinh\eta$ on m is monotonic (and thus invertible) if $\frac{\partial\eta}{\partial m}$ does not change sign in the allowed region of variation for $m \in [m_0, m_c]$. We can obtain a useful and compact expression for $\frac{\partial\eta}{\partial m}$ in two steps. First, we take the derivative of (C.0.1) with respect to m: the final result is expressed in terms of the elliptic trigonometric functions and the second elliptic integral $\mathbb{E}(\sqrt{n}\tilde{\sigma}, m)$. This last dependence can be liminated with help of the eq. (4.2.34) for the flux: in fact we can use the derivative of this equation to write down the relevant second elliptic integral $\mathbb{E}(\sqrt{n}\tilde{\sigma}, m)$ in terms of elliptic trigonometric functions. The final expression is relatively simple

$$\left.\frac{\partial\eta}{\partial m}\right|_{\chi,\kappa} = \frac{\left[\frac{n^2(n+1)(mn+1)}{1-m} - m(1-m)\left(\partial_m n - \frac{n(n+1)}{1-m}\right)^2\right]\left(\frac{2g(\tilde{\sigma})g'(\tilde{\sigma})}{2mn^2g(\tilde{\sigma})^2+g(\tilde{\sigma})^4-mj^2n^2} + \frac{\pi-2\chi}{j^3}\right)}{4n\sqrt{-(n+1)(mn+1)}}, \tag{4.3.1}$$

where the derivative is taken at constant χ and κ and

$$n \equiv \frac{j^2-1}{m+1}. \tag{4.3.2}$$

In eq. (4.3.1) $\partial_m n$ denotes the derivative of n with respect to m (n depends on m through the explicit factors in its definition and through the implicit dependence present in j^2, which is fixed by solving the flux equation (4.2.34)). It is not difficult to check that the second factor in (4.3.1) is always positive in the range $n \leq g^2(\sigma) \leq -mn^2$. Thus, the sign of (4.3.1) is entirely controlled by the factor between square brackets.

As discussed in subsec. 4.2.1, given the angle χ and the flux κ, we can find a value m_c of m such that no solution exists for $m > m_c$. This critical value m_c solves the equation (see eq (4.2.36))

$$\mathrm{sn}\left(\frac{(\pi-2\chi)}{2\sqrt{m_c+1}}|m_c\right) = \frac{\sqrt{2}}{\sqrt{m_c+1+\sqrt{(m_c-1)^2-4m_c\kappa^2}}}. \tag{4.3.3}$$

We can now easily expand n around m_c and at the leading order we find[4]

$$n = \frac{x^2}{1-(m+1)x^2} = \frac{c_0}{m_c-m} + O(1) \quad \text{with} \quad 0 < c_0 < 1\,, \tag{4.3.4}$$

namely n blows up at $m = m_c$. The bounds on the constant c_0 are equivalent to the fact that x decreases for $m < m_c$. Instead the combination $\sqrt{n}\tilde{\sigma}$ is finite when m approaches m_c (i.e. $\sqrt{n}\tilde{\sigma} \mapsto \frac{\pi-2\chi}{2\sqrt{1+m_c}}$). In this limit it is quite straightforward to show that η vanishes. In fact, the argument of $\tanh^{-1}$ in eq. (4.2.16) behaves as $1/\sqrt{n}$, while $v(\tilde{\sigma})$ vanishes as $1/\sqrt{n}$ (see appendix C).

If we use the above behavior of n close to m_c, we can also check that the derivative of η in m_c and thus of the distance diverges to $-\infty$ as the $\sqrt{n}$. This is consistent with the behaviour of the curves plotted in fig. 4.7. When we decrease m the parameter η increases, i.e. we are moving away from the brane. To understand if this occurs for all the range spanned by m at fixed κ and χ, we shall investigate the sign of $\frac{\partial\eta}{\partial m}$ on the other boundary of the allowed region, namely the red curve in fig. 4.4. The value m_0 lying on this second boundary is determined only by the angle χ and it satisfies

$$\chi = \frac{\pi}{2} - \mathbb{K}(m_0). \tag{4.3.5}$$

[4]The explicit form of c_0 is not relevant at the moment.

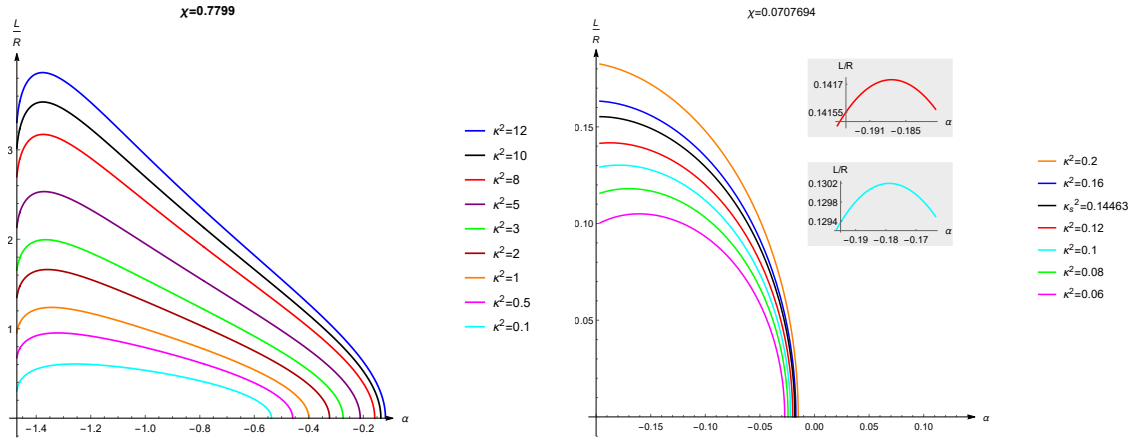

(a) (b)

Figure 4.7: We have plotted the distance L as a function of $\alpha = \arctan(m)$. In (a) we have chosen an angle $\chi > \chi_s$: the different curves corresponds to different value of the flux. All the curves display a maximum. In (b) we have chosen an $\chi < \chi_s$. When we are above the critical flux $\kappa > \kappa_s$ (the black curve), the curves are monotonic. On the contrary, as κ becomes smaller than κ_s (i.e. we are below the black curve) again a maximum appears.

Then the derivative of η with respect to m computed at $m = m_0$ is given by (see app. D for a derivation of this result)

$$\begin{aligned}\left.\frac{\partial\eta}{\partial m}\right|_{m=m_0} &= \frac{(1-m_0)\left(\mathbb{E}(m_0)+(m_0-1)\mathbb{K}(m_0)\right)^2}{2\kappa(1-m_0)(-m_0)^{3/2}\sqrt{1-(\kappa^2+1)m_0}}+\\ &+\frac{m_0\kappa^2\left(1-\left(\mathbb{E}(m_0)+(m_0-1)\mathbb{K}(m_0)\right)^2\right)}{2\kappa(1-m_0)(-m_0)^{3/2}\sqrt{1-(\kappa^2+1)m_0}}\end{aligned} \tag{4.3.6}$$

The sign of this quantity is controlled by the sign of the coefficient of the term linear in κ^2 in the numerator of the second addend of (4.3.6) since the other term is manifestly positive for negative values of m_0. In fig. 4.8 we have plotted the coefficient of κ^2. We recognize that there is a critical value $m_s \simeq -1.45221$ for which this coefficient vanishes, namely

$$(m_s-1)\,\mathbb{K}(m_s)+\mathbb{E}(m_s)+1=0. \tag{4.3.7}$$

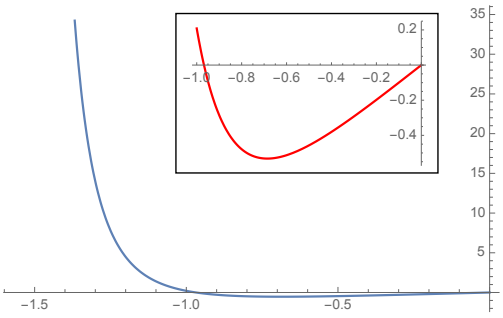

Figure 4.8: Plot of the coefficient of κ^2 in the numerator of the second addend of (4.3.6) (we have set $m_0 = \tan\alpha$ with $\alpha \in (-\pi/2, 0]$). It is negative between zero and and a critical value $m_s = \tan\alpha_s = -1.45221$. For $m < m_s$ the coefficient is always positive.

We can translate m_s into an equivalent critical angle $\chi_s = \frac{\pi}{2} - \mathbb{K}(m_s) \simeq 0.331147$. The angle χ_s separates two distinct regions of parameters:

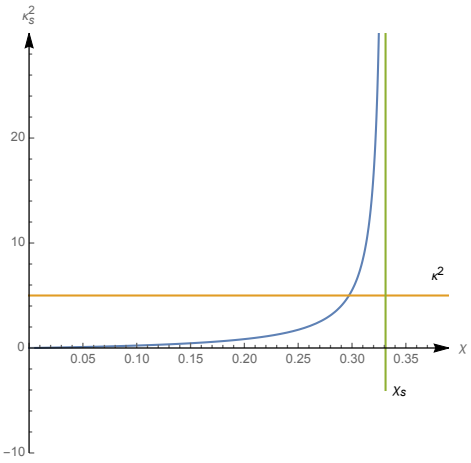

Figure 4.9: The blue curve illustrates the behavior of the critical flux in the interval $[0, \chi_s]$, where it exists. It is a monotonic function of χ and it ranges from 0 to ∞.

(1): $\mathbf{m_0 \leq m_s}$ (or $\boldsymbol{\chi_s \leq \chi \leq \frac{\pi}{2}}$). The coefficient of κ^2 and thus the derivative in $m = m_0$ are positive independently of the value of the flux. Since the same derivative diverges to $-\infty$ on the other extremum of the interval $m = m_c$, the dependence of η on m cannot be monotonic and we cannot invert (4.2.16) on the entire range of the allowed m's. In fact, as illustrated in fig. 4.7 (a), when we decrease m starting from the value m_c defined by (4.3.3) the distance from the brane starts increasing, it reaches a maximum and then decreases to the value reached for $m = m_0$.

(2): $\mathbf{m_s < m_0 < 0}$ (or $\boldsymbol{0 < \chi < \chi_s}$). The derivative of η with respect to m computed at $m = m_0$ is always negative unless the flux κ^2 is below a the critical value κ_s^2 given by

$$\kappa_s^2 = \frac{m_0 - 1}{m_0 \left(\frac{1}{((m_0-1)K(m_0)+E(m_0))^2} - 1 \right)}. \tag{4.3.8}$$

We find more instructive to view this critical flux κ_s^2 defined in (4.3.8) as a function of the angle χ (instead of m_0) by exploiting eq. (4.3.5). If we draw the curve $\kappa_s^2(\chi)$ we obtain the blue curve in fig. 4.9. Given the angle χ (with $0 < \chi < \chi_s$) we can determine a critical value of the flux κ_s by means of the plot 4.9. The black curve in fig. 4.7 (b) displays the behavior of the distance with m for the critical value of the flux: it is monotonic and has vanishing derivative at $m = m_0$. If we choose a flux greater than κ_s (the curves above the black one), the distance is a monotonic function of m, namely its derivative never vanishes. Below this critical value of the flux (i.e. the curves below the black one) the derivatives vanishes just once: namely when we decrease m starting from the value m_c the distance starts increasing, it reaches a maximum and then decreases to the value reached for $m = m_0$.

The presence of a non-monotonic behavior (for a certain range of parameters) is synonymous of the existence of different branches of solutions. In other words, if either $\chi_s \leq \chi \leq \frac{\pi}{2}$ or $0 < \chi < \chi_s$ and $\kappa^2 < \kappa_s^2$, we can find value of the distance for which we can construct two different extremal connected surfaces. We shall come back to this point when we discuss the area of the extremal surfaces.

In both regions ((1) and (2)) there is a maximal distance L_{max} after which the connected solution does not exist. We can determine analytically the value of L_{max} when $0 < \chi < \chi_s$ and we are above the critical flux κ_s. We are in the range of parameters for which η is a monotonic function of m and η_{max} is obtained when we reach the boundary $m = m_0$. If we use the expansion in App. D and substitute into eq. (C.0.1) we find

$$\eta_{\text{max}} = \tanh^{-1}\sqrt{\frac{\kappa^2 m_0}{\kappa^2 m_0 + m_0 - 1}} \quad \Rightarrow \quad L_{\text{max}} = R\sinh\eta_{\text{max}} = R\sqrt{\frac{\kappa^2 m_0}{m_0 - 1}}\,. \tag{4.3.9}$$

If we are below the critical flux or the angle is in the range $[\chi_s, \frac{\pi}{2}]$ the maximal distance from the brane for which the connected solution exists cannot be determined analytically, but only numerically. In fig. 4.10 we have plotted the maximal distance from the brane as a function of χ for different values of the flux κ^2. Given κ^2, we can always find an angle $\chi_{\kappa^2} \in (0, \chi_s]$ for which κ^2 is exactly the critical flux (see fig. 4.9). For angles in the interval $(0, \chi_{\kappa^2}]$, the maximal distance is given by eq. (4.3.9) and is represented by the dashed curves in fig. 4.10. For angles greater than χ_{κ^2}, the behavior of the distance is described by the continuous lines in fig. 4.10. The merge of the two branches of the distance (dashed and continuous) is continuous with its first derivative as one can show by a direct computation of the left and right derivative in χ_{κ^2}[5]. In fig. 4.10, we have drawn the dashed curves also for values greater than χ_{κ^2} to illustrate that two branches are not given by the same function.

The general behavior displayed in fig. 4.10 is quite easy to summarize: the maximal distance increase with χ at fixed κ^2 and increase with κ^2 at fixed angle. The latter behavior is expected: in fact, when κ^2 grows the slope of the brane becomes smaller

[5]The derivative of η with respect to χ admits a very simple form in terms of n and m

$$\left.\frac{\partial\eta}{\partial\chi}\right|_{\kappa,m} = \frac{(m-1)m\partial_m n + (n+1)(2mn+1)}{j\sqrt{-(n+1)(mn+1)}}.$$

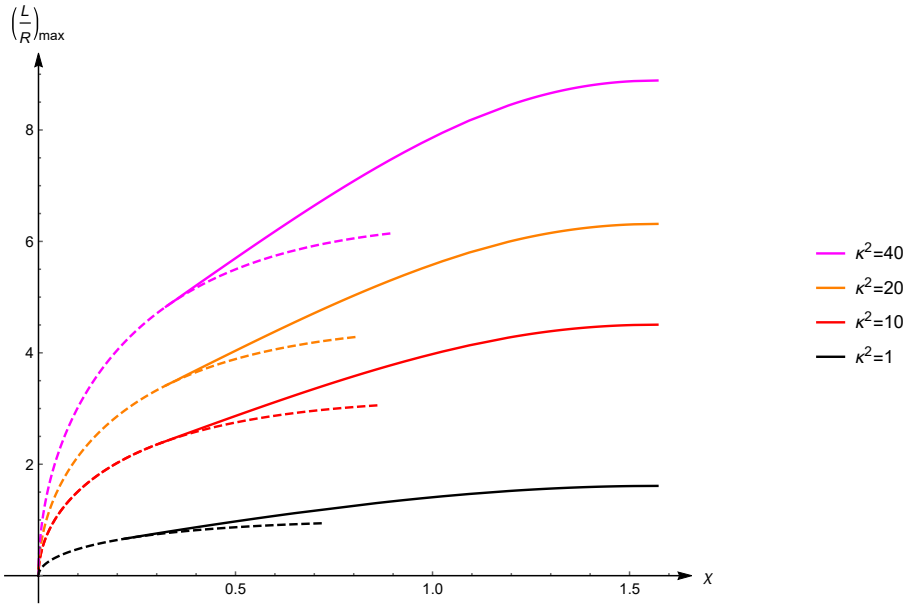

Figure 4.10: The dashed curves are given by (4.3.9) and describe the distance for $\chi < \chi_{\kappa^2}$, while the continuous ones are valid for $\chi > \chi_{\kappa^2}$. Different colors corresponds to different fluxes. We see that the maximal distance grows both with χ and κ^2. We have drawn the dashed curves also for values greater than χ_{κ^2} to show that the merging of the two branches is continuous with its first derivative.

and smaller and the brane is *closer* to the boundary. Therefore the cost in *energy* (*in area*) is low for a larger interval of the distances.

4.3.2 The Area

The regularized area of the connected minimal surfaces is obtained by evaluating the Polyakov action on the classical solution $(r(\sigma), y(\sigma))$:

$$\mathcal{S} = \frac{\sqrt{\lambda}}{4\pi} \int d\tau d\sigma \frac{1}{y^2}(y'^2 + r'^2 + r^2 + c^2 y^4 + j^2 y^2). \tag{4.3.10}$$

We can eliminate the explicit dependence on the integration constants j and c by means of the Virasoro constraint (4.1.14). We find

$$S = \frac{\sqrt{\lambda}}{4\pi} \int_\Sigma d\tau d\sigma \frac{1}{y^2}(y'^2 + r'^2 + r^2 + r^2 - y'^2 - r'^2) = \sqrt{\lambda} \int_{\sigma_\epsilon}^{\tilde{\sigma}} d\sigma \frac{r^2(\sigma)}{y^2(\sigma)} = \sqrt{\lambda} \int_{\sigma_\epsilon}^{\tilde{\sigma}} d\sigma g^2(\sigma), \tag{4.3.11}$$

where we have used that the integrand does not depend on τ to perform the integration over this variable. Remarkably the area depends only on the function $g(\sigma)$.

The integration over σ run from σ_ϵ, the value of σ for which the minimal surface intersects the plane $y=\epsilon$, to $\tilde{\sigma}$, the value of σ for which the minimal surface intersects the brane. The lower extremum σ_ϵ is determined by solving $y(\sigma_\epsilon)=\epsilon$ for small ϵ. At the lowest orders in ϵ we find the following expansion:

$$\sigma_\epsilon = \frac{\epsilon}{R} + \frac{1}{6}(j^2+2)\frac{\epsilon^3}{R^3} + O(\epsilon^4). \tag{4.3.12}$$

Next, we can easily perform the integration over the coordinate σ in terms of the elliptic integral of the second kind and we get

$$\mathcal{S}_\epsilon = \sqrt{\lambda n}\left(\sqrt{n}\sigma - \mathbb{E}\left(\mathrm{am}\left(\sqrt{n}\sigma|m\right)|m\right) - \frac{\mathrm{cn}\left(\sqrt{n}\sigma|m\right)\mathrm{dn}\left(\sqrt{n}\sigma|m\right)}{\mathrm{sn}\left(\sqrt{n}\sigma|m\right)}\right)\Bigg|_{\sigma_\epsilon}^{\tilde{\sigma}}. \tag{4.3.13}$$

The expected ultraviolet linear divergence arises when we evaluate the primitive in the lower extremum. Since the term ϵ^2 is absent in the expansion of σ_ϵ, the lower extremum does not give any non-vanishing contribution in the limit $\epsilon \to 0$. The only contribution to the renormalized area originates from the upper extremum:

$$\mathcal{S}_{\text{ren.}} = \sqrt{\lambda n}\left(\sqrt{n}\tilde{\sigma} - \mathbb{E}\left(\mathrm{am}\left(\sqrt{n}\tilde{\sigma}|m\right)|m\right) - \frac{\mathrm{cn}\left(\sqrt{n}\tilde{\sigma}|m\right)\mathrm{dn}\left(\sqrt{n}\tilde{\sigma}|m\right)}{\mathrm{sn}\left(\sqrt{n}\tilde{\sigma}|m\right)}\right) \equiv \sqrt{\lambda}\hat{\mathcal{S}}_{\text{ren.}}. \tag{4.3.14}$$

The behavior of the renormalized action as a function of the distance from the defect can be investigated by computing its derivative with respect to m at fixed κ and χ. We proceed by following the same two steps performed for the evaluation of $\left.\frac{\partial\eta}{\partial m}\right|_{\kappa,\chi}$ and we get the remarkable identity

$$\left.\frac{\partial\hat{\mathcal{S}}_{\text{ren.}}}{\partial m}\right|_{\kappa,\chi} = \sqrt{-(n+1)(mn+1)}\ \left.\frac{\partial\eta}{\partial m}\right|_{\kappa,\chi}, \tag{4.3.15}$$

namely the derivative of the action and of $\eta-$parameter (the distance) are proportional through a positive definite factor. Thus the derivative of the $\hat{\mathcal{S}}_{\text{ren.}}$ with respect to η or equivalently to L has a very simple form[6]

$$\left.\frac{\partial\hat{\mathcal{S}}_{\text{ren.}}}{\partial L}\right|_{\kappa,\chi} = \frac{1}{R\sqrt{1+\frac{L^2}{R^2}}}\left.\frac{\partial\hat{\mathcal{S}}_{\text{ren.}}}{\partial\eta}\right|_{\kappa,\chi} = \frac{\sqrt{-(n+1)(mn+1)}}{R\sqrt{1+\frac{L^2}{R^2}}} = c(L,\kappa,\chi), \tag{4.3.16}$$

[6]This relation immediately implies that $\mathcal{S}_{\text{ren.}}$ does not depend on L when $c=0$, which apparently contradicts eq. (24) and (25) in [24]. But this is not case. In fact if we keep χ and κ fixed the area [24] does not change with L: it is a function only of χ.

where c is the integration constant appearing in eq. (4.1.12) for x_3. A similar relation was found in [93] for the quark-antiquark potential at finite temperature. There it was speculated that this kind of relation might enjoy some sort of universality.

Because of (4.3.15), the area and the distance possess a similar behavior as functions of m:

(S_1) $\boldsymbol{\chi_s \leq \chi \leq \frac{\pi}{2}}$ or $\boldsymbol{0 < \chi < \chi_s}$ and $\boldsymbol{\kappa < \kappa_s}$: when we move away from the D5-brane by decreasing m from its critical value m_c (corresponding to vanishing distance) both the area and the distance increase and reach their maximum value for the same value of m. Then both decrease up to $m = m_0$ (i.e. the curved red boundary in fig. 4.5).

(S_2) $\boldsymbol{0 < \chi < \chi_s}$ and $\boldsymbol{\kappa \geq \kappa_s}$: both the area and the distance monotonically increase when m is lowered from m_c to m_0.

In fig. 4.11 we have plotted the area as a function of $\alpha \equiv \arctan(m)$ for a fixed angle $\chi = 0.155059$ in the range $0 < \chi < \chi_s$. On the left gray box we have zoomed on the behavior of the area for different value of the flux in the proximity of the value m_0 on the curved red boundary in fig. 4.4. Below the critical value of the flux (black curve) determined by (4.3.8) all the lines possess a maximum, while above κ_s^2 they are monotonically decreasing. However, independently of the flux, all of them terminate in the same point since the boundary value on the red curve in fig. 4.4 does not depend on the flux. On the right gray box we have zoomed in the region close to the brane, the action always diverges when m approaches the values m_c, obtained by solving (4.3.3). The typical behavior of the area in the region $\chi_s \leq \chi \leq \frac{\pi}{2}$ as function of $\alpha = \arctan(m)$ is displayed in fig. 4.12. Independently of κ^2 all the curves terminate on the same point $(m_0, \chi_0 = \frac{\pi}{2} - \mathbb{K}(m_0))$ and possess a maximum for the same value of m for which the distance does (see left gray box).

We conclude this section with an amusing observation about the derivative of the area with respect the two other parameters. It is not difficult to check that both of them can be rewritten in terms of the same derivative of η:

$$
\begin{aligned}
(A_1): \quad & \frac{\partial \mathcal{A}}{\partial \chi} = \sqrt{-(n+1)(mn+1)}\, \frac{\partial \eta}{\partial \chi} - j \\
(A_2): \quad & \kappa \frac{\partial \mathcal{A}}{\partial \kappa} = \sqrt{-(n+1)(mn+1)}\, \kappa \frac{\partial \eta}{\partial \kappa} + \frac{g'(\tilde{\sigma})}{g(\tilde{\sigma})}.
\end{aligned}
\tag{4.3.17}
$$

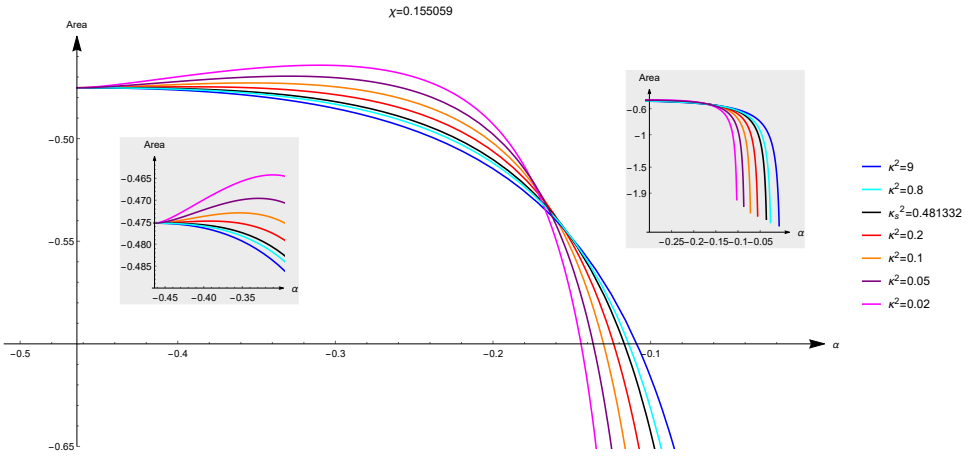

Figure 4.11: We have plotted the behaviour of the area as a function of $\alpha = \arctan(m)$ for a fixed value of the angle χ (below χ_s) but for different values of the flux. On the left we have zoomed the region close to the red curved boundary in fig. 4.4. Independently of κ^2 all the curves terminate on the same point $(m_0, \chi_0 = \frac{\pi}{2} - \mathbb{K}(m_0))$. For values of $\kappa^2 \leq \kappa_s^2$, these curves display a maximum, instead they are monotonic if we are above the critical flux κ_s. On the right we have plotted the same curves in the region close to $m_c = \tan \alpha_c$, namely the value for which the distance from the brane vanishes. The area diverges for all value of the flux.

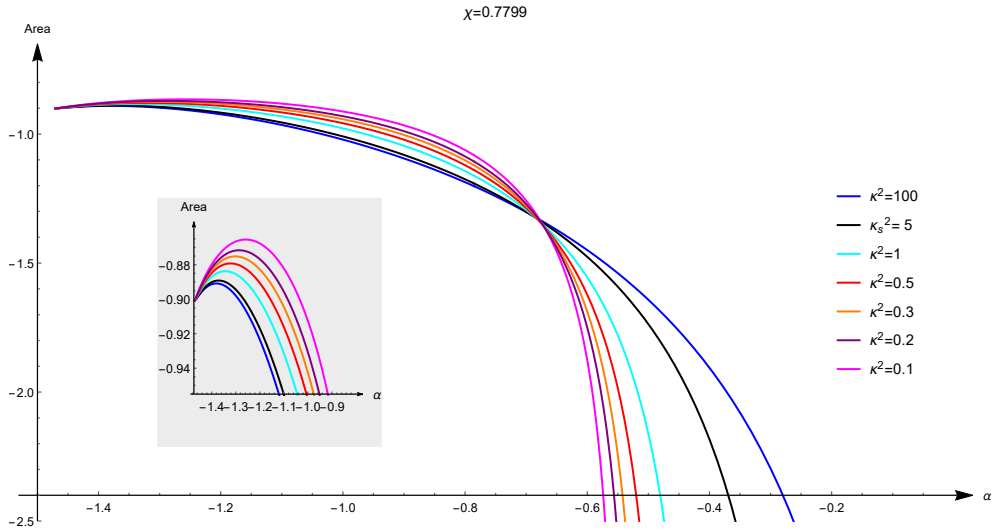

Figure 4.12: We have plotted the behaviour of the area as a function of $\alpha = \arctan(m)$ for a value of the angle above χ_s and for different values of the flux. Independently of κ^2 all the curves terminate on the same point $(m_0, \chi_0 = \frac{\pi}{2} - \mathbb{K}(m_0))$ and display a maximum. On the left we have zoomed in the region close to m_0 to show the presence of a maximum value for the area.

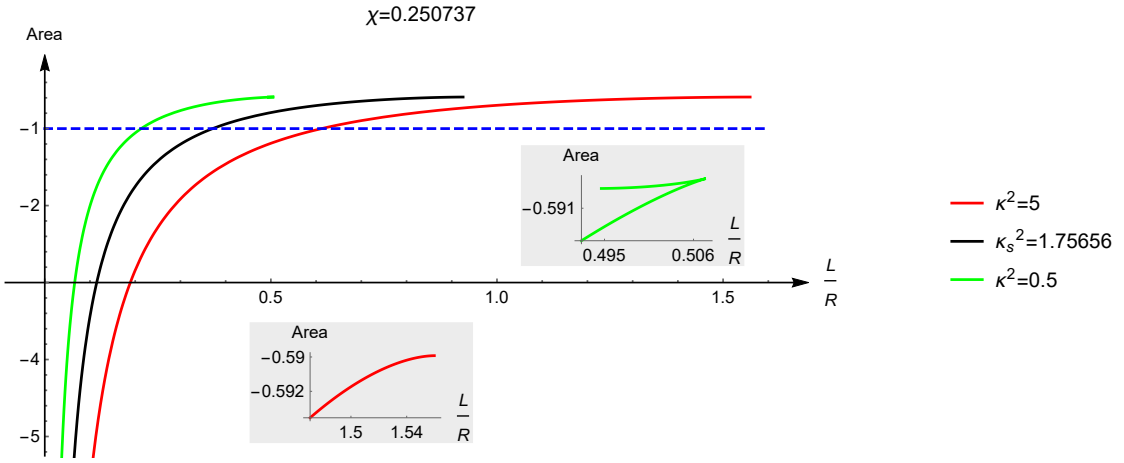

Figure 4.13: This graphic displays the behavior of the area as a function of the distance L/R for a fixed value of the angle $\chi = 0.250737 < \chi_s$. In this range there is a critical flux $\kappa_s^2 = 1.75656$ and the area for this value of the flux is the black curve. Above the critical flux, the typical behavior is given by the red curve, namely the area is a monotonic function of the distance and the solution stops existing after a maximal value of the distance. Below the critical flux, the typical behavior is described, instead, by the green curve. In the latter case there are two branches of solutions. However the upper one is always subdominant. In this plot we normalized the area functional so that the area of the dome is -1.

4.3.3 Transition: connected solution vs dome

To understand when the connected solution becomes dominant with respect to the usual dome we have to plot the area as a function of the distance from the brane. This can be done by exploiting the result of the previous two sections. We have to distinguish two cases depending on the angle χ governing the coupling with the scalars:

$0 < \chi < \chi_s$: Above the critical flux κ_s (represented by the black curve in fig. 4.13) the area is a monotonic function of the distance (see e.g. the red curve in fig. 4.13). If we are approaching from infinity the connected solution starts to exist at certain maximal distance, which depends on χ. The area is larger than the one of the dome, which, therefore, still dominates. While we are getting closer the area keep decreasing and we reach a critical distance where the connected solution and the disconnected one have the same area. In fig. 4.13 the critical distance is realized when the red curve crosses the blue line. After this value of the distance, the connected solution becomes the dominant one: in fact the area keep decreasing

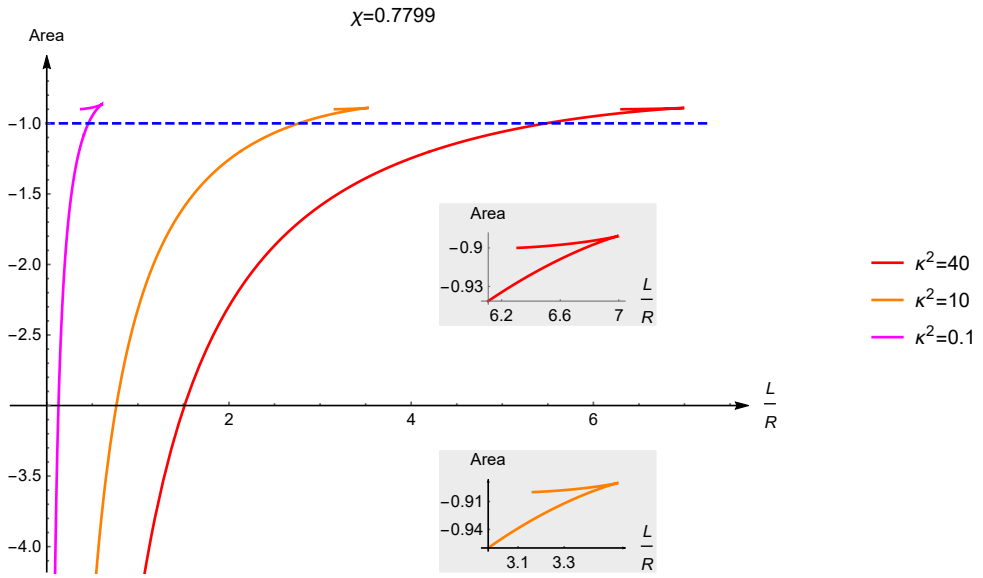

Figure 4.14: This plot displays the behavior of the area as a function of the distance L/R for a fixed value of the angle $\chi = 0.7799 > \chi_s$. For this value of χ there is no critical flux. The typical behavior is described by the three curves (red, orange and purple). There are always two branches of solutions. However, the upper one is always subdominant. In this plot we normalized the area functional so that the area of the dome is -1.

and diverges to $-\infty$ when we reach the brane.

The typical behavior of the area below the critical flux κ_s is described by the green curve in fig. 4.13. There is still a maximal distance, at which the connected solution starts to exist, but when the distance decreases there are two different branches of solutions: namely we have two connected extremal surfaces with the same angle χ, flux κ and distance L. In fig. 4.13, this is clearly displayed in the zoom of the region close to the maximal distance. The upper branch corresponds to the values of the modular parameter m ranging from m_0, lying on the red curved boundary in fig. 4.4, to the value corresponding to the maximal distance. The lower one is instead obtained when m runs from the value corresponding to the maximal distance to m_c, for which the distance from the brane vanishes. The area of the solution in the upper branch, when it exists, is always subdominant with respect to the one in the lower branch. Therefore, we can focus on the latter.

$\chi_s \leq \chi \leq \frac{\pi}{2}$: The behavior of the area as function of the distance in this range of angles is displayed in fig. 4.14. The situation is analogous to what occurs in the

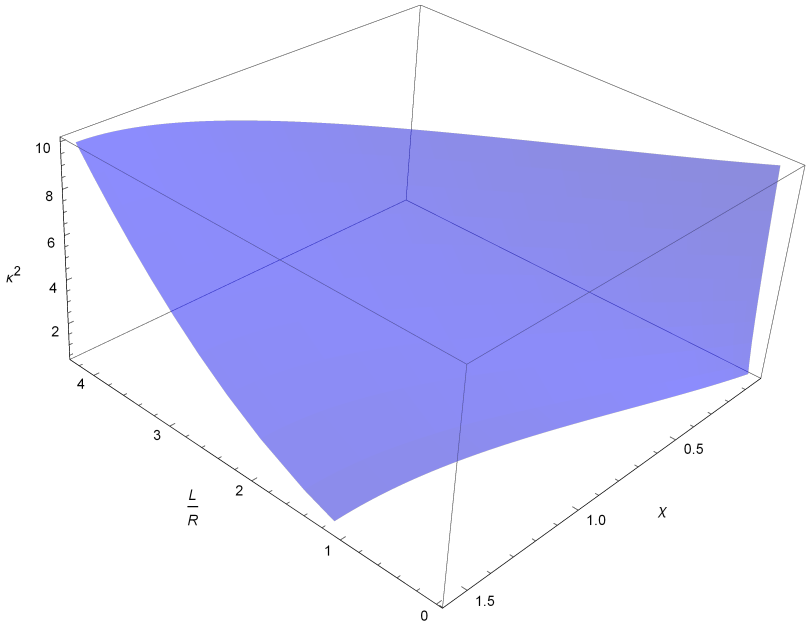

Figure 4.15: In the parameter space $(\chi, L/R, \kappa^2)$ we have plotted the critical surface, namely the set of point for which the area of the connected solution is equal to the one of the dome.

other region below the critical flux. Starting from the maximal distance for which the connected solution exists, we have two families of extremal surfaces when the distance decreases. However, as we can see in in fig. 4.14, the shorter one is always subdominant. The one relevant for us will be the lower branch running from the maximal distance to the brane. The length of the subdominant branch increases with the flux.

In both regions there is always a value of the distance for which the area of the dome is equal to the area of the connected solution and below which the connected solution becomes dominant. In other words we have a phase transition of the Gross-Ooguri type [26]. In fact, above this critical distance, the dominant solution is the usual emisphere and area is constant (the dashed blue line in fig. 4.13 and 4.14). The transition is of the first order since the area is continuous but not its first derivative. In fact, the derivative (4.3.16) for the connected solution is different from zero, whereas for the dome it always vanishes being the area constant.

In fig. 4.15, in the parameter space $(\chi, L/R, \kappa^2)$ we have drawn the critical surface that corresponds to the locus of the first order phase transition for values of the fluxes up to ten and distances up to four. The critical distance increases with the

flux, as one expects. The surface when χ approaches to 0 collapses to a point again suggesting that there is no connected BPS solution.

Chapter 5

Circular Wilson loop in defect $\mathcal{N} = 4$: weak coupling

5.1 Perturbation theory: the non-BPS case

In order to obtain explicit results at perturbative level one should consider field configurations expanded around the supersymmetric vacuum (3.1.4): the determination of the effective propagators and interaction vertices in this background needs a careful and non-trivial diagonalization procedure, that has been presented in [20]. Moreover, limiting the investigation at one-loop order, the form of the three-dimensional boundary Lagrangian is not important and the effect of the defect is entirely encoded into bulk propagators and vertices. The full Wilson loop expectation value is therefore given at this order by the tree-level and one-loop contributions

$$\langle \mathcal{W} \rangle = \langle \mathcal{W} \rangle_{(0)} + \langle \mathcal{W} \rangle_{(1)} \ . \tag{5.1.1}$$

In fact, it is convenient to split the generalized connection $\mathcal{A}$ as

$$\mathcal{A} = \mathcal{A}^{\rm cl} + \tilde{\mathcal{A}} \, , \tag{5.1.2}$$

where $\mathcal{A}^{\rm cl}$ is the tree level term and $\tilde{\mathcal{A}}$ takes into account one-loop contributions which come in two varieties: tadpoles and ladders. The propagator along $\mathcal{C}$ and its classical part can be defined as

$$U(\alpha, \beta) = \mathcal{P} \exp \int_\alpha^\beta d\tau \mathcal{A}(\tau) \qquad U^{\rm cl}(\alpha, \beta) = \mathcal{P} \exp \int_\alpha^\beta d\tau \mathcal{A}^{\rm cl}(\tau) \, . \tag{5.1.3}$$

The classical part of the generalised connection receives contribution from $\phi_3^{\rm cl}$

$$\mathcal{A}^{\rm cl}(\tau) = -R\sin\chi\,\phi_3^{\rm cl} = \frac{R}{L}\sin\chi\left(t_3 \oplus 0_{(N-k)(N-k)}\right)\,, \tag{5.1.4}$$

and the classical propagator reads

$$U^{\rm cl}(0,2\pi) = e^{2\pi\frac{R}{L}\sin\chi\left(t_3\oplus 0_{(N-k)(N-k)}\right)}\,. \tag{5.1.5}$$

The relevant computation has been already presented in [24]: indeed, already at tree-level, they found

$$\langle\mathcal{W}\rangle_{(0)} = {\rm Tr}\left(U^{\rm cl}(0,2\pi)\right) = N-k+\sum_{l=1}^{k} e^{2\pi\frac{R}{L}\sin\chi\,d_{k,l}} = N-k+\frac{\sinh\left(\frac{\pi R\sin\chi}{L}k\right)}{\sinh\left(\frac{\pi R\sin\chi}{L}\right)}, \tag{5.1.6}$$

with $N-k$ corresponding to the standard tree-level contribution for the circular Wilson loop while the second term is the interesting one for the comparison with the connected string result. To perform the trace over the t_3 one has to use the matrix representations given in app. A.

At one-loop, the contribution of tadpole diagrams has the form

$$\langle\mathcal{W}\rangle_{\rm tad} = R\left(\int_0^{2\pi} d\alpha\left(e^{\alpha\frac{R}{L}\sin\chi t_3}\right)_{ij}\left\langle\tilde{\mathcal{A}}(\alpha)\right\rangle_{jl}\left(e^{(2\pi-\alpha)\frac{R}{L}\sin\chi t_3}\right)_{li} + \int_0^{2\pi} d\alpha\left\langle\tilde{\mathcal{A}}(\alpha)\right\rangle_{aa}\right)\,, \tag{5.1.7}$$

where $i,j,..=1,..,k$ and $a=k+1,..,N$ label the matrix elements of t_3 in the upper $k\times k$ block and in the lower $(N-k)\times(N-k)$ block, respectively. The one-point functions of massless gauge fields vanish $\left\langle\tilde{\mathcal{A}}(\alpha)\right\rangle_{aa}=0$. In a supersymmetric-preserving regularization scheme those of the massive fields vanish as well, $\left\langle\tilde{\mathcal{A}}(\alpha)\right\rangle_{ij}=0$, as computed in [17, 20]. Thus, the total contribution to $\langle\mathcal{W}\rangle_{(1)}$ of tadpole diagrams is zero and the one-loop part is given by the ladder diagrams contribution

$$\langle\mathcal{W}\rangle_{(1)} = R^2\int_0^{2\pi} d\alpha\int_\alpha^{2\pi} d\beta\left\langle{\rm tr}\left(U^{\rm cl}(0,\alpha)\tilde{\mathcal{A}}(\alpha)U^{\rm cl}(\alpha,\beta)\tilde{\mathcal{A}}(\beta)U^{\rm cl}(\beta,2\pi)\right)\right\rangle\,. \tag{5.1.8}$$

This contibution can be decomposed into two different terms

$$\langle\mathcal{W}\rangle_{(1)} = W_{(1)}+W_{(2)}\,, \tag{5.1.9}$$

where $W_{(1)}$ contains the standard contribution for the non-broken theory with $N\to(N-k)$ and a term scaling a k^2. Because we want to compare the string result with the perturbative computation, we can safely discard both of them, the latter

being subleading with the others in the large-N limit while the former should come from string solutions that do not end on the D5-brane, not giving $\frac{\lambda}{k^2}$ dependent corrections. The pieces involving the off-diagonal blocks of the generalized connection contribute to $W_{(2)}$ as follows

$$\begin{aligned} W_{(2)} =& R^2 \int_0^{2\pi} d\alpha \int_\alpha^{2\pi} d\beta \sum_{i=1}^{k} e^{\frac{2\pi-\beta+\alpha}{L} R \sin\chi d_{k,i}} \left\langle \tilde{\mathcal{A}}(\alpha)_{ia} \tilde{\mathcal{A}}(\beta)_{ai} \right\rangle + \\ &+ R^2 \int_0^{2\pi} d\alpha \int_\alpha^{2\pi} d\beta \sum_{i=1}^{k} e^{\frac{\beta-\alpha}{L} R \sin\chi d_{k,i}} \left\langle \tilde{\mathcal{A}}(\alpha)_{ai} \tilde{\mathcal{A}}(\beta)_{ia} \right\rangle . \end{aligned} \tag{5.1.10}$$

The free correlators of the scalar and gauge fields with mixed indices are evaluated in terms of the massive scalar propagators [20]. Thus, we have

$$\begin{aligned} \left\langle \tilde{\mathcal{A}}(\alpha)_{ia} \tilde{\mathcal{A}}(\beta)_{aj} \right\rangle = \left\langle \tilde{\mathcal{A}}(\alpha)_{ai} \tilde{\mathcal{A}}(\beta)_{ja} \right\rangle = \delta_{ij}(N-k) \Big[(1-\cos(\beta-\alpha)) K_{\frac{k}{2}}(\alpha,\beta) + \\ + \sin^2\chi \left(\frac{k-1}{2k} K_{\frac{k+2}{2}}(\alpha,\beta) + \frac{k+1}{2k} K_{\frac{k-2}{2}}(\alpha,\beta) - K_{\frac{k}{2}}(\alpha,\beta) \right) \Big] , \end{aligned} \tag{5.1.11}$$

where $K_\nu(\alpha,\beta)$ is the propagator defined in app. B. Following the steps of [24], one obtains

$$W_{(2)} = \frac{g_{YM}^2 (N-k) R}{4\pi L} \int_0^\infty dr\, r \int_{-\pi}^{\pi} d\delta \frac{\sinh\left(\frac{(\pi-\delta)R\sin\chi}{2L} k\right)}{\sinh\left(\frac{(\pi-\delta)R\sin\chi}{2L}\right)} \left(\mathcal{I}_1 + \sin^2\chi \mathcal{I}_2 \right) , \tag{5.1.12}$$

where $\delta = \beta - \alpha - \pi$. More explicitly we have

$$\mathcal{I}_1 = 2\cos\frac{\delta}{2} \sin\left(\frac{2Rr}{L}\right) I_{\frac{k}{2}}(r)\, K_{\frac{k}{2}}(r) , \tag{5.1.13}$$

$$\begin{aligned} \mathcal{I}_2 =& \frac{\sin\left(\frac{2Rr}{L}\cos\frac{\delta}{2}\right)}{\cos\frac{\delta}{2}} \left(\frac{k-1}{2k} I_{\frac{k+2}{2}}(r)\, K_{\frac{k+2}{2}}(r) + \frac{k+1}{2k} I_{\frac{k-2}{2}}(r)\, K_{\frac{k-2}{2}}(r) - \right. \\ & \left. - I_{\frac{k}{2}}(r)\, K_{\frac{k}{2}}(r) \right) . \end{aligned} \tag{5.1.14}$$

As expected these expressions depend on R and L only through the ratio $\frac{R}{L}$. When $\chi \neq 0$ the integrals are very difficult to be performed analytically but, in the limit of large k, they can be evaluated to extract their λ/k^2 behavior. The relevant technique has been already settled in [24], where the focus was on the limit $L/R \to 0$. As far as $\sin\chi \neq 0$ both $\langle \mathcal{W} \rangle_{(0)}$ and $\langle \mathcal{W} \rangle_{(1)}$ exhibit an exponential behavior in k, that can be evaluated elementary in $\langle \mathcal{W} \rangle_{(0)}$ and through a saddle-point approximation in the integrals defining $\langle \mathcal{W} \rangle_{(1)}$. We stress that the ratio R/L can be taken finite in this

computation, sending just the parameter k to infinity[1]. Repeating the same steps as in [24] we end up with

$$\log\langle\mathcal{W}\rangle \simeq -\frac{k\pi R}{L}\left[\sin\chi+\frac{\lambda}{4\pi^2k^2}\left(\frac{\pi}{2}-\chi-\frac{1}{2}\sin 2\chi\right)\sec^3\chi\left(\sin^2\chi+\left(\frac{L}{R}\right)^2\right)+ +O\left(\frac{\lambda^2}{\pi^4k^4}\right)\right]. \tag{5.1.15}$$

We see that a perfect match with the strong coupling result at order $\frac{\lambda}{k^2}$ is obtained, without resorting to any limit on R/L.

5.1.1 Comparing perturbative analysis with the strong coupling analysis

Usually, in the AdS/CFT correspondence, perturbative computations and the supergravity analysis live in opposite regime and cannot be successfully compared. For this class of defect conformal field theories, one can consider a double scaling limit [16, 91] that open a new window. Gravity computations, which are valid for large 't Hooft coupling λ, can be considered for large k in such a way that λ/k^2 is kept small and the results are found to be expressible in powers of λ/k^2. Thus, in this regime, it is possible to successfully compare gauge and gravity results providing further non-trivial verifications of the AdS/CFT correspondence.
In the strong coupling regime, this limit is equivalent to expand our classical solution in power of $\frac{1}{\kappa^2}$, namely for large value of the flux. The flux diverges when the denominator in (4.2.34) vanishes, but the numerator does not. This occurs when x, m and χ satisfy the relation

$$m\,x^2\,\mathrm{cn}\left(\frac{1}{2}x(\pi-2\chi)\middle|\,m\right)^2+x^2-1=0. \tag{5.1.16}$$

Even though we are considering the regime in which κ^2 is very large and eventually diverges, we require that the (adimensional) distance L/R of the Wilson loop from the defect remains finite. The parameter $\eta=\mathrm{arcsinh}\frac{L}{R}$ in terms of x, m and χ is the sum of two positive contributions. In fact, in eq. (4.2.16) the first term is

[1] Of course in so doing we get also other terms, coming from the sinh factors at denominator. It is easy to realize that they could not be produced from the classical connected string solution. we argue that they could be obtained from the one-loop corrections at strong coupling.

the integral of a positive function, while the second one is the $\tanh^{-1}$ of a positive argument. If use the eq. (4.2.34) we can recast the argument of $\tanh^{-1}$ in the following form:

$$\sqrt{\frac{2\kappa^2\,(1-t)}{\kappa^2\,(1-t)-t+\sqrt{\left(\kappa^2\,(1-t)-t\right)^2-4\,(\kappa^2+1)\,mx^4+2}}}, \tag{5.1.17}$$

which allows us to study easily its behavior for large κ^2. Here we define $t \equiv (m+1)x^2$. If the m and x are finite when $\kappa^2 \to \infty$ and the combination $1-(m+1)x^2$ does not vanish, it is straightforward to realize that the quantity in (5.1.17) approaches 1. Therefore its contribution to the distance ($\tanh^{-1}(1)$) diverges. To avoid this conclusion we must require

$$x = \frac{1}{\sqrt{1+m}} + O\left(\frac{1}{\kappa^2}\right) \qquad \kappa \to \infty. \tag{5.1.18}$$

If we use the definition of the unknown x, the above result is equivalent to require that $j^2 = O(\kappa^2)$, therefore we are in the region (A). In this limit, with the help of the expansion (5.1.18), eq. (5.1.16) collapses to

$$\frac{m}{m+1}\,\mathrm{sn}\left(\frac{1}{2\sqrt{1+m}}x(\pi-2\chi)\middle|\, m\right)^2 = 0 \quad \Rightarrow \quad m = 0. \tag{5.1.19}$$

The requirement that the distance is kept finite and different from zero fixes as m must vanishfor large κ: $m = O\left(\frac{1}{\kappa^2}\right)$. Therefore, in this regime we can safely assume the following expansion for the parameters:

$$m = \sum_{n=1}^{\infty} \frac{a_{2n}}{\kappa^{2n}} \qquad\qquad x = 1 + \sum_{n=1}^{\infty} \frac{b_{2n}}{\kappa^{2n}}. \tag{5.1.20}$$

The coefficients can be determined by solving iteratively the equation for the flux and the condition fixing the distance (see app. E). At the lowest order we get

$$m = \frac{\sec^2\chi}{\kappa^2}\left(1-\left(\frac{L^2}{R^2}+1\right)\sec^2\chi\right) + O\left(\frac{1}{\kappa^4}\right) \tag{5.1.21a}$$

$$x = 1 + \frac{1}{2\kappa^2}\left(\frac{L^2}{R^2}+1\right)\tan^2\chi\sec^2\chi + O\left(\frac{1}{\kappa^4}\right). \tag{5.1.21b}$$

The subsequent terms in the expansion are quite cumbersome and their explicit form up to $1/\kappa^4$ is given in app. E. We can now use this expansion (see app. E) to

determine the first two terms in the large κ expansion

$$S = -\frac{\sqrt{\lambda}\kappa R}{L}\left[\sin\chi + \frac{1}{4\kappa^2}\left(\frac{\pi}{2}-\chi-\frac{1}{2}\sin 2\chi\right)\sec^3\chi\left(\sin^2\chi+\frac{L^2}{R^2}\right)\right] + O\left(\kappa^{-2}\right) = \\ = -\frac{\pi k R}{L}\left[\sin\chi + \frac{\lambda}{4\pi^2 k^2}\left(\frac{\pi}{2}-\chi-\frac{1}{2}\sin 2\chi\right)\sec^3\chi\left(\sin^2\chi+\frac{L^2}{R^2}\right) + O\left(\frac{\lambda^2}{\pi^4 k^4}\right)\right], \tag{5.1.22}$$

where we have replaced the strong coupling quantity κ with its expression in terms of $\sqrt{\lambda}$ and the integer flux k. A simple power-counting of the coupling constant immediately shows that these are the only two terms which can be compared with our perturbative computation.

5.1.2 Perturbation theory: the BPS case

At $\chi = 0$, when the Wilson loop only couples to the mass-less scalar ϕ_6 and we are therefore at the BPS point, a dramatic simplification occurs. In fact the non trivial contribution at one-loop reduces to

$$\langle\mathcal{W}\rangle_{(1)} = W_{(1)} + \frac{g_{YM}^2\,(N-k)\,R}{4\pi L} k \int_0^\infty dr\, r \int_{-\pi}^{\pi} d\delta\;\; 2\cos\frac{\delta}{2}\sin\left(\frac{2Rr}{L}\cos\frac{\delta}{2}\right) I_{\frac{k}{2}}(r)\, K_{\frac{k}{2}}(r)\ . \tag{5.1.23}$$

The integral over the angular variable δ can be performed in terms of the Bessel function J_1 and we get

$$\langle\mathcal{W}\rangle_{(1)} = W_{(1)} + \frac{g_{YM}^2\,(N-k)\,R}{4\pi L} 4\pi k \int_0^\infty dr\, r\, J_1\left(\frac{2Rr}{L}\right) I_{\frac{k}{2}}(r)\, K_{\frac{k}{2}}(r)\ . \tag{5.1.24}$$

The radial integral can be now performed in terms of Meijer G Functions:

$$\langle\mathcal{W}\rangle_{(1)} = W_{(1)} + \frac{g_{YM}^2\,(N-k)\,kL}{4\sqrt{\pi}R}\, G^{2,2}_{3,3}\left(\frac{R^2}{L^2}\middle|\begin{matrix}1, 1-\frac{k}{2}, \frac{k+2}{2}\\ \frac{1}{2}, \frac{3}{2}, \frac{1}{2}\end{matrix}\right)\ . \tag{5.1.25}$$

Below, we shall explore two interesting limits of this exact result. First, we investigate the behavior of $\langle\mathcal{W}\rangle_{(1)}$ when the parameter k goes to ∞. This limit is easier to discuss if we step back to the integral form of the result and perform the change of variables $r \to \frac{k}{2}r$

$$\langle\mathcal{W}\rangle_{(1)} = W_{(1)} + \frac{g_{YM}^2\,(N-k)\,R}{4\pi L}\pi k^3 \int_0^\infty dr\, r\, J_1\left(\frac{Rkr}{L}\right) I_{\frac{k}{2}}\left(\frac{kr}{2}\right) K_{\frac{k}{2}}\left(\frac{kr}{2}\right). \tag{5.1.26}$$

Then, we can use the following asymptotic expansions for the product of the modified Bessel functions

$$K_{\frac{k}{2}}\left(\frac{kr}{2}\right)I_{\frac{k}{2}}\left(\frac{kr}{2}\right)=\frac{1}{k(1+r^2)^{1/2}}\sum_{n=0}^{\infty}\frac{2^{2n}}{k^{2n}}\sum_{m=0}^{2n}(-1)^m U_{2n-m}((1+r^2)^{-\frac{1}{2}})U_m((1+r^2)^{-\frac{1}{2}}), \tag{5.1.27}$$

which is obtained by combining the expansion 10.41.3 and 10.41.4 of [94]. The $U_n(x)$ are polinomuials that can be constructed recursively (see sec. 10.41 in [94] for details): $U_0(x)=1, U_1(x)=\frac{x}{8}-\frac{5x^3}{24},\dots$. If we are interested at the leading order in k, it is sufficient to consider the first term in the expansion:

$$\begin{aligned}\langle\mathcal{W}\rangle_{(1)}\simeq W_{(1)}+\frac{g_{YM}^2\,(N-k)\,R}{4L}k^2\int_0^\infty dr J_1\left(\frac{Rkr}{L}\right)\frac{r}{(1+r^2)^{1/2}}=\\ =W_{(1)}+\frac{g_{YM}^2\,(N-k)\,L}{4R}\frac{2}{\sqrt{\pi}}G^{2,1}_{1,3}\left(\frac{k^2R^2}{4L^2}\middle|\begin{matrix}1\\ \frac{1}{2},\frac{3}{2},\frac{1}{2}\end{matrix}\right)=\\ =W_{(1)}+\frac{g_{YM}^2\,(N-k)\,L}{4R}\left(1+O\left(\frac{1}{k^2}\right)\right).\end{aligned} \tag{5.1.28}$$

The BPS circle does not possess the correct scaling to match a potential connected string solution. Its expansion does not organize in a series in λ/k^2. This corroborates the absence of a connected solution in the BPS case.

The second limit we shall consider is $R\to 0$, namely when we shrink the loop to a point. Since we are dealing with a conformal field theory, it is the dimensionless combination $x=R/L$, which approaches 0. We find

$$\begin{aligned}\langle\mathcal{W}\rangle_{(1)}=W_{(1)}+\frac{g_{YM}^2k(N-k)}{4}\left[1-\frac{1}{4}\left(1-k^2\right)x^2\left(\psi\left(\frac{k+1}{2}\right)+\gamma_E+\log x-\log 2\right)-\right.\\ \left.-\frac{x^2}{2}+O\left(x^4\right)\right].\end{aligned} \tag{5.1.29}$$

As expected, the leading term scales as a constant in this limit, and when combined with $W_{(1)}$ it reconstructs at this order the circular operator in absence of the defect. The next term in the expansion can be easily understood in terms of the operator product expansion of the circular BPS Wilson loop. In absence of the defect, when the radius R of the circle shrinks to zero, we can write that (see sec. 2.5)

$$\frac{\mathcal{W}}{\langle\mathcal{W}\rangle_0}=\mathbb{1}+\sum_k c_k R^{\Delta_k}\mathcal{O}^{(k)}(x), \tag{5.1.30}$$

where $\mathcal{O}^{(k)}(x)$ is a local operator of scaling dimension Δ_k evaluated at the center of the circle. The constant c_k are the Wilson coefficients and depends on the coupling constant. The expansion is normalized using the vacuum expectation value (VEV) $\langle\mathcal{W}\rangle_0$ in the absence of the defect. At the lowest order, namely if we consider operators with classical dimension less or equal to 2, the above expansion is given by (2.5.14) together with the definitions (2.5.4)

$$\begin{aligned}\frac{\mathcal{W}}{\langle\mathcal{W}\rangle_0} = \mathbb{1} + R^{\Delta_K}\left[\frac{\pi^2}{3N} + \frac{4\pi^2 C_2\lambda}{\sqrt{3}N} + \cdots\right]\mathrm{Tr}(\phi^i\phi_i) + \\ + R^{\Delta_O}\left[\frac{2\pi^2}{N} - \frac{\lambda\pi^2}{12N} + \cdots\right] Y_a C^a_{ij}\mathrm{Tr}(\phi^i\phi^j) + \text{higher scaling dimension.}\end{aligned} \tag{5.1.31}$$

In (5.1.31) the dots denotes the higher order terms in λ^2 in the expansion of the Wilson coefficient. The Wilson coefficient at order λ in (5.1.31) for the chiral primary operator is obtained expanding the r.h.s of (2.5.9) for λ small. The coefficient C_2 for the Konishi operator is not know. For the definition of C^a_{ij} and Y^a see app. G. Thus, at this order (leading in N) we find

$$\begin{aligned}\frac{\langle\mathcal{W}\rangle_{\text{defect}}}{\langle\mathcal{W}\rangle_0} =& \mathbb{1} + x^2(1+\Delta^{(1)}\log x)\frac{\pi^2}{3N}(-\frac{1}{4}k(1-k^2) + L^2\langle\mathrm{Tr}(\phi^i\phi_i)\rangle_{1-\text{loop}}) - \\ & - x^2\frac{\lambda k(1-k^2)}{\sqrt{3}N}C_2\pi^2 + \frac{2x^2\pi^2}{N}\left[\frac{k(1-k^2)}{24} - \frac{\lambda k}{16\pi^2}\right] - x^2\frac{\lambda k(1-k^2)\pi^2}{288N} + \cdots,\end{aligned} \tag{5.1.32}$$

where $\Delta^{(1)} = \frac{3\lambda}{4\pi^2}$ is the one-loop correction to the anomalous dimension of the Konishi operator. Substituting in (5.1.32) the expression for $\langle\mathrm{Tr}(\phi^i\phi_i)\rangle_{1-\text{loop}}$ given in app. (G), we get

$$\begin{aligned}\frac{\langle\mathcal{W}\rangle_{\text{defect}}}{\langle\mathcal{W}\rangle_0} = \mathbb{1} + x^2\Bigg[&-\frac{\lambda}{16N}k(1-k^2)\log x - \frac{\lambda k}{8N} - \\ &-\frac{\lambda}{16N}k\left(1-k^2\right)\left(\psi\left(\frac{k+1}{2}\right) + \gamma_E - \log 2 + \frac{5}{6}\right) - \\ &- \frac{\lambda\pi^2}{288N}k(1-k^2) - \frac{\lambda C_2\pi^2}{\sqrt{3}N}k(1-k^2)\Bigg].\end{aligned} \tag{5.1.33}$$

The quantity between the square brackets matches the expansion of the Wilson loop given in (5.1.29) if

$$C_2 = -\frac{15+\pi^2}{96\sqrt{3}\pi^2}\,. \tag{5.1.34}$$

Thus, from the OPE for the Wilson loop in the defect case we give a prediction for the Wilson coefficient of the Konishi operator at order λ^2 in (2.5.14). This prediction could be verified performing the two-loop point-function of the Konishi operator with the circular Wilson loop.

It is intriguing also to consider the expansion of eq. (5.1.28) in the limit $L \to 0$ namely $x \to \infty$. In this limit the Wilson loop gets closer to the defect. For odd value of k we find an expansion in inverse odd power of x:

$$\langle \mathcal{W} \rangle_{(1)} = W_{(1)} + \frac{g_{YM}^2 (N-k)}{4} \left[\frac{1}{x} - \frac{3}{(8-2k^2)\, x^3} + O\left(\left(\frac{1}{x} \right)^4 \right) \right] \tag{5.1.35}$$

For even k we have also logarithmic corrections that start at the order x^{-k-1}. For instance, if $k=4$ we find

$$W_{(1)} + g_{YM}^2 (N-4) \left[\frac{1}{4x} + \frac{1}{32x^3} + \frac{3(120 \log(8x) - 289)}{8192 x^5} - \frac{25(168 \log(8x) - 367)}{65536 x^7} + \right. \\ \left. + O\left(\frac{1}{x^8} \right) \right] . \tag{5.1.36}$$

It would be intriguing to interpret this result as an OPE of the Wilson loop in terms of the defect operators, but this expansion appears to depends crucially on k. For odd k we should have only protected operators, while for even k also non protected operators enter in the expansion. This different behavior makes the above interpretation quite puzzling.

Chapter 6

Correlator of two circles in the defect case

The study of a single circular Wilson loop in $\mathcal{N} = 4$ SYM theory in the presence of a defect, considered in the previous chapters, can be extended to the case in which two circles are inserted in the set-up realized by the D3-D5 intersection.

In the usual $\mathcal{N} = 4$ SYM theory with no defect present, Gross and Ooguri pointed out that the correlator between two circles experiments a sort of phase transition [26]. This is because the area of the surface bounded by the two loops can have two competing saddle points. The minimal surface can have the topology of an annulus connecting the two circles or can consist of two separated disk solutions that interact among themselves by the exchange of light supergravity modes. The two-point function of two concentric circular Wilson loops with the same constant internal space orientation has been studied both for equal [95] or different radii [96]. In [93] the correlator of Wilson loops with the same radii is examined at both zero and finite temperature. The result is that for large separation between the two loops, the preferred configuration is the one given by separated surfaces. In fact, the area of the annulus increases with the separation between the loops and becomes energetically less favourite. In [97] this study further generalizes to concentric loops with both spacial and internal separation. From a perturbative point of view, to analyze this phase transition, in principle, one has to sum all planar diagrams. Thus, if one consider the strong coupling limit of the ladder diagrams resummation does not expect to match the string theory computation because the interacting diagrams are not taken into account. Nevertheless, it is possible to find a qualitative matching since the ladders resummation presents a phase transition that resembles the Gross-Ooguri transition [97–99].

If we consider the same two-point function for the circles in the defect case, the situation becomes more intricate but even intriguing. In the D3-D5 system, besides the two different saddle points described above, the minimal area configuration can be given by two connected cylindrical surfaces, or we can also have an intermediate case with a cylindrical surface for one of the loops and a disk for the other one. If we choose two loops with equal radii, we can describe them in terms of the flux κ, the distance from the defect L/R, the angle χ, that in principle can be different for the two circles, and the relative distance h/R between them.

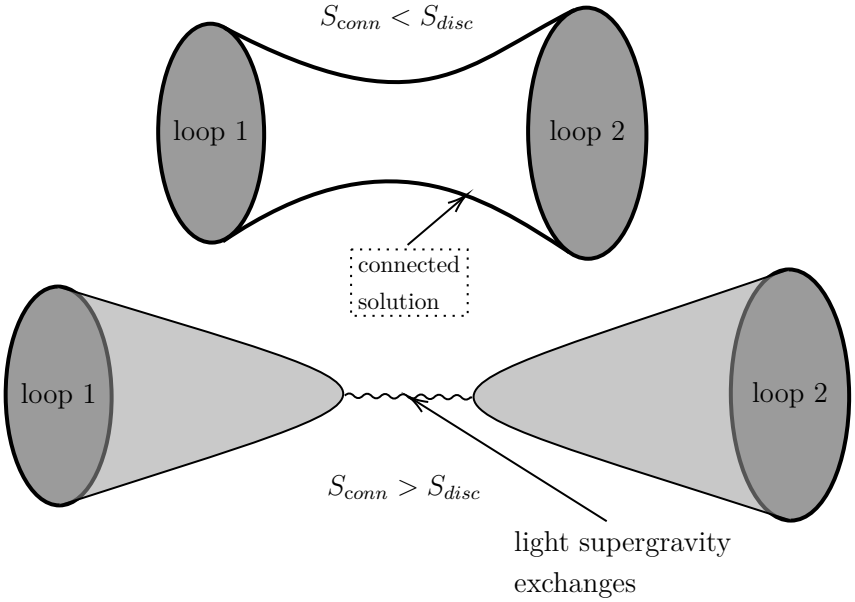

Figure 6.1: Gross-Ooguri phase transition without the defect: when the two circles are close enough, the minimal surface has the topology of an annulus. Above a critical separation distance, the connected surface becomes unstable, and the disconnected solution starts to dominate. In the latter case, the connected correlator is saturated by lightest supergravity modes exchanges.

6.1 String solutions between two concentric circles without the defect

In this section we briefly review the results obtained for the connected minimal surface corresponding to the fundamental string world-sheet stretched between

two concentric circles located at the boundary. To be more general as possible, we consider two circles of radii R_1 and R_2 separated by a distance h along the x_3 coordinate in AdS_5. Moreover, we allow the loops to possess also an internal separation parametrized by the angle γ in the S^5. This configuration considered in [97] provides a generalization of the computations given in [93, 95, 96, 100]. Indeed, from our set of solutions one can recover the configurations found in [98] by setting $\gamma = 0$. The connected correlation function of two Wilson loops in $\mathcal{N} = 4$ SYM at strong coupling is given by the minimal area of a surface in $AdS_5 \times S^5$ whose boundaries are the two circles C_1 and C_2

$$\langle W(C_1)\, W(C_2)\rangle_{\text{conn}} = \exp\left(-S_{\text{NG}}\right). \tag{6.1.1}$$

We consider the metric

$$ds^2_{AdS_5\times S^5} = \frac{1}{y^2}(-dt^2 + dy^2 + dr^2 + r^2 d\phi^2 + dx_3^2) + d\Omega_5^2\,, \tag{6.1.2}$$

where $d\Omega_5^2$ is given in (4.1.4). The ansatz for the string embedding is the same of (4.1.7), and the Nambu-Goto action that describes the world-sheet reads [1]

$$S_{\text{NG}} = \frac{\sqrt{\lambda}}{2\pi}\int d\tau d\sigma \frac{r}{y^2}\sqrt{x_3'^2 + r'^2 + y'^2 + y^2\theta'^2}\,. \tag{6.1.3}$$

Performing the integration over $\tau \in [0, 2\pi]$, we get

$$S_{\text{NG}} = \sqrt{\lambda}\int d\sigma \frac{r}{y^2}\sqrt{x_3'^2 + r'^2 + y'^2 + y^2\theta'^2}\,. \tag{6.1.4}$$

To find the equation of motions one has to minimize the Nambu-Goto action. Since there is no dependence in the Lagrangian on θ and x_3, their equation of motions translate into the conservation laws

$$K_x = \frac{r x_3'}{y^2\sqrt{x_3'^2 + r'^2 + y'^2 + y^2\theta'^2}} \qquad \text{and} \qquad K_\theta = \frac{r\theta'}{\sqrt{x_3'^2 + r'^2 + y'^2 + y^2\theta'^2}}\,, \tag{6.1.5}$$

where K_x and K_θ are two integration constants. Without loss of generality we can assume that K_x is positive, and thus the same holds for x_3'. This implies that we can choose the gauge in which $x_3 \equiv x = \sigma$, and the equation of motions for the remaining variables take the form

$$r'' - \frac{r}{K_x^2\, y^4} = 0\,, \qquad y'' + \frac{2r^2}{K_x^2\, y^5} - \frac{K_\theta^2}{{K_x}^2 y^3} = 0, \tag{6.1.6}$$

[1] Notice that we are using the unit in which the radii of AdS_5 and S^5 are 1 and $\frac{1}{\alpha'} = \sqrt{\lambda}$.

where the prime symbol denotes the derivative respect to x. Using the equation of motions for $r(x)$ and $y(x)$ together with the conservation laws (6.1.5), one obtain the condition

$$(y^2 + r^2)'' + 2 = 0 \tag{6.1.7}$$

that integrated gives

$$y^2 + r^2 + (x + \tilde{b})^2 = a^2 \,. \tag{6.1.8}$$

Namely, the connected surface spans a sub-manifold of AdS_5 given by the above equation. The connected solution has to satisfy the following boundary conditions

$$r(L) = R_1 \,, \quad r(L+h) = R_2 \,, \quad y(L) = y(L+h) = 0 \,, \tag{6.1.9}$$

that come from the configuration of the loops: the first loop with radius R_1 is located at $x = L$, while the second loop with radius R_2 is located at $x = L + h$. Since both loops are at the boundary of AdS, we require $y = 0$ at $x = L$ and $x = L + h$. Imposing the boundary conditions (6.1.9), we can fix the constants $\tilde{b}$ and a as

$$\tilde{b} = \frac{R_1^2 - R_2^2}{2h} - \frac{h}{2} - L \qquad a^2 = R_1^2 + \frac{(h^2 - R_1^2 + R_2^2)^2}{4h^2} \,. \tag{6.1.10}$$

Following [95, 96], eq. (6.1.8) can be parametrized in terms of an angle $\psi(x)$ as

$$r(x) = \sqrt{a^2 - \left(x + \tilde{b}\right)^2}\cos\psi\,(x) \;, \qquad y(x) = \sqrt{a^2 - \left(x + \tilde{b}\right)^2}\sin\psi\,(x) \;. \tag{6.1.11}$$

Exploiting the combination of the two conservation laws (6.1.5) and using the above parametrization, we get

$$\frac{d\psi}{dx} = \pm \frac{a}{a^2 - \left(x + \tilde{b}\right)^2} \sqrt{\frac{\cos^2\psi - K_\theta^2 \sin^2\psi}{K_x^2\, a^2 \sin^4\psi} - 1} \,, \tag{6.1.12}$$

where $\psi\,(x) \in [0, \pi/2]$ satisfies (see ((6.1.9)))

$$\psi\,(L) = 0 = \psi\,(L + h) \,. \tag{6.1.13}$$

The angle ψ grows (plus sign in (6.1.12)) up to a maximum value ψ_0 at $x = x_0$, for $L \leq x < x_0$. Then, it decreases (minus sign in (6.1.12)) for $x_0 < x \leq L + h$. Demanding $\psi'(x_0) = 0$, one finds the following relation that defines ψ_0

$$\sin^2\psi_0 = \frac{\sqrt{(1 + K_\theta^2)^2 + 4a^2\, K_x^2} - (1 + K_\theta^2)}{2a^2\, K_x^2} \,. \tag{6.1.14}$$

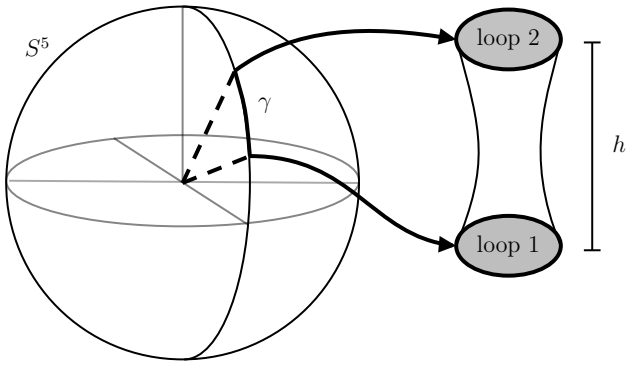

Figure 6.2: Internal separation of the loops in S^5.

The first order differential equation (6.1.12) for $\psi(x)$ can be solved using the method of separation of variable. It is convenient to substitute K_x and K_θ with the new parameter s and t defined as

$$s = \sin^2 \psi_0 \,, \qquad t = a^2 K_x^2 s^2 \,, \tag{6.1.15}$$

where $0 \leq s < 1$ and $t \geq 0$. Following [97], we have that the solution is characterized by the following integrals

$$\mathcal{F}(s,t) = \int_0^1 dz \frac{4\sqrt{st}\, z^2}{\sqrt{(1-z^2)(1-sz^2)(1+tz^2)}} = \ln\left(\frac{a+h+b}{a-h-b}\right) - \ln\left(\frac{a+b}{a-b}\right). \tag{6.1.16}$$

$$\gamma(s,t) = \Delta\theta = \int_0^1 dz \frac{2\sqrt{1-s-t}}{\sqrt{(1-z^2)(1-sz^2)(1+tz^2)}} \tag{6.1.17}$$

$$S_{\text{reg}} = 2\sqrt{\lambda} \int_0^1 \frac{dz}{z^2\sqrt{1-z^2}\sqrt{s}} \left(\frac{\sqrt{1-sz^2}}{\sqrt{1+tz^2}} - 1\right), \tag{6.1.18}$$

where the change of variable $z = \sin\theta/\sqrt{s}$ has been performed and $b = \tilde{b} + L$. Here $\gamma(s,t)$ is the angular separation in the S^5 between the loops, and S_{reg} is the renormalized action fot the connected surface. The above integrals characterizing the classical string solution can be written in terms of elliptic functions

$$\mathcal{F}(s,t) = \sqrt{\frac{t}{s}} \frac{1}{\sqrt{1+t}} \left(\mathbb{K}\left(\frac{s+t}{1+t}\right) - (1-s)\Pi\left(s, \frac{s+t}{1+t}\right)\right) \tag{6.1.19}$$

$$\gamma(s,t) = \frac{2\sqrt{1-s-t}}{\sqrt{1+t}} \mathbb{K}\left(\frac{s+t}{1+t}\right) \tag{6.1.20}$$

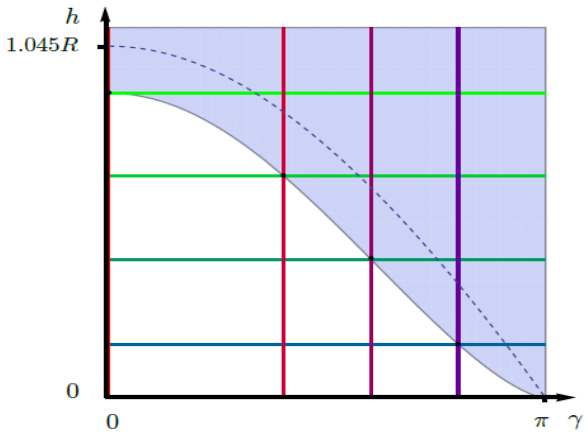

Figure 6.3: In this plot given in [97], the light blue region corresponds to the values of the internal and spatial separation for which the dominant solutions is the disconnected surface (two separate spherical domes). The continuous curve gives the critical distance h_{crit}, at which the transition occurs, for different values of γ. The dashed curve gives the maximal value of h above which no connected solution exists. Here the two loops considered have the same radii.

$$S_{\text{conn}} = -\frac{2\sqrt{\lambda}}{\sqrt{s}}\frac{1}{\sqrt{1+t}}\left[(1+t)\mathbb{E}\left(\frac{s+t}{1+t}\right) - (1-s)\mathbb{K}\left(\frac{s+t}{1+t}\right)\right]. \tag{6.1.21}$$

The reality condition on γ translates into the bound $s \leq 1-t$ for the parameter s. When $t = 1-s$, the internal separation between the loops is zero and the renormalized action (6.1.21) reduces to the result given in [93, 95, 96]. The on-shell action for every value of γ grows with the spatial separations h. At a certain critical value of h, the area of the connected solution becomes equal to $-2\sqrt{\lambda}$, which is the value of the on-shell action for two disconnected spherical dome solutions. Thus, for this value of the spatial separation, we have the Gross-Ooguri phase transition (continuous line in 6.3). The connected solution exists up to a maximal value for h, that for $\gamma = 0$ and $R_1 = R_2$ is determined numerically in [95] and is $h_{\text{max}} = 1.045R$. Both the maximal and the critical value for h decrease when γ increases.

6.2 String solutions for two concentric circles with the defect

In this section, we will present a preliminary study for the case in which we have two circular Wilson loops in the presence of the defect. The two loops are placed on planes parallel to the defect at a distance $x_3 = L$ and $x_3 = L + h$, respectively.

For simplicity, we consider the case in which the circles have the same radius R, namely $R_1 = R_2 = R$. The two Wilson loops can couple with the scalars ϕ_3 and ϕ_6 of the theory with different angles. The first loop, located at $x_3 = L$, will have an internal angle χ_1 while for the second one at $x_3 = L + h$ the coupling with the scalar will be given by χ_2. Thus, the internal separation can be defined as $\gamma = \Delta\chi$, with $\gamma \in [0, \pi/2)$. The parameters that describe the solutions are

$$\kappa, \quad \chi_1, \quad \chi_2, \quad \frac{L}{R} \quad \text{and} \quad \frac{h}{R}\,. \tag{6.2.1}$$

As anticipated, when the defect is present we have richer situations respect to the standard Gross-Ooguri phase transition between the two circles. We expect that when both circles are far away from the defect ($L/R >> 1$), the picture is the one described in the previous section. Depending on h, the dominant solution will be given by the connected surface between the contours or it will consist of two disconnected domes. If we get closer to the defect, we can have a greater variety of configurations for the minimal area. The defect opens the possibility to have also cylindrical surfaces that start from the boundary of AdS and attach to the brane. Since in the two circles case, as described above, we have five different parameters that characterize the solution, to fully describe all the possible configurations is complicated and we are working to fully analyze the parameter space. We can try to semplify the description making a few comments on the figure 6.3. In fact, looking at this plot we immediately recognize that if $h/R > 1.045$ there can be no connected solution between the two circles for any value of γ. Thus, we can have two different situations.

$\boldsymbol{h/R > 1.045}$: if we are far away from the defect, the minimal area is given by the two disconnected domes, and it is equal to $-2\sqrt{\lambda}$. If we get closer to the defect ($L/R << 1$), in such a way that a connected solution to the brane is allowed, three different situations can occur.

(1) $\boldsymbol{\chi_1 \geq \chi_2}$: we found in chapter 4 that the critical distance for the cylindrical surface (stratched between the boundary and the defect) increase with the angle and the flux. Fixing κ, the critical distance for the first loop is bigger than that for the second one. The minimal area for the first circle, which is more close to the defect, is given by the cylindrical surface if

$$\left(\frac{L}{R}\right)_1 \leq \left(\frac{L}{R}\right)_{(1,\text{critical})}\,. \tag{6.2.2}$$

The second loop can be at a distance from the defect such that the dominant solution is still the dome

$$\left(\frac{L+h}{R}\right) > \left(\frac{L}{R}\right)_{(2,\text{critical})} . \tag{6.2.3}$$

(2) $\boldsymbol{\chi_1 \leq \chi_2}$: In this case

$$\left(\frac{L}{R}\right)_{(1,\text{critical})} \leq \left(\frac{L}{R}\right)_{(2,\text{critical})} , \tag{6.2.4}$$

thus there is a region for the parameters in which for the second circle the solution with minimal area is the cylindrical surface, but for the first one the dome can be preferred.

(3) For certain value of the parameters, the minimal area configuration is given by two cylindrical surfaces attached to the defect.

Notice that, as pointed out bay cases (1) and (2), if we change χ_1 with χ_2, the situation is not symmetric. Respect to the case without the defect, where only the difference γ between the two matters, here also the value of the single angle is important. This is due to the fact that the defect breaks the original $SO(6)$ R-symmetry to $SO(3) \times SO(3)$.

$\boldsymbol{h/R < 1.045}$: In addition to the previous cases, it is possible that the minimal area is given by the connected surface between the loops. Fixing γ, we find, as depicted in 6.3, a corrisponding maximal value for h/R above which there is no connected solution between the loops, and we recover the cases listed above in (1), (2) and (3). Since the action (6.1.21) diverges as $h \to 0$, we expect that at finite distance from the defect the connected configuration will be dominant respect to the others when the separation between the loops approaches zero.

Analyzing the case in which also the connected solution can be an option for the minimal area configuration requires much more effort, and we are working to classify all the possible cases. First of all, it is necessary to map the parameter s and t, that describe the connected solution without the defect, in the set of parameters that we use to study the defect case. We have recently made some progress in this direction. Even if we still not have a full description of the problem, we can give an idea of

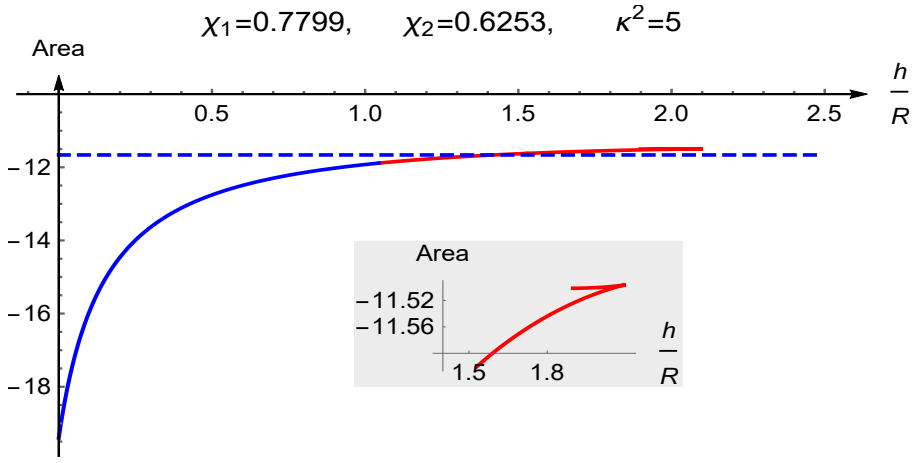

Figure 6.4: We have plotted the sum of the areas of the two cylindrical surfaces for the two circles as a function of the separation between the two. We have fixed the angles, the flux and the distance from the defect of the first loop. The merging point between the red and the continuous blue curve corresponds to $h/R = 1.045$ and for value bigger than this no connected solution between the loops is allowed for any values of γ. The dashed blue line corresponds to the configuration in which for the first loop we have a cylindrical surface with fixed area and the dome for the second loop (the area of the dome is normalized to -1).

what can happen looking at figure 6.4. Here we have fixed two values for the angles $\chi_1 = 0.7799$ and $\chi_2 = 0.6253$. We have also fixed the flux to be $\kappa^2 = 5$. To show the behavior of the action as a function of h/R, we have also fixed the distance from the defect of the first loop $(L/R)_1 = 0.1517$. For this value of the distance, the area of the first loop is $S_1 = -10.66$ and its minimal area configuration is given by the cylindrical surface. Keeping fixed the first loop and approaching from infinity the defect with the second loop, there is a value for the distance at which the cylindrical surface starts to exist also for the second circle. Notice that in 6.4 we plot the sum of the areas of the two circles. We have the transition between the dome and the cylindrical surface for the second loop when $S_1 + S_2 = -10.66 - 1 = -11.66$, this value for the area is given by the dashed blue line. Thus, from the value of h/R at which the red curve crosses the dashed one to the value of h/R that corresponds to the merging between the red and the blue continuous curves, the minimal area configuration is given by two cylindrical surfaces. In fact, the merging corresponds to $h/R = 1.045$. Namely, for distances corresponding to the red curve, we are sure that no connected solution between the loops can exist. If we are along the blue line, there will be a certain value for h/R, which depends on our choice of γ, at which the connected solution between the circles becomes an option. At the present stage

of the work, the only further comment that we can make on the connected solution is that for a small value of h we expect that it will be the dominant one. In fact, for $h \to 0$ the area of the two cylindrical surfaces is finite (since the two loops are at a finite distance from the defect) while the area of the connected surface diverges to $-\infty$.

This is only a preliminary and qualitative analysis since we are still working on this problem. Nevertheless, we are confident of being able to examine in details the various configurations for the two circles in the presence of a defect in a short time.

Conclusions and outlook

In this thesis, we have studied the circular Wilson Loop operator in $\mathcal{N} = 4$ SYM theory in the presence of a codimension-one defect, generalizing previous results presented in [24]. In the following, we comment on the main outputs of our original work presented in chapters 4 and 5, we will also give some insights on a work that we are developing in this moment. Then, we discuss possible further developments.

In chapter 4, we presented the general solution of the equation of motions for the minimal surface connected to the defect. We obtained an explicit expression for the functions that describe the embedding of the string worldsheet into $AdS_5 \times S^5$. The full construction is controlled by the function $g(\sigma)$, which has an explicit expression in terms of Jacobi elliptic functions. The minimal surface is parametrized by three real constants $(m, j, \tilde{\sigma})$ that are highly nonlinearly related to the physical parameters $(L/R, \chi, \kappa)$, once the boundary conditions are imposed. We have analyzed the parameter space of the string solution: using the appropriate boundary conditions and positivity requirements, we have restricted the moduli space into two regions that we called A and B. The evaluation of the area of the minimal surface is obtained by computing the Polyakov action on the solutions. We found that it can be expressed in terms of a bunch of Jacobi elliptic functions and the incomplete elliptic integral of the second kind. The central core of our study is the analysis of the structure of the connected string solution: we have discussed the existence of the minimal surface as a function of the ratio L/R. We found that there is a limiting value beyond that the solution ceases to exist. For some value of the parameters, we were able to determine the maximal distance analitically, and in the other cases, we found it numerically. The maximal distance increases both with the angle and with

the flux. Moreover, there exist regions where a second branch of solutions appears, showing the presence of two competing saddle points to the string action with the same angle, flux, and distance. The final result of this analysis, that singles out a critical angle, χ_s, can be displayed distinguishing two situations.

(1) $\boldsymbol{\chi_s \leq \chi \leq \frac{\pi}{2}}$: In this case we have always two branches for the solutions, no matter of the value of the flux κ

(2) $\boldsymbol{0 < \chi < \chi_s}$: In this region, we can determine a critical value of the flux $\kappa_s(\chi)$: above this value we have a single branch of solutions while below a second branch appears.

The upper branch is always subdominant respect to the lower one. Moreover, the latter turns out to be always physically connected to a vanishing distance from the defect. We compared the area of the dominant connected solution with the disk-like on-shell action: in the different regions we always find that decreasing L/R from $+\infty$, where obviously the disk-like surface is the relevant saddle-point, there exists a critical value (depending on (χ, κ)) below which the connected cylinder start being dominant. The presence of two different string solutions, corresponding to the circular Wilson Loop operator, that are dominant in different regions of the parameters implies that there is a transition of the Gross-Oogury type between the two configurations. We studied the transition finding that it is of the first order. Nicely the spherical dome ceases to be dominant before touching the D5 brane profile.

Chapter 5 is devoted to some perturbative computations, checking the picture emerging from strong coupling: first, we performed the expansion in λ/k^2 of the AdS/CFT solution. We recovered the result of [24] without compromising ourselves with the value of other parameters (taking L/R and χ generic) and showing the consistency with the relevant order of weak-coupling perturbation theory. Then, we discussed the BPS point $\chi = 0$. In this case, a dramatic simplification occurs and the relevant one-loop contribution can be evaluated exactly. We recognize that in the $k \to \infty$ the BPS result does not match the strong coupling expansion for the connected string action. In fact, the expansion for the BPS circle does not organize in a power series in λ/k^2 and it does not possess a connected string counterpart. Moreover, shrinking to a point the BPS circle ($R \to 0$ limit), we found an expansion that can be understood in terms of the OPE of the Wilson loop in the defect case. We performed also

the same expansion in the opposite limit, namely $L \to 0$. In this latter case, the interpretation of the result is more complicated.

In chapter 6 we presented the study, which is a work currently in progress, of the two circles correlator in the presence of a defect. In the standard case without the interface, the minimal area of the string solution can have two competing saddle points: one corresponding to the world-sheet of the fundamental string stretched between the two loops and the other given by two disconnected spherical surfaces interacting among themselves. When the D5 is present, we expect two more possibilities: the minimal area can be given by two cylindrical surfaces attached to the defect or can correspond to a cylindrical surface for one of the circles and the spherical dome for the other. We are still analyzing this plethora of configurations for different values of the parameters that describe the solutions.

An interesting development of our work would be to extend the analysis to the situation where the D3-branes are intersected by a probe D7-brane, which now plays the role of the defect. This case is particularly interesting because supersymmetry is completely broken. Two different cases can be considered. The first with a $SO(3) \times SO(3)$ symmetry where the probe D7-brane profile is $AdS_4 \times S^2 \times S^2$ and where the world-volume $U(1)$ gauge field of the D7 brane has k_1 and k_2 units of magnetic flux on the two 2-spheres. The second with $SO(5)$ symmetry, where the probe brane profile is $AdS_4 \times S^4$ and the world-volume gauge fields form a certain instanton bundle on the S^4 with instanton number d_G. The parameter k of the D3-D5 system is replaced by k_1 and k_2 in the first case and by d_G in the second one. Moreover, the former configuration has a dual defect CFT where all six scalar fields of $\mathcal{N} = 4$ SYM theory are assigned VEVs, and the two gauge group of the theories separated by the defect are now $SU(N)$ and $SU(N - k_1 k_2)$, respectively. In the latter case, only five out of the scalar fields are assigned VEVs, and these transform in an irreducible $SO(5)$ representation. A double scaling limit can be performed in both cases and result for the one-point functions of scalar operators has been reported in [101–103].

Another exciting extension of our work can be to consider what happens to the circular Wilson loop operator when it is placed in ABJM theory, which is a three-dimensional $\mathcal{N} = 6$ superconformal $U(N_1) \times U(N_2)$ Chern–Simons theory with mat-

ter dual to M-theory on $AdS_4 \times S^7/\mathbb{Z}_k$, with a domain wall and how our previous analysis changes in this case.

Acknowledgments

First of all, I am very deeply grateful to my advisor, Domenico Seminara, for initiating me to this interesting area of research, for sharing his knowledge and for patiently guiding me through these three years. Our discussions have been always very stimolating to me. Special thanks are also due to Luca Griguolo for the collaborations and illuminating discussions. I want to thank also Carlo Angelantonj who first got me interested in string theory. A special thank goes also to my officemate Matteo and to all my colleagues for funny days spent together and to Alessio for interesting discussions and a lot of funny moments. A warm thanks goes also to my family for always supporting me during all the stage of my life. Thanks also to all my friends, and to Michela that with her cheerfulness makes my days better. At last but not least, my thanks go to Matteo, for always lovingly encouraging and supporting me.

Appendix A

Representation of $\mathfrak{su}(2)$

We give here the explicit expressions for the $\mathfrak{su}(2)$ generators t_i appearing in the vacuum expectation value of the scalars in the defect version of $\mathcal{N}=4$. Following [21], we define the standard $k\times k$ matrix unities $E^i_{\ j}$ that are zero everywhere except for a 1 at position (i,j). These matrices satisfy the relation

$$E^i_{\ j}E^k_{\ l}=\delta^k_{\ j}E^i_{\ l}. \tag{A.0.1}$$

We introduce the matrices

$$t_+=\sum_{i=1}^{k-1}c_{k,i}E^i_{\ i+1}\,,\qquad t_-=\sum_{i=1}^{k-1}c_{k,i}E^{i+1}_{\ i}\,,\qquad t_3=\sum_{i=1}^{k}d_{k,i}E^i_{\ i} \tag{A.0.2}$$

with the constants

$$c_{k,i}=\sqrt{i(k-i)}\,,\qquad d_{k,i}=\frac{1}{2}(k-2i+1). \tag{A.0.3}$$

The standard k-dimensional representation of the $\mathfrak{su}(2)$ Lie algebra is defined as

$$t_1=\frac{t_++t_-}{2}\,,\qquad t_2=\frac{t_+-t_-}{2}\,,\qquad \text{and}\quad t_3. \tag{A.0.4}$$

Notice that all these matrices are traceless and satisfy the $\mathfrak{su}(2)$ commutation relations (3.1.10). If $k=2$, the representation matrices are multiples of the Pauli matrices: $t_i\,|_{k=2}=\frac{1}{2}\sigma_i$.

Appendix B

Massive propagators

The scalar and fermionic propagators in the defect theory have been derived in [17, 20] by expressing them in terms of propagators in AdS_{d+1}. The transverse coordinate x_3 to the defect plays the role of the radial coordinate of an auxiliary AdS_4 space with the defect as its boundary. In terms of the AdS_4 scalar propagator, satisfying

$$\left(-\nabla^\mu \nabla_\mu + \tilde{m}^2\right) K_{AdS}(x,y) = \frac{\delta(x-y)}{\sqrt{g}} \tag{B.0.1}$$

where $g_{\mu\nu} = (x_3)^{-2}\eta_{\mu\nu}$, one can define

$$K(x,y) = \frac{g_{YM}^2 K_{AdS}(x,y)}{2x_3 y_3} \tag{B.0.2}$$

which is a solution for

$$\left(-\partial^\mu \partial_\mu + \frac{m}{(x_3)^2}\right) K(x,y) = \frac{g_{YM}^2}{2}\delta(x-y) \tag{B.0.3}$$

with the identification $\tilde{m}^2 = m^2 - 2$. We use for the scalar propagators the following integral representation [104]

$$K_\nu(x,y) = \frac{g_{YM}^2\sqrt{x_3 y_3}}{2}\int \frac{d^3\vec{k}}{(2\pi)^3} e^{i\vec{k}\cdot(\vec{x}-\vec{y})} I_\nu\left(\left|\vec{k}\right| x_3\right) K_\nu\left(\left|\vec{k}\right| y_3\right), \tag{B.0.4}$$

where $\vec{k}$, $\vec{x}$ and $\vec{y}$ are 3d vectors in the (x_0, x_1, x_2) directions, I_ν and K_ν are modified Bessel functions and ν is related to the mass of the propagating mode

$$\nu = \sqrt{m^2 + \frac{1}{4}}\,. \tag{B.0.5}$$

Since fermionic modes do not contribute in 1-loop computation of the circular Wilson loop expectation value, we do not present the corresponding propagators. In the following table we report the pattern for the masses and ν's obtained by diagonalizing the mass matrix coming from the action (1.1.47) by expanding the lagrangian around the classical solution $\phi_i^{\rm cl}$ $(i = 1, 2, 3)$:

Multiplicity	$\nu\left(\tilde{\phi}_{4,5,6},\, A_{0,1,2},\, c\right)$	$m\left(\psi_{1,2,3,4}\right)$	$\nu\left(\tilde{\phi}_{1,2,3},\, A_3\right)$
$l+1$	$l+\frac{1}{2}$	$-l$	$l-\frac{1}{2}$
l	$l+\frac{1}{2}$	$l+1$	$l+\frac{3}{2}$
$(k-1)(N-k)$	$\frac{k}{2}$	$\frac{k+1}{2}$	$\frac{k+2}{2}$
$(k+1)(N-k)$	$\frac{k}{2}$	$-\frac{k-1}{2}$	$\frac{k-2}{2}$
$(N-k)(N-k)$	$\frac{1}{2}$	0	$\frac{1}{2}$

where $l = 1, ..., k-1$. Here the ψ_j $(j = 1, .., 4)$ are four-dimensional Majorana fermions and c is a massive ghost field coming from the gauge fixing of the action.

Appendix C

Expression for the distance from the defect

The distance (4.2.16) from the defect brane can be also expressed in terms of Elliptic integral of the third kind if we explicitly perform the integral defining the function $v(\sigma)$. We get

$$\begin{aligned}\eta =&\sqrt{-\frac{(j^2m+1)(j^2+m)}{(m+1)(j^2-1)}}\left[\sqrt{\frac{j^2-1}{m+1}}\tilde{\sigma}-\Pi\left(-\frac{m+1}{j^2-1};\,\mathrm{am}\left(\sqrt{\frac{j^2-1}{m+1}}\tilde{\sigma}\middle|\, m\right)\middle|\, m\right)\right]+\\&+\tanh^{-1}\left(-\sqrt{-\frac{(m+1)^2}{(j^2m+1)(j^2+m)}}\frac{g'(\tilde{\sigma})}{g(\tilde{\sigma})}\right)= \qquad \text{(C.0.1)}\\ =&\sqrt{-\frac{(n+1)(nm+1)}{n}}\left[\sqrt{n}\tilde{\sigma}-\Pi\left(-\frac{1}{n};\mathrm{am}(\sqrt{n}\tilde{\sigma}|m)\middle|\, m\right)\right]+\\&+\tanh^{-1}\left(\frac{-\frac{g'(\tilde{\sigma})}{g(\tilde{\sigma})}}{\sqrt{-(nm+1)(n+1)}}\right),\end{aligned}$$

where we have introduced the short-hand notation

$$n\equiv\frac{j^2-1}{m+1}. \qquad \text{(C.0.2)}$$

The parameter n is always positive both in region (A) and (B). As m approaches m_c, the argument of the arctanh behaves like

$$\sim\frac{\sqrt{n}}{n\sqrt{-m_c}}\frac{\mathrm{cn}(\sqrt{n}\tilde{\sigma}|m)\mathrm{dn}(\sqrt{n}\tilde{\sigma}|m)}{\mathrm{sn}(\sqrt{n}\tilde{\sigma}|m)}=\frac{s_0}{\sqrt{n}}, \qquad \text{(C.0.3)}$$

where we have used that the combination $\sqrt{n}\tilde{\sigma}$ is finite in this limit. The remaining contribution can be seen to vanish with the same behavior if we use the following property

$$\Pi(\tilde{n},z,m)\simeq F(z,m)+c(z,m)\tilde{n}+O(\tilde{n}^2)\qquad(\tilde{n}\to 0). \qquad \text{(C.0.4)}$$

Appendix D

Expansion of n, $g(\tilde{\sigma})$ and $\frac{\partial \eta}{\partial m}$ around the boundary $j^2 = -1/m^2$.

This boundary is the curved red line plotted in fig. 4.4. The values of χ and m along this curve are related by eq. (4.2.30). We shall now fix a value for the angle $\chi = \chi_0$; eq. (4.2.30) allows us to translate it in a value m_0 for m. Given the couple (χ_0, m_0), the value x is fixed by eq. (4.2.28) to be

$$x_0 = 1. \tag{D.0.1}$$

We now expand around this configuration. Specifically, we keep the angle χ_0 fixed and we allow m to be different from m_0, but close to it. Then, we can write x as series expansion around m_0:

$$x = 1 + s_1(m - m_0) + s_2(m - m_0)^2 + O((m - m_0)^3). \tag{D.0.2}$$

The coefficients s_i can be determined by solving perturbatively eq. (4.2.34) and one finds

$$x = 1 + \frac{(m - m_0)^2 \left(\kappa^2 m_0 + m_0 - 1\right) \left((m_0 - 1)\,\mathbb{K}(m_0) + \mathbb{E}(m_0)\right)^2}{8\kappa^2 (m_0 - 1)\, m_0^2} + O\left((m - m_0)^3\right). \tag{D.0.3}$$

The expansion for n around $m = m_0$ is then easily recovered

$$\begin{aligned} n = \frac{x^2}{1 - (m+1)x^2} &= -\frac{1}{m_0} + \frac{m - m_0}{m_0^2} - \frac{a_0}{m_0^3}(m - m_0)^2 + O((m - m_0)^3) \\ \text{with} \qquad a_0 &= 1 - \frac{\left(\kappa^2 m_0 + m_0 - 1\right) \left((m_0 - 1)\,\mathbb{K}(m_0) + \mathbb{E}(m_0)\right)^2}{4\kappa^2 (m_0 - 1)\, m_0}. \end{aligned} \tag{D.0.4}$$

We can also use (D.0.3) to evaluate the expansion of $g(\tilde{\sigma})$ and $g'(\tilde{\sigma})$, two quantities that often appears in our analysis. In fact, by means of eq. (4.2.34), we can write

$$\begin{aligned} g(\tilde{\sigma}) =& \sqrt{-\frac{2fmnx^2}{\kappa^2+(\kappa^2+1)\left(-(m+1)\right)x^2+\sqrt{\left(\kappa^2-f(m+1)x^2\right)^2-4fmx^4}}} = \\ =& \frac{1}{\sqrt{-m_0}}+\frac{m-m_0}{2\left(-m_0\right)^{3/2}}+ \\ &+\frac{(4a_0-1)(m_0-1)-\left((m_0-1)\,\mathbb{K}(m_0)+\mathbb{E}(m_0)\right)^2}{8(m_0-1)\left(-m_0\right)^{5/2}}\left(m-m_0\right)^2+ \\ &+O\left(\left(m-m_0\right)^3\right), \end{aligned} \tag{D.0.5}$$

where $f \equiv \kappa^2+1$ and

$$\begin{aligned} g'(\tilde{\sigma}) =& -\kappa\sqrt{-mn^2-g^2(\tilde{\sigma})} = \frac{(m-m_0)\left((m_0-1)\,\mathbb{K}(m_0)+\mathbb{E}(m_0)\right)}{2m_0^2}+ \\ &+O\left(\left(m-m_0\right)^2\right). \end{aligned} \tag{D.0.6}$$

If we now plug these expansions in (4.3.1) we find

$$\begin{aligned} \left.\frac{\partial\eta}{\partial m}\right|_{m=m_0} =& \frac{(1-m_0)\left(\mathbb{E}(m_0)+(m_0-1)\mathbb{K}(m_0)\right)^2}{2\kappa(1-m_0)\left(-m_0\right)^{3/2}\sqrt{1-(\kappa^2+1)\,m_0}}+ \\ &+\frac{m_0\kappa^2\left(1-\left(\mathbb{E}(m_0)+(m_0-1)\,\mathbb{K}(m_0)\right)^2\right)}{2\kappa(1-m_0)\left(-m_0\right)^{3/2}\sqrt{1-(\kappa^2+1)\,m_0}}. \end{aligned} \tag{D.0.7}$$

Appendix E

The Expansion of the area and comparison with the perturbative results

To perform this analysis we have to expand the elliptic functions around $m = 0$, vanishing modulus, keeping in mind that all the the other entries depend on m explicitly or implicitly (through $x(m)$). First, we consider the expansion of the eq. (4.2.34) of the flux. Since $x \to 1$ while $m \to 0$, we can first expand the elliptic function for for small modulus keeping x fixed and then expand $x(m)$ for small m. If we write the expansion of m and x for large flux as follows

$$m = \sum_{n=1}^{\infty} \frac{a_{2n}}{\kappa^{2n}} \qquad x = 1 + \sum_{n=1}^{\infty} \frac{b_{2n}}{\kappa^{2n}},$$

the eq. (4.2.34) determining the flux reads

$$\begin{aligned}\kappa^2 =& \frac{\kappa^2}{a_2 \cos^2\chi + 2\, b_2 \cot^2\chi} + \frac{1}{8\left(a_2 \sin^2\chi + 2\, b_2\right)^2}\Big[\tan\chi\left(-4\tan\chi\left(a_4 \sin^2\chi + 2b_4\right) + \right.\\ &+ 2a_2 b_2 \sec^2\chi\left((\pi - 2\chi)\left(\sin^2 2\chi + 2\cos 2\chi\right) - 4\sin 2\chi - \sin 4\chi\right) - \\ &- a_2^2 \sin\chi \tan^2\chi(4\chi\sin\chi - 2\pi\sin\chi + 7\cos\chi + \cos 3\chi) \\ &\left. + \; 4b_2^2(8\chi + 3\sin 2\chi - 4\pi)\sec^2\chi\right)\Big] + O\left(\kappa^{-2}\right) .\end{aligned} \tag{E.0.1}$$

We can perform the same analysis for the distance

$$\frac{L}{R}=\tanh^{-1}\left(\frac{\sqrt{-\frac{(a_2+2b_2)\tan^2\chi}{b_2}}}{\sqrt{2}}\right)+\frac{1}{2\sqrt{2}\kappa^2}\Bigg[(-a_2-2b_2)^{1/2}\sqrt{b_2}(\pi-2\chi-\sin 2\chi)-$$
$$-\frac{2\left(2a_2^2b_2+a_2\left(11b_2^2-b_4\right)+2b_2\left(a_4+b_2^2+b_4\right)\right)\sin^2\chi}{b_2\left(a_2+4b_2-a_2\cos 2\chi\right)\sqrt{-\frac{(a_2+2b_2)\tan^2\chi}{b_2}}}+ \tag{E.0.2}$$
$$+\frac{(a_2+2b_2)\left(a_2\sin 4\chi-2(\pi-2\chi)\left(a_2-4b_2\right)\right)+2\left(4a_2b_2+2a_2^2+a_4-6b_2^2+2b_4\right)\sin 2\chi}{2\left(a_2+4b_2-a_2\cos 2\chi\right)\sqrt{-\frac{(a_2+2b_2)}{b_2}}}\Bigg]+$$
$$+O\left(\kappa^{-4}\right).$$

We can now solve iteratively this combined system of equations and determines $\{a_2,a_4,b_2,b_4\}$ in terms of L/R and χ. We get

$$a_2=\frac{1}{2}\sec^4\chi\left(-\frac{2L^2}{R^2}+\cos 2\chi-1\right), \tag{E.0.3}$$
$$b_2=\frac{1}{2}\left(\frac{L^2}{R^2}+1\right)\tan^2\chi\sec^2\chi, \tag{E.0.4}$$
$$a_4=-\frac{1}{32}\sec^9\chi\left(-\frac{2L^2}{R^2}+\cos 2\chi-1\right)\left(-\frac{88L^2\chi\sin\chi}{R^2}+\frac{44\pi L^2\sin\chi}{R^2}+\right.$$
$$\frac{8L^2\chi\sin 3\chi}{R^2}-\frac{4\pi L^2\sin 3\chi}{R^2}-2\left(\frac{16L^2}{R^2}+5\right)\cos\chi-84\chi\sin\chi+42\pi\sin\chi+$$
$$\left.+12\chi\sin 3\chi-6\pi\sin 3\chi+9\cos 3\chi+\cos 5\chi\right), \tag{E.0.5}$$
$$b_4=-\frac{1}{64}\left(\frac{L^2}{R^2}+1\right)\tan\chi\sec^8\chi\left(-\frac{112L^2\chi}{R^2}-\frac{52L^2\sin 2\chi}{R^2}+\frac{2L^2\sin 4\chi}{R^2}-\right.$$
$$-8(\pi-2\chi)\left(\frac{5L^2}{R^2}+6\right)\cos 2\chi+\frac{56\pi L^2}{R^2}-84\chi-31\sin 2\chi+14\sin 4\chi+$$
$$\left.+\sin 6\chi+6(\pi-2\chi)\cos 4\chi+42\pi\right). \tag{E.0.6}$$

We can perform an expansion in terms of the above parameters for the area as well and one gets

$$\frac{S}{\sqrt{\lambda}}=-\kappa\sqrt{-\frac{1}{a_2+2b_2}}\tan\chi-\frac{1}{8\kappa}\left(-\frac{1}{a_2+2b_2}\right)^{3/2}\sec^2\chi\left[4b_2(\pi-2\chi)\left(a_2+2b_2\right)+\right.$$
$$+\left.\left(a_2^2+a_4-6b_2^2\right)\sin 2\chi+2\left(a_2b_2+b_4\right)\sin 2\chi+a_2(\pi-2\chi)\left(a_2+2b_2\right)\cos 2\chi\right]+$$
$$+O\left(\kappa^{-3/2}\right). \tag{E.0.7}$$

Exploiting the explicit form of the coefficients a_2, a_4, b_2 and b_4 we find

$$\frac{S}{\sqrt{\lambda}} = -\frac{\kappa R \sin\chi}{L} - \frac{R(2\chi + \sin 2\chi - \pi)\sec^3\chi\left(-\frac{2L^2}{R^2} + \cos 2\chi - 1\right)}{16\kappa L} + O\left(\kappa^{-2}\right). \tag{E.0.8}$$

Appendix F

Connected solution as correlator between two circle of different radii

Let us examine more carefully the geometric structure of our solution. In AdS_5 the surface is spanned by

$$y(\sigma) = \frac{R\cosh\eta}{\sqrt{1+g^2(\sigma)}}\text{sech}[v(\sigma)-\eta] \qquad r(\sigma) = R\cosh\eta\frac{g(\sigma)}{\sqrt{1+g^2(\sigma)}}\text{sech}[v(\sigma)-\eta]$$
$$x_3(\sigma) = -R\cosh\eta\tanh[v(\sigma)-\eta]. \tag{F.0.1}$$

This parametric form draws a sub-manifold inside the following S^3 in AdS_5:

$$\begin{aligned} x^2+y^2+r^2 =& R^2\cosh^2\eta\Big[\frac{\text{sech}^2[v(\sigma)-\eta]}{1+g^2(\sigma)} + \frac{g^2(\sigma)}{1+g^2(\sigma)}\text{sech}^2[v(\sigma)-\eta]+ \\ &+\tanh^2[v(\sigma)-\eta]\Big] = \\ =& R^2\cosh^2\eta = \sqrt{L^2+R^2}. \end{aligned} \tag{F.0.2}$$

This surfaces intersects the boundary of AdS_5 at $\sigma = 0$ and if we extend the range of the world-sheet coordinate σ beyond $\tilde{\sigma}$, it reaches again the boundary at $\hat{\sigma} = \frac{2}{\sqrt{n}}\mathbb{K}(m)$ for which

$$v(\hat{\sigma}) = 2\sqrt{\frac{\epsilon_0}{n}}\left[\mathbb{K}(m) - \Pi\left(-\frac{1}{n},m\right)\right]. \tag{F.0.3}$$

This second intersection with the boundary of AdS_5 is again a circle of radius

$$\hat{R} = R\cosh\eta\ \text{sech}\left(2\sqrt{\frac{\epsilon_0}{n}}\left[\mathbb{K}(m) - \Pi\left(-\frac{1}{n},m\right)\right] - \eta\right). \tag{F.0.4}$$

This second circle is located at

$$\begin{aligned} x_3(\hat{\sigma}) =& - R\cosh\eta\tanh[v(\hat{\sigma})-\eta] = R\sinh\eta - R\sinh v(\hat{\sigma})\text{sech}\,(v(\hat{\sigma})-\eta) = \\ =& R\sinh\eta - \hat{R}\text{sech}\eta\sinh v(\hat{\sigma}) \end{aligned} \tag{F.0.5}$$

and the distance ℓ in the transverse direction x_3 between this circle and the one at $\sigma = 0$ is

$$\ell = \hat{R}\text{sech}\eta\sinh v(\hat{\sigma}). \tag{F.0.6}$$

The angle χ describing the scalars coupling to the two circles is different and the $\Delta\chi$ between the two loops is

$$\Delta\chi = \frac{2j}{\sqrt{n}}\mathbb{K}(m). \tag{F.0.7}$$

Appendix G

Basis for chiral primary operators

In our framework, the only operators built from scalars that can have one-point functions different from zero are those invariant under $SO(3)\times SO(3)$. If we consider the case of operator with classical dimension 2 we can construct only two operators of this type:

$$\mathrm{Tr}(\phi_i\phi^i) \tag{G.0.1}$$

and the chiral primary operator

$$\mathcal{O}_1(x) = \sqrt{\frac{1}{6}}\mathrm{Tr}\left[\phi_1^2+\phi_2^2+\phi_3^2-\phi_4^2-\phi_5^2-\phi_6^2\right]. \tag{G.0.2}$$

The list of CPO's is completed by 4 diagonal operators:

$$\begin{aligned}
\mathcal{O}_2(x) &= \sqrt{\frac{1}{2}}\mathrm{Tr}\left[\phi_1^2-\phi_3^2\right] \qquad & \mathcal{O}_3(x) &= \sqrt{\frac{1}{6}}\mathrm{Tr}\left[\phi_1^2-2\phi_2^2+\phi_3^2\right]\\
\mathcal{O}_4(x) &= \sqrt{\frac{1}{2}}\mathrm{Tr}\left[\phi_4^2-\phi_6^2\right] \qquad & \mathcal{O}_5(x) &= \sqrt{\frac{1}{6}}\mathrm{Tr}\left[\phi_4^2-2\phi_5^2+\phi_6^2\right]
\end{aligned} \tag{G.0.3}$$

and 15 off-diagonal ones $\mathcal{O}_{ij}(x) = \sqrt{2}\mathrm{Tr}\left[\phi_i\phi_j\right]$ with $i<j$. When performing integrability calculation, one usually computes the expectation values of the CPO $\mathrm{Tr}(Z^2)$. We want to expand this operator in our basis, we find

$$\begin{aligned}
\mathrm{Tr}(Z^2) =& \mathrm{Tr}(\phi_3^2-\phi_6^2)+2i\mathrm{Tr}(\phi_3\phi_6) = \\
=& \sqrt{\frac{2}{3}}\mathcal{O}_1(x) - \sqrt{\frac{1}{2}}\mathcal{O}_2(x) + \sqrt{\frac{1}{6}}\mathcal{O}_3(x) + \sqrt{\frac{1}{2}}\mathcal{O}_4(x) - \sqrt{\frac{1}{6}}\mathcal{O}_5(x) + \sqrt{2}i\mathcal{O}_{36}(x).
\end{aligned} \tag{G.0.4}$$

Then, we have the following relation between the VEV's:

$$\langle \mathcal{O}_1(x)\rangle_0 = \sqrt{\frac{3}{2}}\langle \mathrm{Tr}(Z^2)\rangle_0. \tag{G.0.5}$$

Actually in the Wilson loop operator appears the following linear combination of CPO $Y_a(\theta)C^a_{ij}\mathrm{Tr}(\phi^i\phi^j)$, where $Y^a(\theta) = (C^a_{ij}\theta^i\theta^j) = \left(-\sqrt{\frac{1}{6}}, 0, 0, -\sqrt{\frac{1}{2}}, \sqrt{\frac{1}{6}}, \mathbf{0}\right)$ is a 20 component vector. The boldface zero indicates that the remaining 15 components vanish and the C^a_{ij} form the basis of the symmetric traceless tensors that we used for constructing the CPO. Then

$$\langle Y_a C^a_{ij}\mathrm{Tr}(\phi^i\phi^j)\rangle_0 = \langle Y_1\mathcal{O}^1(x)\rangle_0 = -\frac{1}{2}\langle \mathrm{Tr}(Z^2)\rangle_0\,. \tag{G.0.6}$$

Now if we use eq (28) of [23], we find

$$\begin{aligned}\langle \mathrm{Tr}(Z^2)\rangle_0 =& -\frac{1}{12L^2}k(1-k^2) + \frac{g^2_{YM}}{8\pi^2L^2}\Bigg(k(N-k) + \frac{(k-1)}{2} + \\ &+ \sum_{i=0}^{\left[\frac{k-2}{2}\right]}(H_{k-i-1} - H_i)(k-2i-1)\Bigg) = \\ =& -\frac{1}{12L^2}k(1-k^2) + \frac{g^2_{YM}}{8\pi^2L^2}\left(k(N-k) + \frac{k^2-1}{2}\right).\end{aligned} \tag{G.0.7}$$

Therefore

$$\begin{aligned}\langle Y_a C^a_{ij}\mathrm{Tr}(\phi^i\phi^j)\rangle_0 = -\frac{1}{2}\langle \mathrm{Tr}(Z^2)\rangle_0 =& \frac{1}{24L^2}k(1-k^2) - \\ &- \frac{g^2_{YM}}{16\pi^2L^2}\left(k(N-k) + \frac{k^2-1}{2}\right).\end{aligned} \tag{G.0.8}$$

If we the explicit expression of the background fields is not difficult to compute

$$\langle \mathrm{Tr}(\phi^i\phi_i)\rangle_{tree} = \mathrm{Tr}(\phi^{cl}_i\phi^i_{cl}) = -\frac{1}{4L^2}k(1-k^2)\,. \tag{G.0.9}$$

At one-loop we have [23]

$$\langle \mathrm{Tr}(\phi^i\phi_i)\rangle_{1\mathrm{loop}} = -\frac{3\lambda}{16\pi^2L^2}k\left(1-k^2\right)\left(\psi\left(\frac{k+1}{2}\right) + \gamma_E - \log 2 + \frac{5}{6}\right). \tag{G.0.10}$$

Bibliography

[1] Gerard 't Hooft. "A Planar Diagram Theory for Strong Interactions". In: *Nucl. Phys.* B72 (1974). [,337(1973)], p. 461. DOI: 10.1016/0550-3213(74)90154-0.

[2] Leonard Susskind. "The World as a hologram". In: *J. Math. Phys.* 36 (1995), pp. 6377–6396. DOI: 10.1063/1.531249. arXiv: hep-th/9409089 [hep-th].

[3] Juan Martin Maldacena. "The Large N limit of superconformal field theories and supergravity". In: *AIP Conf. Proc.* 484.1 (1999), p. 51. DOI: 10.1063/1.59653.

[4] S. S. Gubser, Igor R. Klebanov, and Alexander M. Polyakov. "Gauge theory correlators from noncritical string theory". In: *Phys. Lett.* B428 (1998), pp. 105–114. DOI: 10.1016/S0370-2693(98)00377-3. arXiv: hep-th/9802109 [hep-th].

[5] Edward Witten. "Anti-de Sitter space and holography". In: *Adv. Theor. Math. Phys.* 2 (1998), pp. 253–291. DOI: 10.4310/ATMP.1998.v2.n2.a2. arXiv: hep-th/9802150 [hep-th].

[6] Juan Martin Maldacena. "Wilson loops in large N field theories". In: *Phys. Rev. Lett.* 80 (1998), pp. 4859–4862. DOI: 10.1103/PhysRevLett.80.4859. arXiv: hep-th/9803002 [hep-th].

[7] Soo-Jong Rey and Jung-Tay Yee. "Macroscopic strings as heavy quarks in large N gauge theory and anti-de Sitter supergravity". In: *Eur. Phys. J.* C22 (2001), pp. 379–394. DOI: 10.1007/s100520100799. arXiv: hep-th/9803001 [hep-th].

[8] David Eliecer Berenstein et al. "The Operator product expansion for Wilson loops and surfaces in the large N limit". In: *Phys. Rev.* D59 (1999), p. 105023. DOI: 10.1103/PhysRevD.59.105023. arXiv: hep-th/9809188 [hep-th].

[9] Nadav Drukker, David J. Gross, and Hirosi Ooguri. "Wilson loops and minimal surfaces". In: *Phys. Rev.* D60 (1999), p. 125006. DOI: 10.1103/PhysRevD.60.125006. arXiv: hep-th/9904191 [hep-th].

[10] Vasily Pestun. "Localization of gauge theory on a four-sphere and supersymmetric Wilson loops". In: *Commun. Math. Phys.* 313 (2012), pp. 71–129. DOI: 10.1007/s00220-012-1485-0. arXiv: 0712.2824 [hep-th].

[11] Andreas Karch and Lisa Randall. "Open and closed string interpretation of SUSY CFT's on branes with boundaries". In: *JHEP* 06 (2001), p. 063. DOI: 10.1088/1126-6708/2001/06/063. arXiv: hep-th/0105132 [hep-th].

[12] Andreas Karch and Lisa Randall. "Locally localized gravity". In: *JHEP* 05 (2001). [,140(2000)], p. 008. DOI: 10.1088/1126-6708/2001/05/008. arXiv: hep-th/0011156 [hep-th].

[13] Oliver DeWolfe, Daniel Z. Freedman, and Hirosi Ooguri. "Holography and defect conformal field theories". In: *Phys. Rev.* D66 (2002), p. 025009. DOI: 10.1103/PhysRevD.66.025009. arXiv: hep-th/0111135 [hep-th].

[14] Johanna Erdmenger, Zachary Guralnik, and Ingo Kirsch. "Four-dimensional superconformal theories with interacting boundaries or defects". In: *Phys. Rev.* D66 (2002), p. 025020. DOI: 10.1103/PhysRevD.66.025020. arXiv: hep-th/0203020 [hep-th].

[15] Davide Gaiotto and Edward Witten. "Supersymmetric Boundary Conditions in N=4 Super Yang-Mills Theory". In: *J. Statist. Phys.* 135 (2009), pp. 789–855. DOI: 10.1007/s10955-009-9687-3. arXiv: 0804.2902 [hep-th].

[16] Koichi Nagasaki, Hiroaki Tanida, and Satoshi Yamaguchi. "Holographic Interface-Particle Potential". In: *JHEP* 01 (2012), p. 139. DOI: 10.1007/JHEP01(2012)139. arXiv: 1109.1927 [hep-th].

[17] Isak Buhl-Mortensen et al. "One-loop one-point functions in gauge-gravity dualities with defects". In: *Phys. Rev. Lett.* 117.23 (2016), p. 231603. DOI: 10.1103/PhysRevLett.117.231603. arXiv: 1606.01886 [hep-th].

[18] Koichi Nagasaki and Satoshi Yamaguchi. "Expectation values of chiral primary operators in holographic interface CFT". In: *Phys. Rev.* D86 (2012), p. 086004. DOI: 10.1103/PhysRevD.86.086004. arXiv: 1205.1674 [hep-th].

[19] Charlotte Kristjansen, Gordon W. Semenoff, and Donovan Young. "Chiral primary one-point functions in the D3-D7 defect conformal field theory". In: *JHEP* 01 (2013), p. 117. DOI: 10.1007/JHEP01(2013)117. arXiv: 1210.7015 [hep-th].

[20] Isak Buhl-Mortensen et al. "A Quantum Check of AdS/dCFT". In: *JHEP* 01 (2017), p. 098. DOI: 10.1007/JHEP01(2017)098. arXiv: 1611.04603 [hep-th].

[21] Marius de Leeuw, Charlotte Kristjansen, and Konstantin Zarembo. "One-point Functions in Defect CFT and Integrability". In: *JHEP* 08 (2015), p. 098. DOI: 10.1007/JHEP08(2015)098. arXiv: 1506.06958 [hep-th].

[22] Isak Buhl-Mortensen et al. "One-point Functions in AdS/dCFT from Matrix Product States". In: *JHEP* 02 (2016), p. 052. DOI: 10.1007/JHEP02(2016)052. arXiv: 1512.02532 [hep-th].

[23] Isak Buhl-Mortensen et al. "Asymptotic One-Point Functions in Gauge-String Duality with Defects". In: *Phys. Rev. Lett.* 119.26 (2017), p. 261604. DOI: 10.1103/PhysRevLett.119.261604. arXiv: 1704.07386 [hep-th].

[24] Jeremias Aguilera-Damia, Diego H. Correa, and Victor I. Giraldo-Rivera. "Circular Wilson loops in defect Conformal Field Theory". In: *JHEP* 03 (2017), p. 023. DOI: 10.1007/JHEP03(2017)023. arXiv: 1612.07991 [hep-th].

[25] S. Bonansea et al. "Circular Wilson loops in defect $\mathcal{N}$=4 SYM: phase transitions, double-scaling limits and OPE expansion". In: (2019). arXiv: 1911.07792 [hep-th].

[26] David J. Gross and Hirosi Ooguri. "Aspects of large N gauge theory dynamics as seen by string theory". In: *Phys. Rev.* D58 (1998), p. 106002. DOI: 10.1103/PhysRevD.58.106002. arXiv: hep-th/9805129 [hep-th].

[27] Nadav Drukker et al. "Supersymmetric Wilson loops on S**3". In: *JHEP* 05 (2008), p. 017. DOI: 10.1088/1126-6708/2008/05/017. arXiv: 0711.3226 [hep-th].

[28] Simone Giombi, Vasily Pestun, and Riccardo Ricci. "Notes on supersymmetric Wilson loops on a two-sphere". In: *JHEP* 07 (2010), p. 088. DOI: 10.1007/JHEP07(2010)088. arXiv: 0905.0665 [hep-th].

[29] A. Bassetto et al. "Correlators of supersymmetric Wilson-loops, protected operators and matrix models in N=4 SYM". In: *JHEP* 08 (2009), p. 061. DOI: 10.1088/1126-6708/2009/08/061. arXiv: 0905.1943 [hep-th].

[30] Sidney R. Coleman and J. Mandula. "All Possible Symmetries of the S Matrix". In: *Phys. Rev.* 159 (1967), pp. 1251–1256. DOI: 10.1103/PhysRev.159.1251.

[31] Rudolf Haag, Jan T. Lopuszanski, and Martin Sohnius. "All Possible Generators of Supersymmetries of the s Matrix". In: *Nucl. Phys.* B88 (1975). [,257(1974)], p. 257. DOI: 10.1016/0550-3213(75)90279-5.

[32] G. Mack and Abdus Salam. "Finite component field representations of the conformal group". In: *Annals Phys.* 53 (1969), pp. 174–202. DOI: 10.1016/0003-4916(69)90278-4.

[33] Lars Brink, John H. Schwarz, and Joel Scherk. "Supersymmetric Yang-Mills Theories". In: *Nucl. Phys.* B121 (1977), pp. 77–92. DOI: 10.1016/0550-3213(77)90328-5.

[34] F. Gliozzi, Joel Scherk, and David I. Olive. "Supersymmetry, Supergravity Theories and the Dual Spinor Model". In: *Nucl. Phys.* B122 (1977), pp. 253–290. DOI: 10.1016/0550-3213(77)90206-1.

[35] M. Rocek M. T. Grisaru and W. Siegel. "Zero Three Loop beta Function in N=4 Super Yang-Mills Theory". In: *Phys. Rev. Lett.* 45 (1980), pp. 1063–1066.

[36] William E. Caswell and Daniela Zanon. "Vanishing Three Loop Beta Function in $N = 4$ Supersymmetric Yang-Mills Theory". In: *Phys. Lett.* 100B (1981), pp. 152–156. DOI: 10.1016/0370-2693(81)90764-4.

[37] William E. Caswell and Daniela Zanon. "Zero Three Loop Beta Function in the $N = 4$ Supersymmetric Yang-Mills Theory". In: *Nucl. Phys.* B182 (1981), p. 125. DOI: 10.1016/0550-3213(81)90461-2.

[38] Stanley Mandelstam. "Light Cone Superspace and the Ultraviolet Finiteness of the N=4 Model". In: *Nucl. Phys.* B213 (1983), pp. 149–168. DOI: 10.1016/0550-3213(83)90179-7.

[39] Lars Brink, Olof Lindgren, and Bengt E. W. Nilsson. "The Ultraviolet Finiteness of the N=4 Yang-Mills Theory". In: *Phys. Lett.* 123B (1983), pp. 323–328. DOI: 10.1016/0370-2693(83)91210-8.

[40] D. J. Gross and Frank Wilczek. "Asymptotically Free Gauge Theories - I". In: *Phys. Rev.* D8 (1973), pp. 3633–3652. DOI: 10.1103/PhysRevD.8.3633.

[41] C. Montonen and David I. Olive. "Magnetic Monopoles as Gauge Particles?" In: *Phys. Lett.* 72B (1977), pp. 117–120. DOI: 10.1016/0370-2693(77)90076-4.

[42] Eric D'Hoker and Daniel Z. Freedman. "Supersymmetric gauge theories and the AdS / CFT correspondence". In: *Strings, Branes and Extra Dimensions: TASI 2001: Proceedings*. 2002, pp. 3–158. arXiv: hep-th/0201253 [hep-th].

[43] Jacob D. Bekenstein. "Black Holes and Entropy". In: *Phys. Rev. D* 7 (8 Apr. 1973), pp. 2333–2346. DOI: 10.1103/PhysRevD.7.2333. URL: https://link.aps.org/doi/10.1103/PhysRevD.7.2333.

[44] S. W. Hawking. "Black holes and thermodynamics". In: *Phys. Rev. D* 13 (2 Jan. 1976), pp. 191–197. DOI: 10.1103/PhysRevD.13.191. URL: https://link.aps.org/doi/10.1103/PhysRevD.13.191.

[45] J. Polchinski. "String Theory vol. I, II". In: CUP (1998).

[46] Joseph Polchinski. "Dirichlet Branes and Ramond-Ramond Charges". In: *Phys. Rev. Lett.* 75 (26 Dec. 1995), pp. 4724–4727. DOI: 10.1103/PhysRevLett.75.4724. URL: https://link.aps.org/doi/10.1103/PhysRevLett.75.4724.

[47] Gary T. Horowitz and Andrew Strominger. "Black strings and P-branes". In: *Nucl. Phys.* B360 (1991), pp. 197–209. DOI: 10.1016/0550-3213(91)90440-9.

[48] Massimo Bianchi, Daniel Z. Freedman, and Kostas Skenderis. "Holographic renormalization". In: *Nucl. Phys.* B631 (2002), pp. 159–194. DOI: 10.1016/S0550-3213(02)00179-7. arXiv: hep-th/0112119 [hep-th].

[49] Kostas Skenderis. "Lecture notes on holographic renormalization". In: *Class. Quant. Grav.* 19 (2002), pp. 5849–5876. DOI: 10.1088/0264-9381/19/22/306. arXiv: hep-th/0209067 [hep-th].

[50] Kenneth G. Wilson. "Confinement of quarks". In: *Phys. Rev. D* 10 (8 Oct. 1974), pp. 2445–2459. DOI: 10.1103/PhysRevD.10.2445. URL: https://link.aps.org/doi/10.1103/PhysRevD.10.2445.

[51] K. Zarembo. "Supersymmetric Wilson loops". In: *Nucl. Phys.* B643 (2002), pp. 157–171. DOI: 10.1016/S0550-3213(02)00693-4. arXiv: hep-th/0205160 [hep-th].

[52] Z. Guralnik and B. Kulik. "Properties of chiral Wilson loops". In: *JHEP* 01 (2004), p. 065. DOI: 10.1088/1126-6708/2004/01/065. arXiv: hep-th/0309118 [hep-th].

[53] Z. Guralnik, S. Kovacs, and B. Kulik. "Less is more: Non-renormalization theorems from lower dimensional superspace". In: *Int. J. Mod. Phys.* A20 (2005), pp. 4546–4553. DOI: 10.1142/S0217751X05028193. arXiv: hep-th/0409091 [hep-th].

[54] A. Dymarsky et al. "Calibrated surfaces and supersymmetric Wilson loops". In: *JHEP* 09 (2006), p. 057. DOI: 10.1088/1126-6708/2006/09/057. arXiv: hep-th/0604058 [hep-th].

[55] Nadav Drukker et al. "More supersymmetric Wilson loops". In: *Phys. Rev.* D76 (2007), p. 107703. DOI: 10.1103/PhysRevD.76.107703. arXiv: 0704.2237 [hep-th].

[56] J. K. Erickson, G. W. Semenoff, and K. Zarembo. "Wilson loops in N=4 supersymmetric Yang-Mills theory". In: *Nucl. Phys.* B582 (2000), pp. 155–175. DOI: 10.1016/S0550-3213(00)00300-X. arXiv: hep-th/0003055 [hep-th].

[57] Nadav Drukker and David J. Gross. "An Exact prediction of N=4 SUSYM theory for string theory". In: *J. Math. Phys.* 42 (2001), pp. 2896–2914. DOI: 10.1063/1.1372177. arXiv: hep-th/0010274 [hep-th].

[58] Gleb Arutyunov, Jan Plefka, and Matthias Staudacher. "Limiting geometries of two circular Maldacena-Wilson loop operators". In: *JHEP* 12 (2001), p. 014. DOI: 10.1088/1126-6708/2001/12/014. arXiv: hep-th/0111290 [hep-th].

[59] K. Konishi. "Anomalous Supersymmetry Transformation of Some Composite Operators in SQCD". In: *Phys. Lett.* 135B (1984), pp. 439–444. DOI: 10.1016/0370-2693(84)90311-3.

[60] Damiano Anselmi. "The N=4 quantum conformal algebra". In: *Nucl. Phys.* B541 (1999), pp. 369–385. DOI: 10.1016/S0550-3213(98)00848-7. arXiv: hep-th/9809192 [hep-th].

[61] Massimo Bianchi et al. "On the logarithmic behavior in N=4 SYM theory". In: *JHEP* 08 (1999), p. 020. DOI: 10.1088/1126-6708/1999/08/020. arXiv: hep-th/9906188 [hep-th].

[62] Massimo Bianchi et al. "Anomalous dimensions in N=4 SYM theory at order g4". In: *Nuclear Physics B* 584 (Sept. 2000), pp. 216–232. DOI: 10.1016/S0550-3213(00)00312-6.

[63] Massimo Bianchi et al. "Properties of the Konishi multiplet in Script N = 4 SYM theory". In: *Journal of High Energy Physics - J HIGH ENERGY PHYS* 5 (May 2001). DOI: 10.1088/1126-6708/2001/05/042.

[64] Gleb Arutyunov, Sergey Frolov, and Anastasios C. Petkou. "Operator product expansion of the lowest weight CPOs in $\mathcal{N} = 4$ SYM_4 at strong coupling". In: *Nucl. Phys.* B586 (2000). [Erratum: Nucl. Phys.B609,539(2001)], pp. 547–588. DOI: 10.1016/S0550-3213(01)00266-8,10.1016/S0550-3213(00)00439-9. arXiv: hep-th/0005182 [hep-th].

[65] Gleb Arutyunov, Sergey Frolov, and Anastasios Petkou. "Perturbative and instanton corrections to the OPE of CPOs in $\mathcal{N} = 4$ SYM_4". In: *Nucl. Phys.* B602 (2001). [Erratum: Nucl. Phys.B609,540(2001)], pp. 238–260. DOI: 10.1016/S0550-3213(01)00118-3,10.1016/S0550-3213(01)00265-6. arXiv: hep-th/0010137 [hep-th].

[66] G. Arutyunov et al. "Exceptional nonrenormalization properties and OPE analysis of chiral four point functions in N=4 SYM(4)". In: *Nucl. Phys.* B620 (2002), pp. 380–404. DOI: 10.1016/S0550-3213(01)00569-7. arXiv: hep-th/0103230 [hep-th].

[67] Silvia Penati and Alberto Santambrogio. "Superspace approach to anomalous dimensions in N=4 SYM". In: *Nucl. Phys.* B614 (2001), pp. 367–387. DOI: 10.1016/S0550-3213(01)00414-X. arXiv: hep-th/0107071 [hep-th].

[68] Steven S. Gubser and Igor R. Klebanov. "Absorption by branes and Schwinger terms in the world volume theory". In: *Phys. Lett.* B413 (1997), pp. 41–48. DOI: 10.1016/S0370-2693(97)01099-X. arXiv: hep-th/9708005 [hep-th].

[69] D. Anselmi et al. "Nonperturbative formulas for central functions of supersymmetric gauge theories". In: *Nucl. Phys.* B526 (1998), pp. 543–571. DOI: 10.1016/S0550-3213(98)00278-8. arXiv: hep-th/9708042 [hep-th].

[70] Eric D'Hoker, Daniel Z. Freedman, and Witold Skiba. "Field theory tests for correlators in the AdS / CFT correspondence". In: *Phys. Rev.* D59 (1999), p. 045008. DOI: 10.1103/PhysRevD.59.045008. arXiv: hep-th/9807098 [hep-th].

[71] B. Eden, Paul S. Howe, and Peter C. West. "Nilpotent invariants in N=4 SYM". In: *Phys. Lett.* B463 (1999), pp. 19–26. DOI: 10.1016/S0370-2693(99)00705-4. arXiv: hep-th/9905085 [hep-th].

[72] Anastasios Petkou and Kostas Skenderis. "A Nonrenormalization theorem for conformal anomalies". In: *Nucl. Phys.* B561 (1999), pp. 100–116. DOI: 10.1016/S0550-3213(99)00514-3. arXiv: hep-th/9906030 [hep-th].

[73] Paul S. Howe et al. "Explicit construction of nilpotent covariants in N=4 SYM". In: *Nucl. Phys.* B571 (2000), pp. 71–90. DOI: 10.1016/S0550-3213(99)00768-3. arXiv: hep-th/9910011 [hep-th].

[74] S. Penati, A. Santambrogio, and Daniela Zanon. "Two point functions of chiral operators in N=4 SYM at order g**4". In: *JHEP* 12 (1999), p. 006. DOI: 10.1088/1126-6708/1999/12/006. arXiv: hep-th/9910197 [hep-th].

[75] Silvia Penati, Alberto Santambrogio, and Daniela Zanon. "More on correlators and contact terms in N=4 SYM at order g**4". In: *Nucl. Phys.* B593 (2001), pp. 651–670. DOI: 10.1016/S0550-3213(00)00633-7. arXiv: hep-th/0005223 [hep-th].

[76] Gordon W. Semenoff and K. Zarembo. "More exact predictions of SUSYM for string theory". In: *Nucl. Phys.* B616 (2001), pp. 34–46. DOI: 10.1016/S0550-3213(01)00455-2. arXiv: hep-th/0106015 [hep-th].

[77] Sangmin Lee et al. "Three point functions of chiral operators in D = 4, N=4 SYM at large N". In: *Adv. Theor. Math. Phys.* 2 (1998), pp. 697–718. DOI: 10.4310/ATMP.1998.v2.n4.a1. arXiv: hep-th/9806074 [hep-th].

[78] John L. Cardy. "Conformal Invariance and Surface Critical Behavior". In: *Nucl. Phys.* B240 (1984), pp. 514–532. DOI: 10.1016/0550-3213(84)90241-4.

[79] W. Nahm. "A Simple Formalism for the BPS Monopole". In: *Phys. Lett.* 90B (1980), pp. 413–414. DOI: 10.1016/0370-2693(80)90961-2.

[80] Duiliu-Emanuel Diaconescu. "D-branes, monopoles and Nahm equations". In: *Nucl. Phys.* B503 (1997), pp. 220–238. DOI: 10.1016/S0550-3213(97)00438-0. arXiv: hep-th/9608163 [hep-th].

[81] Neil R. Constable, Robert C. Myers, and Oyvind Tafjord. "The Noncommutative bion core". In: *Phys. Rev.* D61 (2000), p. 106009. DOI: 10.1103/PhysRevD.61.106009. arXiv: hep-th/9911136 [hep-th].

[82] Andreas Karch and Lisa Randall. "Localized gravity in string theory". In: *Phys. Rev. Lett.* 87 (2001), p. 061601. DOI: 10.1103/PhysRevLett.87.061601. arXiv: hep-th/0105108 [hep-th].

[83] Amit Giveon and David Kutasov. "Brane dynamics and gauge theory". In: *Rev. Mod. Phys.* 71 (1999), pp. 983–1084. DOI: 10.1103/RevModPhys.71.983. arXiv: hep-th/9802067 [hep-th].

[84] Robert C. Myers and Matthias C. Wapler. "Transport Properties of Holographic Defects". In: *JHEP* 12 (2008), p. 115. DOI: 10.1088/1126-6708/2008/12/115. arXiv: 0811.0480 [hep-th].

[85] Yoshiaki Susaki, Yastoshi Takayama, and Kentaroh Yoshida. "Open semiclassical strings and long defect operators in AdS/dCFT correspondence". In: *Phys. Rev. D* 71 (12 June 2005), p. 126006. DOI: 10.1103/PhysRevD.71.126006. URL: https://link.aps.org/doi/10.1103/PhysRevD.71.126006.

[86] Tristan McLoughlin and Ian Swanson. "Open string integrability and AdS/CFT". In: *Nucl. Phys.* B723 (2005), pp. 132–162. DOI: 10.1016/j.nuclphysb.2005.06.014. arXiv: hep-th/0504203 [hep-th].

[87] Yoshiaki Susaki, Yastoshi Takayama, and Kentaroh Yoshida. "Integrability and Higher Loops in AdS/dCFT Correspondence". In: *Physics Letters B* 624 (Apr. 2005). DOI: 10.1016/j.physletb.2005.07.058.

[88] Keisuke Okamura, Yastoshi Takayama, and Kentaroh Yoshida. "Open spinning strings and AdS/dCFT duality". In: *JHEP* 01 (2006), p. 112. DOI: 10.1088/1126-6708/2006/01/112. arXiv: hep-th/0511139 [hep-th].

[89] Marius de Leeuw et al. "Two-point functions in AdS/dCFT and the boundary conformal bootstrap equations". In: *JHEP* 08 (2017), p. 020. DOI: 10.1007/JHEP08(2017)020. arXiv: 1705.03898 [hep-th].

[90] Konstantin Zarembo. "Localization and AdS/CFT Correspondence". In: *J. Phys.* A50.44 (2017), p. 443011. DOI: 10.1088/1751-8121/aa585b. arXiv: 1608.02963 [hep-th].

[91] Marius de Leeuw et al. "One-loop Wilson loops and the particle-interface potential in AdS/dCFT". In: *Phys. Lett.* B768 (2017), pp. 192–197. DOI: 10.1016/j.physletb.2017.02.047. arXiv: 1608.04754 [hep-th].

[92] Michelangelo Preti, Diego Trancanelli, and Edoardo Vescovi. "Quark-antiquark potential in defect conformal field theory". In: *JHEP* 10 (2017), p. 079. DOI: 10.1007/JHEP10(2017)079. arXiv: 1708.04884 [hep-th].

[93] Hungsoo Kim et al. "Gross-Ooguri phase transition at zero and finite temperature: Two circular Wilson loop case". In: *JHEP* 03 (2001), p. 003. DOI: 10.1088/1126-6708/2001/03/003. arXiv: hep-th/0101235 [hep-th].

[94] "NIST Digital Library of Mathematical Functions." In: (). DOI: http://dlmf.nist.gov/,Release1.0.22of2019-03-15..

[95] K. Zarembo. "Wilson loop correlator in the AdS / CFT correspondence". In: *Phys. Lett.* B459 (1999), pp. 527–534. DOI: 10.1016/S0370-2693(99)00717-0. arXiv: hep-th/9904149 [hep-th].

[96] P. Olesen and K. Zarembo. "Phase transition in Wilson loop correlator from AdS / CFT correspondence". In: (2000). arXiv: hep-th/0009210 [hep-th].

[97] Diego H. Correa, Pablo Pisani, and Alan Rios Fukelman. "Ladder Limit for Correlators of Wilson Loops". In: *JHEP* 05 (2018), p. 168. DOI: 10.1007/JHEP05(2018)168. arXiv: 1803.02153 [hep-th].

[98] K. Zarembo. "String breaking from ladder diagrams in SYM theory". In: *JHEP* 03 (2001), p. 042. DOI: 10.1088/1126-6708/2001/03/042. arXiv: hep-th/0103058 [hep-th].

[99] Diego Correa et al. "Dyson equations for correlators of Wilson loops". In: *JHEP* 12 (2018), p. 100. DOI: 10.1007/JHEP12(2018)100. arXiv: 1811.03552 [hep-th].

[100] Nadav Drukker and Bartomeu Fiol. "On the integrability of Wilson loops in $AdS_5 \times S^5$: Some periodic ansatze". In: *JHEP* 01 (2006). hep-th/0506058, p. 056. DOI: 10.1088/1126-6708/2006/01/056. arXiv: hep-th/0506058 [hep-th].

[101] Aleix Gimenez Grau et al. "A Quantum Check of Non-Supersymmetric AdS/dCFT". In: *JHEP* 01 (2019), p. 007. DOI: 10.1007/JHEP01(2019)007. arXiv: 1810.11463 [hep-th].

[102] Marius de Leeuw, Charlotte Kristjansen, and Georgios Linardopoulos. "One-point functions of non-protected operators in the SO(5) symmetric D3–D7 dCFT". In: *J. Phys.* A50.25 (2017), p. 254001. DOI: 10.1088/1751-8121/aa714b. arXiv: 1612.06236 [hep-th].

[103] Marius de Leeuw, Charlotte Kristjansen, and Kasper E. Vardinghus. "A non-integrable quench from AdS/dCFT". In: (2019). DOI: 10.1016/j.physletb.2019.134940. arXiv: 1906.10714 [hep-th].

[104] Hong Liu and Arkady A. Tseytlin. "On four point functions in the CFT / AdS correspondence". In: *Phys. Rev.* D59 (1999), p. 086002. DOI: 10.1103/PhysRevD.59.086002. arXiv: hep-th/9807097 [hep-th].